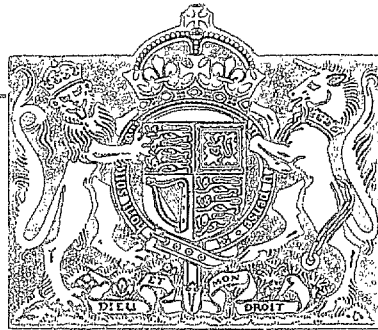


N. A. E.

R. & M. No. 2870
(11,268, 11,747)
A.R.C. Technical Report



MINISTRY OF SUPPLY

AERONAUTICAL RESEARCH COUNCIL
REPORTS AND MEMORANDA

The Diffusion of Load into a
Semi-infinite Sheet

Parts I and II

By

E. H. MANSFIELD, M.A.

Crown Copyright Reserved

LONDON: HER MAJESTY'S STATIONERY OFFICE

1953

SIXTEEN SHILLINGS NET

The Diffusion of Load into a Semi-infinite Sheet

Parts I* and II

By

E. H. MANSFIELD, M.A.

COMMUNICATED BY THE PRINCIPAL DIRECTOR OF SCIENTIFIC RESEARCH (AIR),
MINISTRY OF SUPPLY

Reports and Memoranda No. 2670†
June, 1948

Summary.—In Part I, the rigorous and the 'stringer-sheet' stress solutions are given for a point load applied in the plane of a semi-infinite sheet and at a finite distance from the boundary which is assumed to be free. From these are derived, by integration, some of the stresses produced by distributed loads applied along lines normal to the free boundary; attention is concentrated on the stresses along the line of action of the applied loads.

The problem of finding the shear stresses adjacent to a load-carrying boom attached to the sheet and normal to the free edge is also investigated and integral equations for the shear stresses are derived. The integral equation obtained from the rigorous theory is not readily soluble, but it is shown that, as in the stringer-sheet solution, very large shear stresses are present adjacent to the boom and near the free edge of the sheet.

The required variation of boom cross-sectional area along its length to cause any particular variation of shear stress adjacent to the boom is also given.

In Part II, a theoretical investigation is made into the problem of stiffening a sheet to relieve the high stresses near the free edge and adjacent to a direct load-carrying boom attached to the sheet.

For booms of constant cross-section the stress distribution depends, with certain assumptions, on two non-dimensional parameters, and curves are included for determining the peak stresses in the sheet and the loads in the stiffening structure over the practical range of these parameters.

It is shown that if a given weight of stiffening material is to be distributed uniformly along the free edge of the sheet there is a particular shape of stiffener which gives lowest peak stresses in the sheet.

The influence of rivet flexibility between boom and sheet is examined theoretically.

PART I

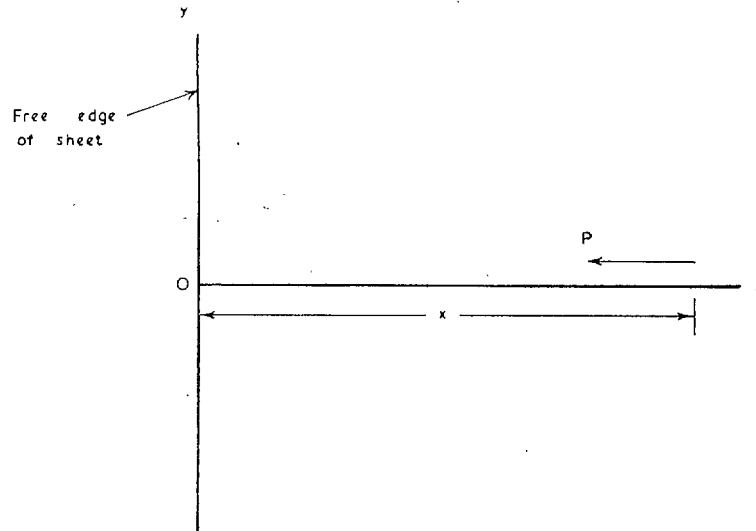
1. *Introduction.*—The diffusion of load from a boom or stringer into a sheet is one of the fundamental stressing problems in aircraft engineering and has been considered by a number of writers^{1 to 5}. All these give approximate solutions as they employ the stringer-sheet or 'stringer-shear-web-stringer' simplifications. Adjacent to the boom and near the root these simplifications are not justifiable for we are concerned with a *localised* effect, and nearby stringers, if any, naturally have an insignificant effect; this applies particularly to the shear stresses adjacent to the boom.

* Part I, November, 1947.

† R.A.E. Report Structures 11, received 17th February, 1948.

R.A.E. Report Structures 27, received 30th August, 1948.

A rigorous solution of this problem seemed necessary, but great difficulties are encountered in satisfying all the boundary conditions. An attempt to overcome these difficulties by solving the subsidiary problem of a point load applied to a semi-infinite sheet near to and normal to the free boundary was made and from it was derived an integral equation for the shear stresses adjacent to a boom of varying and arbitrary section. This equation (containing only one variable) is not readily soluble, but by choosing different forms for the shear stress it is possible to find the boom area to give the assumed shear stress. Since negative boom areas must be avoided in the analysis the correct stress function corresponds to an infinite shear stress at the root. This is not possible in practice, and there must be a certain amount of rivet slip or plastic yielding at the root; this emphasises the importance of stiffening and careful design in the neighbourhood of the root.



DIAG. 1. Co-ordinate axes and position of point load P .

List of Symbols

- | | |
|--------------------------|---|
| Ox, Oy | Co-ordinate axes as shown in Diag. 1 above. x is measured from the free boundary of the sheet |
| f_x | Direct tensile stress along Ox at point $(x, 0)$ |
| f_y | Transverse tensile stress at point $(x, 0)$ |
| q | Shear stress applied along Ox |
| e_x | Strain along Ox at point $(x, 0)$ |
| P | Point load applied normal to the free edge |
| X | Distance from free edge of point of application of load P |
| t | Thickness of sheet (constant) |
| t_s | Stringer-sheet thickness |
| E, G | Elastic Moduli |
| k | $(Et_s/Gt)^{1/2}$ |
| m | Poisson's ratio |
| w | Width of panel |
| A | Cross-sectional area of boom |
| f_{xx}, f_{yy}, q_{xy} | Stresses at a point (x, y) |

2. *Rigorous Stress Solution.*—2.1. *Point Load Applied at a Distance from the Free Edge.*
 A rigorous (stress-function) solution for this loading is obtained in Appendix I; the stresses O_x along are given by:

$$f_x = \frac{-2Px^2\{(2+m)X+x\}}{\pi t(X-x)(X+x)^3}, \quad \dots \dots \dots (1)$$

$$f_y = \frac{+2PX^2(X-mx)}{\pi t(X-x)(X+x)^3}, \quad \dots \dots \dots (2)$$

shear stress = 0,

and these are plotted, together with the simplified stringer-sheet results, in Figs. 1 and 2.

It will be noticed that at the root

$$\left. \begin{aligned} f_x &= 0 \\ f_y &= \frac{2P}{\pi tX} \end{aligned} \right\} \dots \dots \dots (3)$$

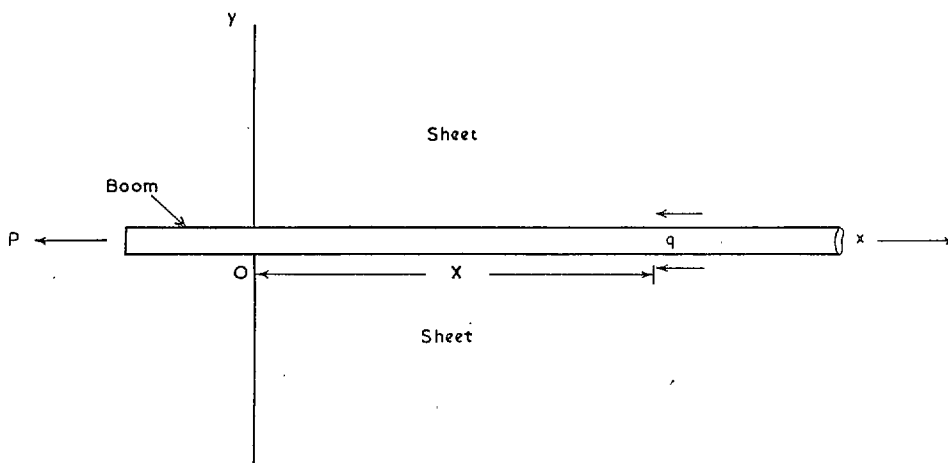
and which is positive for all values of X provided P acts towards the free boundary. The strain at the root, therefore, given by

$$\left. \begin{aligned} e_x &= (f_x - mf_y)/E \\ &= \frac{-2mP}{\pi tXE} \end{aligned} \right\} \dots \dots \dots (4)$$

is always negative.

Expressions for the stresses elsewhere in the sheet are given in Appendix I; they are complicated and are not necessary for the present purposes. Expressions for the stresses when the point load is applied in a direction parallel to the free edge are also given and they may be of interest to other investigators. (See also Ref. 8.)

2.2. *Distributed Load Applied by a Boom* (Integral equation for the shear stress adjacent to a boom).

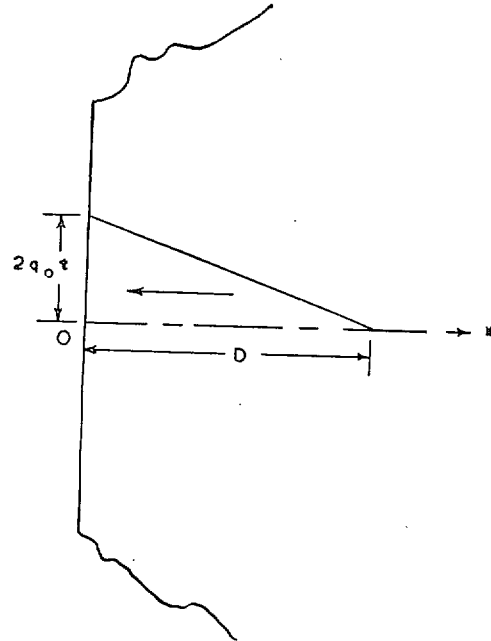


DIAG. 2. Boom and semi-infinite sheet.

If q is the shear stress applied by the boom to an element of the sheet at a distance X from the free edge (see Diag. 2) it can be represented by a point load of

$$dP = 2qt dX, \quad \dots \dots \dots (5)$$

2.3.2. *Linearly distributed shear.*—For a linearly varying shear/unit length ($2q_0t(1 - x/D)$) applied to the sheet as indicated in Diag. 4, the direct strain along the line of the applied shears is given by:



DIAG. 4.

$$\begin{aligned} \frac{Ee_x}{q_0} = & \frac{(3 - m)(1 + m)(D - x)}{2\pi D} \log\left(\frac{D + x}{D - x}\right) \\ & - \frac{4m(2 + m)x}{\pi D} \log\left(\frac{D + x}{x}\right) - \frac{4m}{\pi} \log\left(\frac{D + x}{x}\right) \\ & + \frac{2(1 + 4m + m^2)D^2 + (5 + 18m + 5m^2)Dx + (3 + m)(1 + 3m)x^2}{\pi(D + x)^2}, \quad \dots \quad (10) \end{aligned}$$

which has been plotted in Fig. 4, where it will be seen that the strain becomes negative near the free edge, as it did for the uniformly distributed shear case.

It is worth noting here that since the strain becomes negative near the free edge it is impossible to design a boom which will feed the load in it into the surrounding sheet in the above prescribed manners because this would necessitate a negative boom area in this region.

2.3.3. *Other shear distributions.*—The effect of parabolic and other shear distributions may be found by direct substitution. Alternatively, the linear distribution discussed above may be used as a unit load line, and other smooth shear distributions obtained from it, approximately by summation or exactly by integration. It will be seen that all die-away forms that are not infinite in value at the root will give a negative boom strain in the neighbourhood of the root.

But if we take for example

$$q = K/\sqrt{x} \quad \dots \quad (11)$$

which becomes infinite at the root, we find that

$$Ee_x = \left(\frac{3 - m}{2}\right)^2 K/\sqrt{x} \quad \dots \quad (12)$$

which, although it is positive even near the root, now becomes infinitely large at the root; this would necessitate a zero boom area at the root.

3. *Simplified Stringer-sheet Solution.*—Using stringer-sheet theory the stresses in a sheet due to a point load have been found in Appendix I.

For a point load P applied at the origin and along the x -axis in an *infinite* sheet the stresses throughout are given by

$$\text{and} \quad \left. \begin{aligned} f_{xx} &= \frac{kP}{2\pi t_s} \left\{ \frac{x}{x^2 + k^2y^2} \right\} \\ q_{xy} &= \frac{kP}{2\pi t} \left\{ \frac{y}{x^2 + k^2y^2} \right\} \end{aligned} \right\} \dots \quad (13)$$

where t_s is the thickness of the stringer-sheet and $k^2 = Et_s/Gt$.

3.1. *Point Load Applied at a Distance from the Free Edge.*—When the load is applied towards the free boundary of a semi-infinite sheet and distance X from it (as in section 2.1):

$$\left. \begin{aligned} f_{xx} &= \frac{kP}{\pi t_s} \frac{x(x^2 + k^2y^2 - X^2)}{\{(x+X)^2 + k^2y^2\}\{(x-X)^2 + k^2y^2\}} \\ q_{xy} &= \frac{kP}{\pi t} \frac{y(x^2 + k^2y^2 + X^2)}{\{(x+X)^2 + k^2y^2\}\{(x-X)^2 + k^2y^2\}} \end{aligned} \right\} \dots \dots \dots (14)$$

Along the line of action of the applied load ($y = 0$) these equations reduce to

$$\left. \begin{aligned} f_x &= \frac{-kPx}{\pi t_s(X^2 - x^2)} \\ q_{xy} &= 0 \end{aligned} \right\} \dots \dots \dots (15)$$

3.2. *Distributed Load applied by a Boom (Integral equation for the shear stress adjacent to the boom).*—From reasoning similar to that given in section 2.2 we can derive an integral equation for the shear stress (q) adjacent to a boom. The equation for q corresponding to equation (7) is

$$\int_x^\infty q(X) dX + \frac{Akx}{\pi t_s} \int_0^\infty \frac{q(X) dX}{X^2 - x^2} = 0 \dots \dots \dots (16)$$

and if the boom area is constant the solution of this equation may be expressed in closed form in terms of trigonometrical functions and the sine and cosine integrals

$$\left(\int_x^\infty \frac{\sin t}{t} \cdot dt \text{ and } - \int_x^\infty \frac{\cos \cdot t}{t} \cdot dt \right)$$

which are tabulated in Ref. 9.

$$q/f_0 = \frac{-2t_s}{\pi kt} \{ \cos \varrho \text{ Ci } \varrho + \sin \varrho \text{ si } \varrho \} \dots \dots \dots (16a)$$

where $\varrho = 2xt_s/Ak$ and f_0 the boom stress at the root. This has been plotted in Fig. 5.

3.2.1. *Estimation of shear yielding that occurs in practice.*—From Fig. 5 or equation (16a) it will be noticed that the shear stress becomes infinitely great when x is zero; in fact, for small x the expression inside the brackets of equation (16a) behaves like $\log \gamma \varrho = \log x - \log (Ak/2\gamma t_s)$ where

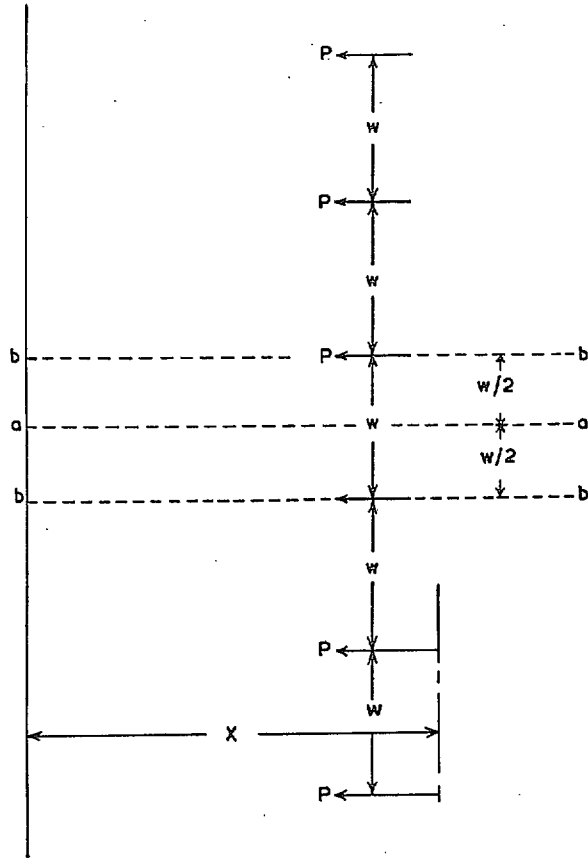
$$\log \gamma = 0.5772 = \text{Euler's constant.}$$

Using these expressions for integrating the area under the q -curve it is possible to estimate the proportion of load taken (theoretically) by shear beyond the elastic limit, and this has been done in Fig. 6. In Fig. 7 an attempt has been made to estimate the actual shear stress distribution, assuming that the boom tensile stress at the root, f_0 , is at the yielding point and that the yielding shear stress of the sheet is $f_0/2$.

Fig. 7 gives an indication of the extent of possible shear yielding and suggests how much stiffening may be necessary.

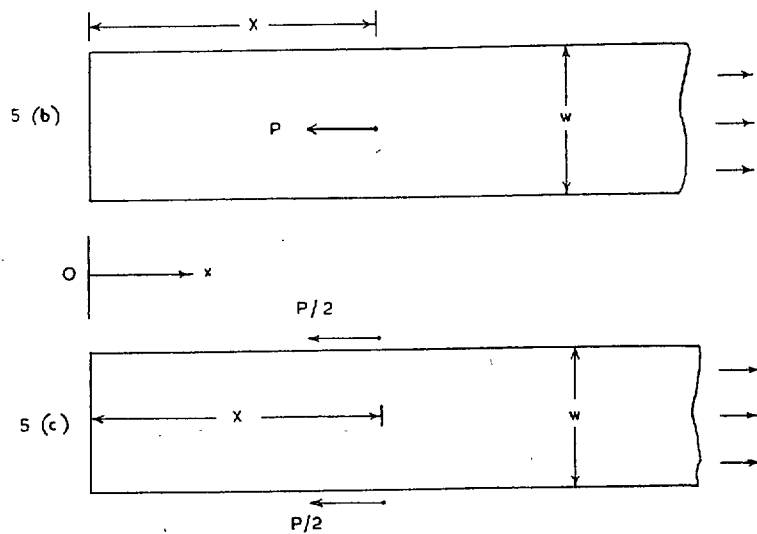
3.3. *Comparison with the Rigorous Solution.*—The broken curves in Figs. 1, 2, 3 and 4 compare the stringer-sheet solution with the rigorous solution for the simple cases considered there. It will be seen that agreement with exact theory is not as good as is generally believed.⁶

4. *Panels of Finite Width (stringer-sheet solution).*—The solution obtained above for the infinitely wide sheet with single point load can be adapted to the case of a panel of finite width by a method of 'images'. Consider the case of a large number of loads applied as indicated in Diag. 5a.



DIAG. 5a. Multiple loads applied to semi-infinite sheet.

The solution for this case can be obtained from that for a single load by a process of summation. It is clear from symmetry that there will be no shear stresses along such lines as a-a or b-b. Also, under the assumptions made in stringer-sheet theory, stresses normal to these lines do not affect the solution. This means that we can cut the sheet along lines a-a or b-b without affecting the stress distribution, and so obtain the solution to the systems in Diags. 5b or 5c.

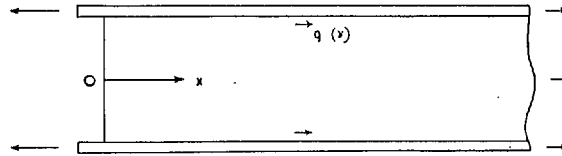


DIAGS. 5b and c. Equivalent loads applied to finite panels.

The direct stress along the line of action of the applied loads for cases (b) and (c) above, is given by

$$f_x = \frac{P}{2wt_s} \left[\coth \left\{ \frac{(x - X)\pi}{kw} \right\} + \coth \left\{ \frac{(x + X)\pi}{kw} \right\} \right]. \quad \dots \dots \dots (17)$$

4.1. *Distributed Loads Applied by Booms (Integral equation for the shear stress adjacent to the booms).*—From reasoning similar to that given in section 2.2 we can derive an integral equation for the shear stress (q) adjacent to the booms (assumed to be of constant area A each) of a panel of finite width.



DIAG. 6. Panel absorbing load from booms.

Regarding the loads $P/2$ of Diag. 5c to be elemental loads of a continuous system along the length of the boom-sheet junction we find that

$$\int_x^\infty q(X) dX - \frac{A}{wt_s} \int_0^\infty q(X) \left[\coth \left\{ \frac{(x - X)\pi}{kw} \right\} + \coth \left\{ \frac{(x + X)\pi}{kw} \right\} \right] dx = 0, \quad \dots \dots (18)$$

the solution of which is

$$q(x) = K \int_0^\infty \frac{\cos(x\lambda/kw) d\lambda}{1 + \alpha\lambda \coth \lambda/2} \quad \dots \dots \dots (18a)$$

where K is $-2A(1 + 2A/wt_s)/t\pi kw$ times the boom stress at the root and $\alpha = A/wt_s$.

5. *Conclusions.*—The stresses in a sheet due to a point applied at a finite distance from the free edge of the sheet can be derived by the method given in this report, and from them can also be derived an integral equation for the shear stresses adjacent to a boom of arbitrary section. The method permits attention to be concentrated on the shear stresses adjacent to the boom and shows that these stresses are very large.

Comparisons with the simplified stringer-sheet theory show that this simplified theory is not as good as is generally believed. Unlike the corresponding stringer-sheet equation, the integral equation obtained in the present report is not readily soluble.

Part II of this report extends the present work to include the effect of a stiffening flange attached to the free boundary of the sheet and efficient methods of design with particular reference to weight saving.

REFERENCES

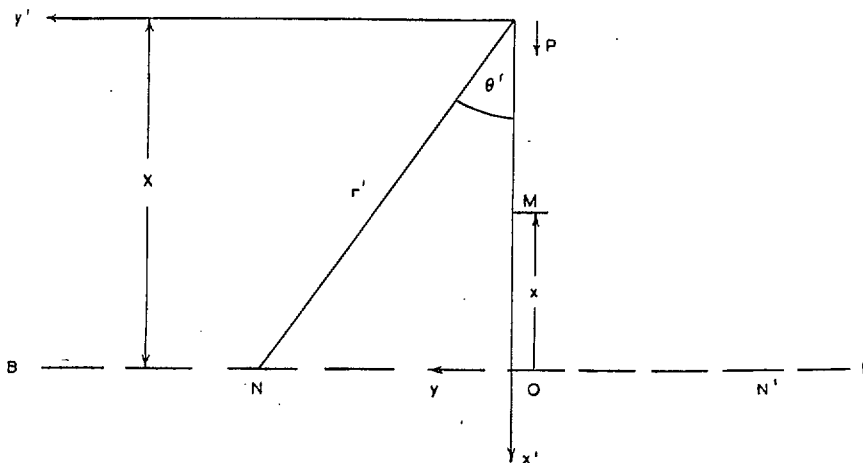
No.	Author	Title, etc.
1	W. J. Duncan	Diffusion of Load in Certain Sheet-stringer Combinations. R. & M. 1825. January, 1938.
2	D. Williams, R. D. Starkey and R. H. Taylor.	The Distribution of Stress between Spar Flanges and Stringers for a Wing under Distributed Loading. R. & M. 2098. June, 1939.
3	J. Hadji-Argyris	The Diffusion of Anti-symmetrical Concentrated End Loads and Edge Loads into Parallel Stiffened Panels and Analysis of Parallel Panels under Transverse Loads. A.R.C. Report 9662. May, 1946. (To be published.)
4	H. L. Cox	Diffusion of Concentrated Loads into Monocoque Structures. III. R. & M. 1860. September, 1938.
5	J. Hadgi-Argyris and H. L. Cox ..	Diffusion of Load into Flat Stiffened Panels of Varying Cross-section. R. & M. 1969. May, 1944.
6	M. Fine	A Comparison of Plain and Stringer-reinforced Sheet from the Shear Lag Standpoint. A.R.C. Report 5549. October, 1941. (Unpublished.)
7	S. Timoshenko	<i>Theory of Elasticity</i> , pp. 83-103.
8	E. Melan	<i>Z. angew. Math. Mech.</i> , Vol. 12, p. 343.
9	E. Jahnke and F. Emde	<i>Tables of Functions</i> .
10	A. E. H. Love	Biharmonic Analysis and its Applications. <i>Proc. Lond. Math. Soc.</i> (2), Vol. 29. 1929.

APPENDIX I

The stress-function solution for a point load applied in the plane of an *infinite* sheet is known, and so the stresses acting along such a line as BB in Diag. 7 are known. If the sheet is cut along BB, we can represent the stresses throughout by the original stresses superimposed on the stresses due to an equal-and-opposite 'liquidating' stress distribution applied along BB to the *semi-infinite* sheet—the exact stress distribution due to loads applied along the boundary of a semi-infinite sheet also being known.

In the first part of this appendix attention is concentrated on the stresses along the line of action of the applied load.

Consider now a load P applied at a point P in the plane of an infinite sheet (as in Diag. 7).



DIAG. 7. Diagram showing notation.

The dashed co-ordinates x' , y' , r' , θ' are with the origin at P . x and y have their origin at O , as in Diag. 7 above.

The stress-function solution is⁷

$$\phi = \frac{(1-m)}{4\pi} P r' \log r' \cdot \cos \theta' - \frac{P r' \theta'}{2\pi} \sin \theta', \quad \dots \dots \dots (19)$$

which satisfies the biharmonic equation and all the boundary conditions. Equation (19) gives stresses (in polar co-ordinates)—

$$\left. \begin{aligned} f_r &= -\frac{(3+m)P}{4\pi r'} \cos \theta' \\ f_{\theta'} &= \frac{(1-m)P}{4\pi r'} \cos \theta', \\ q_{r\theta'} &= \frac{(1-m)P}{4\pi r'} \sin \theta'. \end{aligned} \right\} \dots \dots \dots (20)$$

The stress components in Cartesian co-ordinates are found from

$$\begin{aligned} f_x &= \cos^2 \theta' \cdot f_r + \sin^2 \theta' \cdot f_{\theta'} + q_{r\theta'} \sin 2\theta' \\ &= -\frac{P \cos \theta'}{4\pi r'} \{1-m+2(1+m) \cos^2 \theta'\}, \quad \dots \dots \dots (21) \end{aligned}$$

$$\begin{aligned} f_y &= \sin^2 \theta' \cdot f_r + \cos^2 \theta' \cdot f_{\theta'} - q_{r\theta'} \sin 2\theta' \\ &= \frac{P \cos \theta'}{4\pi r'} \{1-m-2(1+m) \sin^2 \theta'\}, \quad \dots \dots \dots (22) \end{aligned}$$

$$\begin{aligned} q_{xy} &= \sin 2\theta' \cdot (f_{\theta'} - f_r)/2 + \cos 2\theta' \cdot q_{r\theta'}/2 \\ &= -\frac{P \sin \theta'}{4\pi r'} \{1-m+2(1+m) \cos^2 \theta'\} \dots \dots \dots (23) \end{aligned}$$

The stresses, therefore, at M (defined by its distance x from the line BB, BB being normal to the direction of the applied load and distance X from it) are

$$\begin{aligned} f_x &= -\frac{P(3+m)}{4\pi x'} \\ &= -\frac{P(3+m)}{4\pi(X-x)}, \quad \dots \dots \dots (24) \end{aligned}$$

and similarly,

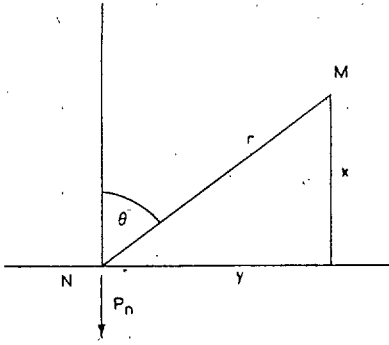
$$f_y = \frac{P(1-m)}{4\pi(X-x)}. \quad \dots \dots \dots (25)$$

The normal and shear stresses at points N along BB are found from equations (21) and (23) by putting $r' = \sqrt{(X^2 + y^2)}$, $\sin \theta' = y/r$ and $\cos \theta' = X/r$, i.e.,

$$f_x = -\frac{P}{4\pi} \left(\frac{X}{X^2 + y^2} \right) \left(1-m + \frac{2(1+m)X^2}{X^2 + y^2} \right), \quad \dots \dots \dots (26)$$

$$q_x = -\frac{P}{4\pi} \left(\frac{y}{X^2 + y^2} \right) \left(1-m + \frac{2(1+m)X^2}{X^2 + y^2} \right). \quad \dots \dots \dots (27)$$

If we make BB a free boundary we must liquidate f_x and q_x by applying equal and opposite stresses along BB. We consider, therefore, the effect of applying normal and shear loads to a free boundary of a semi-infinite sheet.



Normal Load applied to Boundary of Semi-infinite Sheet.—
 In Diag. 8 points M and N correspond with M and N in
 Diag. 7. The stress function solution, $\phi = (P_n/\pi) r\theta \sin \theta$
 gives a simple radial distribution :

$$\left. \begin{aligned} f_r &= 2P_n \cos \theta / \pi r \\ f_\theta &= q_{r\theta} = 0 \end{aligned} \right\} \dots \dots (28)$$

DIAG. 8. Normal load at sheet boundary.

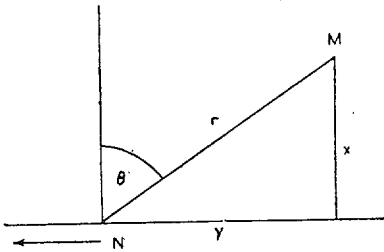
The stresses at M are, in Cartesian co-ordinates,

$$f_x = \frac{2P_n x^3}{\pi(x^2 + y^2)^2} \dots \dots \dots (29)$$

and

$$f_y = \frac{2P_n xy^2}{\pi(x^2 + y^2)^2} \dots \dots \dots (30)$$

We are not concerned with the shear stress, because the effect of a P_n applied to the image point N' in Diag. 7 will be to produce an equal but opposite shear stress, and when we sum the effect of the direct stresses applied all along BB the resultant shear stress at M will be zero. This is also clear from symmetry.



Shear Load applied to Boundary of Semi-infinite Sheet.—
 The stress function solution again gives a simple radial
 distribution :

$$\left. \begin{aligned} f_r &= \frac{2P_s}{\pi r} \sin \theta \\ f_\theta &= q_{r\theta} = 0 \end{aligned} \right\} \dots \dots \dots (31)$$

DIAG. 9. Shear load at sheet boundary.

And the equations corresponding to equations (29) and (30) are:

$$f_x = \frac{2P_s x^2 y}{\pi(x^2 + y^2)^2} \dots \dots \dots (32)$$

$$f_y = \frac{2P_s y^3}{\pi(x^2 + y^2)^2} \dots \dots \dots (33)$$

It is again unnecessary to calculate q_{xy} .

Condition of Zero Stress along the Free Boundary.—We must now choose the magnitude and distribution of the P_n 's and P_s 's to be equal and opposite to the f_x and q_x of equations (26) and (27). For an elemental part δy of the boundary we accordingly have

$$P_n = -f_x \delta y \dots \dots \dots (34)$$

and

$$P_s = -q_x \delta y \dots \dots \dots (35)$$

Substituting for P_n and P_s in equations (29) and (32) for f_x , and equations (30) and (33) for f_y , gives

$$\delta f_x = \frac{-2x^2 \delta y}{\pi(x^2 + y^2)^2} (xf_x + yq_x) \quad \dots \quad (36)$$

$$\delta f_y = \frac{-2y^2 \delta y}{\pi(x^2 + y^2)^2} (xf_x + yq_x) \quad \dots \quad (37)$$

f_x and q_x are given by equations (26) and (27), and, on substitution in equations (36) and (37), give on integrating along the whole of the free boundary:

$$f_x = \frac{Px^2}{2\pi^2} \int_{-\infty}^{+\infty} \frac{(Xx + y^2)\{(3 + m)X^2 + (1 - m)y^2\}}{(X^2 + y^2)^2 (x^2 + y^2)^2} dy \quad \dots \quad (38)$$

and

$$f_y = \frac{P}{2\pi^2} \int_{-\infty}^{+\infty} \frac{(Xx + y^2)\{(3 + m)X^2 + (1 - m)y^2\}y^2}{(X^2 + y^2)^2 (x^2 + y^2)^2} dy \quad \dots \quad (39)$$

These definite integrals may be evaluated using the Calculus of Residues. Denoting the integrals by I we have the relation

$$I_{-\infty}^{+\infty} = 2\pi i \Sigma R^+, \quad \dots \quad (40)$$

where ΣR^+ is the sum of the residuals of the integrand at its poles in the upper half-plane; the variable y regarded as complex. Here the poles are at $y = iX$ and ix , and the residual can therefore be found by making substitutions for y of the form $y = iX + \Delta$ and $ix + \Delta$ and summing the coefficients of $1/\Delta$ in both cases.

Performing this integration gives

$$f_x = P\{8x^2 + (3 + m)(X^2 + 4Xx - x^2)\}/4\pi(X + x)^3$$

and

$$f_y = P\{8X^2 - (1 - m)(X^2 - 4Xx - x^2)\}/4\pi(X + x)^3 \quad \dots \quad (41)$$

Equation (41) represents the stresses at a point M, as indicated in Diag. 7, due to the liquidating stresses applied along the free edge BB, they must be added to the stresses, given by equations (24) and (25), due 'directly' to P . Adding and simplifying gives

$$f_x = \frac{-2Px^2\{(2 + m)X + x\}}{\pi(X - x)(X + x)^3} \quad \dots \quad (42)$$

and

$$f_y = \frac{2PX^2(X - mx)}{\pi(X - x)(X + x)^3} \quad \dots \quad (43)$$

Complete Stress Distribution (see also Ref. 8).—It is clear that the stresses elsewhere in the sheet may be found by a simple extension of the above analysis. Denoting by f_{xx} , f_{yy} and q_{xy} the stresses at a point (x, y) in the plane of an *infinite* sheet, we have from equations (21), (22) and (23):

$$\left. \begin{aligned} f_{xx} &= \frac{-P(X - x)\{(3 + m)(X - x)^2 + (1 - m)y^2\}}{4\pi\{(X - x)^2 + y^2\}^2} \\ f_{yy} &= \frac{P(X - x)\{(1 - m)(X - x)^2 - (1 + 3m)y^2\}}{4\pi\{(X - x)^2 + y^2\}^2} \\ q_{xy} &= \frac{-Py\{(3 + m)(X - x)^2 + (1 - m)y^2\}}{4\pi\{(X - x)^2 + y^2\}^2} \end{aligned} \right\} \dots \quad (44)$$

This may be regarded as corresponding to equations (24) and (25), for it gives the stresses due directly to the applied load P .

If y_1 represents the ordinate along the boundary BB the 'unliquidated' stresses there will be given by equations (26) and (27) with y_1 substituted for y . (This distinction between the y 's was previously unnecessary.)

The stresses due to normal and shear loads applied to the boundary of a semi-infinite sheet will now be given by equations (29), (30), (32) and (33) with y replaced by $(y_1 - y)$. Expressions for the shear stresses will also be needed.

Proceeding along these lines and ensuring that the boundary BB is free from stress we find that the complete stress distribution, due to a concentrated load P applied towards a free boundary and distance X from it, is given by:

$$f_{xx} = \frac{P}{\pi t} \left[\left(\frac{1+m}{2} \right) \left(\frac{(x-X)^3}{r^4} + \frac{(x+X)(x^2+4xX+X^2)}{R^4} - \frac{8xXy^2(x+X)}{R^6} \right) + \left(\frac{1-m}{4} \right) \left(\frac{x-X}{r^2} + \frac{3x+X}{R^2} - \frac{4xy^2}{R^4} \right) \right] \dots \dots \dots (45)$$

$$f_{yy} = \frac{P}{\pi t} \left[\left(\frac{1+m}{2} \right) \left(\frac{(x-X)y^2}{r^4} + \frac{(x+X)(y^2+2X^2)-2y^2X}{R^4} + \frac{8xXy^2(x+X)}{R^6} \right) + \left(\frac{1-m}{4} \right) \left(\frac{X-x}{r^2} + \frac{x+3X}{R^2} - \frac{4xy^2}{R^4} \right) \right] \dots \dots \dots (46)$$

$$q_{xy} = \frac{Py}{\pi t} \left[\left(\frac{1+m}{2} \right) \left(\frac{(x-X)^2}{r^4} + \frac{(x^2-2xX-X^2)}{R^4} + \frac{8xX(x+X)^2}{R^6} \right) + \left(\frac{1-m}{4} \right) \left(\frac{1}{r^2} - \frac{1}{R^2} + \frac{4x(x+X)}{R^4} \right) \right] \dots \dots \dots (47)$$

where

$$\left. \begin{aligned} r^2 &= (x-X)^2 + y^2, \\ R^2 &= (x+X)^2 + y^2. \end{aligned} \right\} \dots \dots \dots (48)$$

Load applied Parallel to the Free Edge (see also Ref. 8).—For completeness the stress distribution is given below for the case where the load is applied parallel to the free boundary. The proof is similar in all respects to that given in this appendix.

$$f_{xx} = \frac{Py}{\pi t} \left[\left(\frac{1+m}{2} \right) \left(\frac{(x-X)^2}{r^4} + \frac{x^2-6xX-X^2}{R^4} + \frac{8xXy^2}{R^6} \right) - \left(\frac{1-m}{4} \right) \left(\frac{1}{r^2} - \frac{1}{R^2} - \frac{4x(x+X)}{R^4} \right) \right] \dots \dots \dots (49)$$

$$f_{yy} = \frac{Py}{\pi t} \left[\left(\frac{1+m}{2} \right) \left(\frac{y^2}{r^4} + \frac{y^2+8xX+6X^2}{R^4} + \frac{8xX(x+X)^2}{R^6} \right) + \left(\frac{1-m}{4} \right) \left(\frac{1}{r^2} + \frac{3}{R^2} - \frac{4x(x+X)}{R^4} \right) \right] \dots \dots \dots (50)$$

$$q_{xy} = \frac{P}{\pi t} \left[\left(\frac{1+m}{2} \right) \left(\frac{y^2(x-X)}{r^4} + \frac{(x+X)(2xX+y^2)}{R^4} - \frac{8xXy^2(x+X)}{R^6} \right) + \left(\frac{1-m}{4} \right) \left(\frac{x-X}{r^2} + \frac{3x+X}{R^2} - \frac{4x(x+X)^2}{R^4} \right) \right], \dots \dots \dots (51)$$

where r and R are given by equation (48).

Stringer-sheet Solution.—The fundamental equation may be written in the form

$$\frac{\partial^2 u}{\partial x^2} + \frac{\partial^2 u}{\partial (ky)^2} = 0,$$

where u is the displacement in the x direction and $k^2 = Et_s/Gt$.

Point Load Applied in Infinite Sheet.—There is a direct analogy between the displacement, u , and the potential function, ϕ , which occurs in irrotational flow and which satisfies

$$\frac{\partial^2 \phi}{\partial x_1^2} + \frac{\partial^2 \phi}{\partial y_1^2} = 0.$$

The potential due to a point source is given by

$$\begin{aligned} \phi &\propto \log r_1 \\ &\propto \log (x_1^2 + y_1^2) \end{aligned}$$

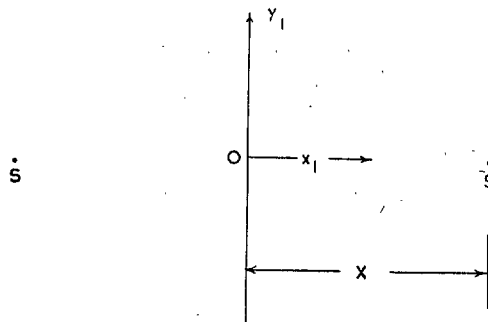
and from the analogy, noting that we can write $x_1 = x$, $y_1 = ky$, we take

$$u = K \log (x^2 + k^2 y^2)$$

as the solution. It can be verified that this equation satisfies the conditions of equilibrium. If the applied load is P , integration of the direct or shear stress along any line gives

$$K = P/4\pi\sqrt{EGt_s}.$$

Point Load applied near Free Edge of Semi-infinite Sheet



DIAG. 10.

This corresponds to two point sources as indicated above, in which case the potential is, by addition

$$\phi \propto \{(x_1 - X)^2 + y_1^2\} + \log \{(x_1 + X)^2 + y_1^2\}$$

and accordingly

$$u = K[\log \{(x - X)^2 + k^2 y^2\} + \log \{(x + X)^2 + k^2 y^2\}]$$

The direct and shear stresses are given by

$$f_{xx} = E \frac{\partial u}{\partial x} \text{ and } q_{xy} = G \frac{\partial u}{\partial y}.$$

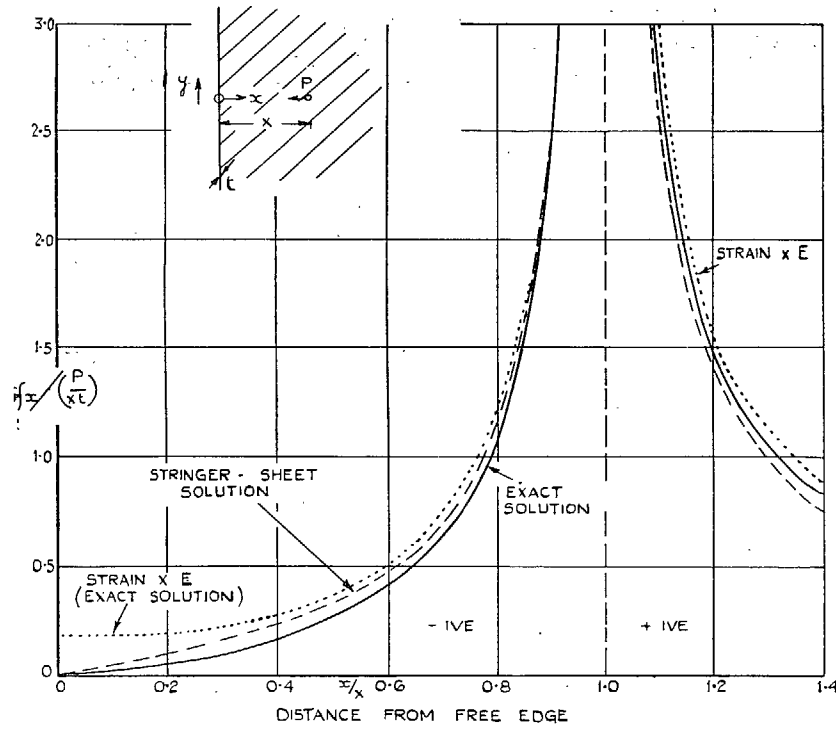


FIG. 1. Direct stresses along line of action of concentrated applied load.

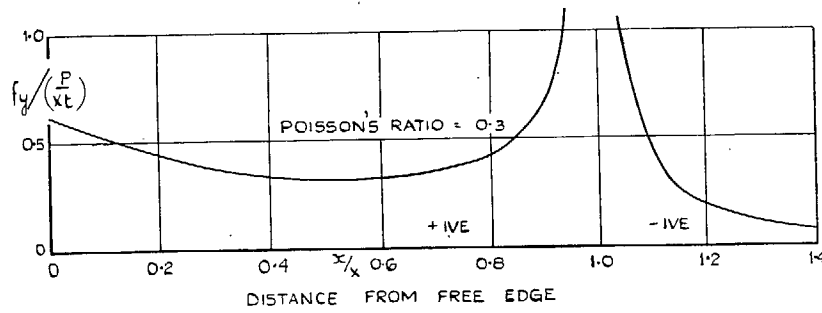


FIG. 2. Transverse stresses along line of action of concentrated applied load.

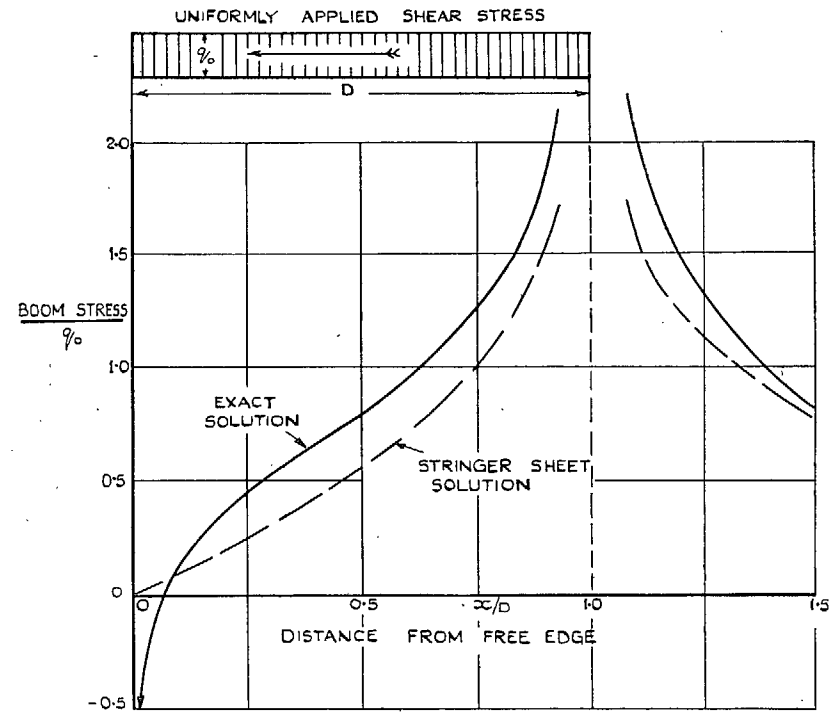


FIG. 3. Direct stress along line of action of uniformly distributed load.

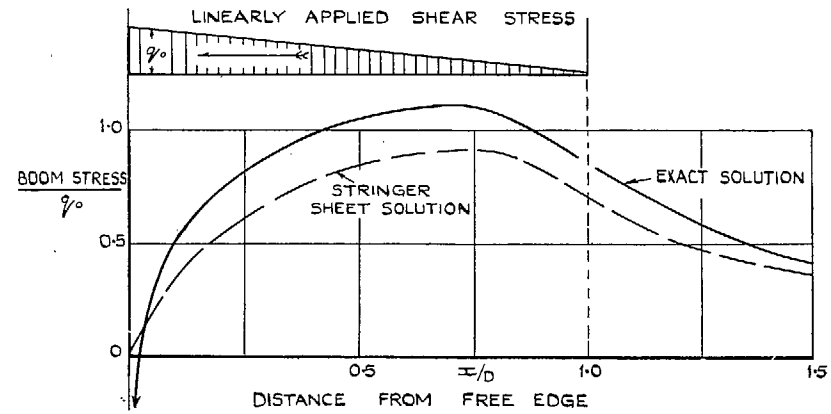


FIG. 4. Direct stress along line of action of linearly distributed load.

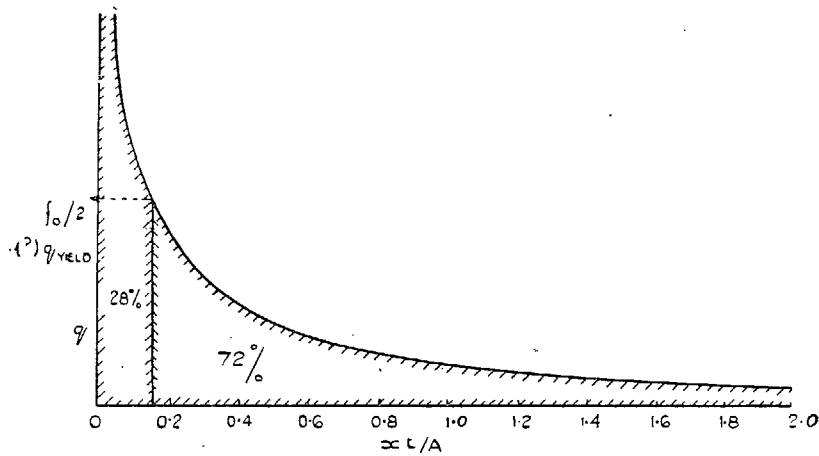


FIG. 6. Curve showing proportion of load taken by shear stresses beyond the elastic limit. (Stringer-sheet theory.)

16

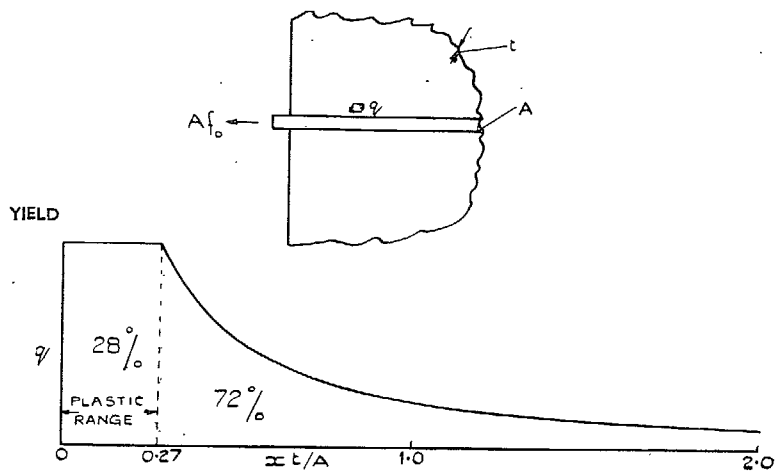


FIG. 7. Modified theoretical curve showing that about 28 per cent of the boom load might be taken by skin in the plastic range which extends about $0.27A/t$ along the boom.

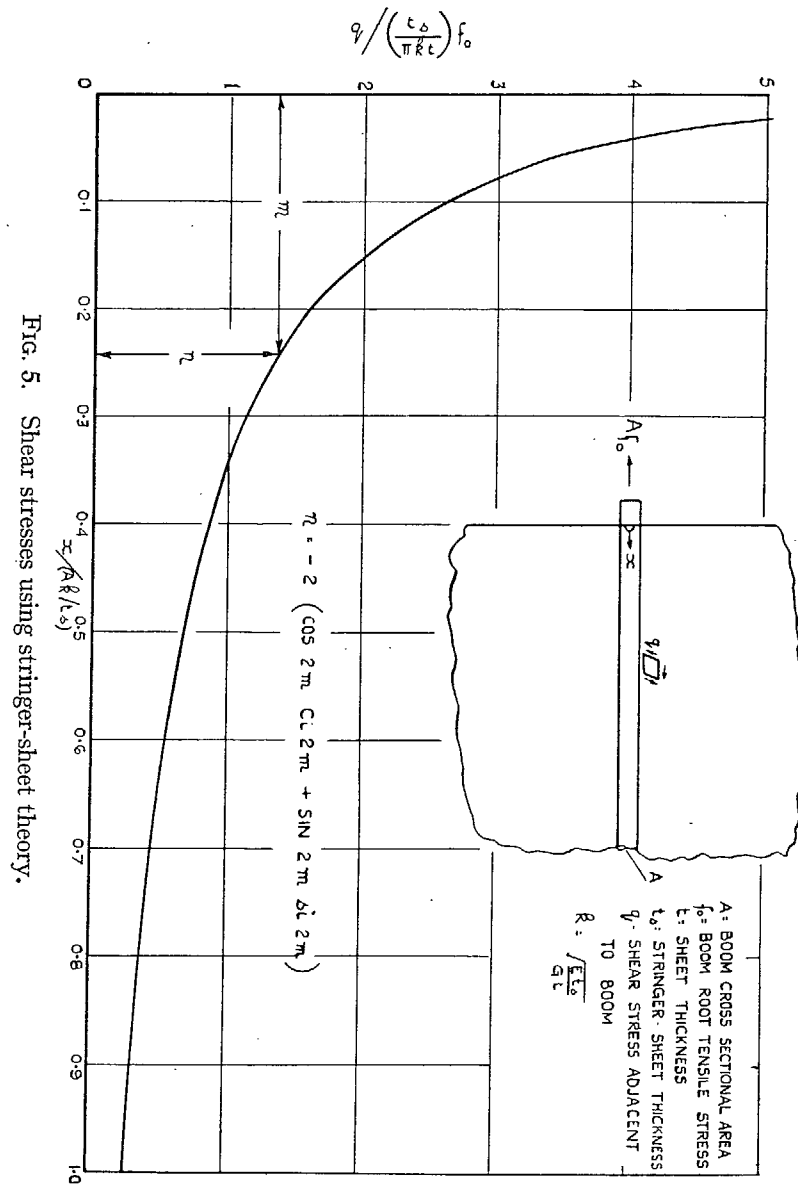
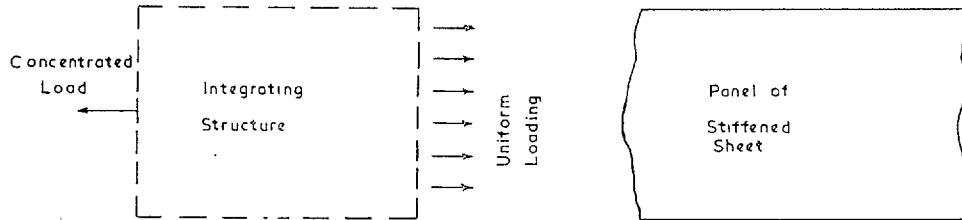


FIG. 5. Shear stresses using stringer-sheet theory.

A: BOOM CROSS SECTIONAL AREA
 f_0 : BOOM ROOT TENSILE STRESS
 l : SHEET THICKNESS
 l_s : STRINGER-SHEET THICKNESS
 q : SHEAR STRESS ADJACENT TO BOOM
 $R = \sqrt{\frac{E I_s}{G t}}$

PART II

6. *Introduction.*—The diffusion of a concentrated load into a stiffened sheet is one of the fundamental problems of design and stress determination in aircraft engineering. Of the many writers^{11 to 17} who have examined this problem, only H. L. Cox¹² has considered it from the standpoint of efficiency. He effected the diffusion by an ‘integrating structure’, the sole function of which was to transform a concentrated load into a uniform loading over a given width of sheet, and he compared the weights of a variety of such structures with the same length of sheet. (See Diag. 11.)

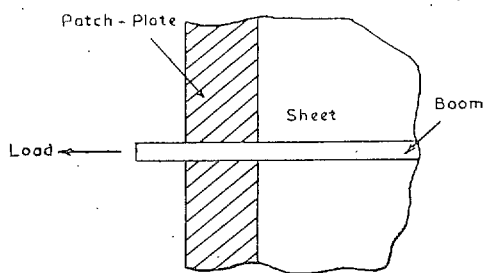


DIAG. 11. Diagrammatic representation of Cox's integrating structure.

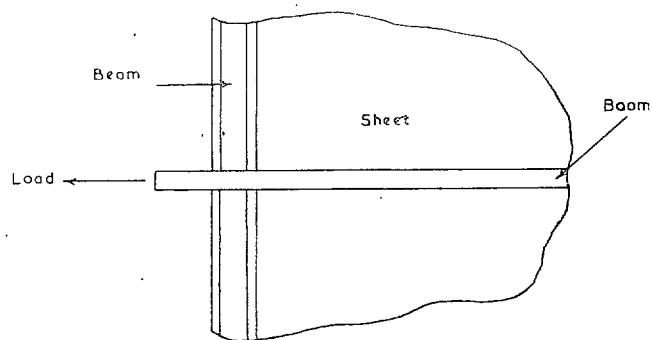
The excess weight of these integrating structures over the weight of the same length of stiffened sheet was very considerable, the main reason lying in the assumption that the sheet was unstressed in shear, that is to say it did not itself contribute to the redistribution of load. The concentrated load is in practice usually applied through a boom which does not terminate at the junction with the sheet (as it did in R. & M. 1780¹²), though its cross-sectional area may decrease as it extends into the sheet because of the load taken by the sheet.

Here we consider the diffusion of load from a continuous boom into a sheet which is capable of taking shear. Unless additional stiffening is present the shear stresses in the sheet are very high in the neighbourhood of the boom and the free edge of the sheet. The additional stiffening commonly employed is either a patch-plate (called here a shear-stiffener) or a flange or beam attached to the free edge of the sheet (called here a bending-stiffener), or both. A shear-stiffener is defined here as a stiffener whose bending flexibility is negligible compared with its shear flexibility (*i.e.*, no deflection due to bending), and a bending-stiffener one whose shear flexibility is negligible compared with its bending flexibility.

These are illustrated in Diags. 12 and 13.



DIAG. 12. Shear-stiffener.



DIAG. 13. Bending-stiffener.

7. *Statement of Problem.*—The diffusion of load is dependent on boom, stiffener, and sheet and the structure must, therefore, be considered as a whole. The present report is concerned with the determination of stresses in such a combination of boom, stiffener and sheet and the design of stiffeners of least weight.

Because of the simplicity of the assumptions the complete stress distribution depends only on a few parameters; for the special cases of constant boom area, which are treated in detail, the distribution depends on two fundamental, non-dimensional parameters. It is, therefore, comparatively easy to plot, or give formulae for, any single function of the stresses (say the peak shear stress in the sheet or the load transferred by the stiffener) over the complete range of possible types of structure.

7.1. *Assumptions.*—The stringer-sheet method^{14,15} is used and the following assumptions are additional to those implicit in this method:—

- (i) The sheet is flat.
- (ii) The shear and bending-stiffeners are attached to the edge of the sheet and are at right angles to the boom and stringers: the bending-stiffener is unbroken by the presence of the boom and each part on either side of the boom may, therefore, be regarded as built-in to the boom.
- (iii) The sheet is infinitely wide and long and the shear and bending-stiffeners infinitely long. It is shown in Appendix II that the results are still useful for sheets with finite dimensions.
- (iv) The stiffeners have constant properties along their length.
- (v) Ordinary bending theory applies to the bending-stiffener, *i.e.*, the bending moment is proportional to the curvature.
- (vi) The shear stress in the shear-stiffener is assumed to be constant over its width. (Separate approximate allowance is made for variations in shear stress over the width whenever it is important.)
- (vii) When both bending and shear deflections of the stiffeners are taken into account the deflections are additive (as in ordinary engineering theory).

8. *No Edge Stiffener; Boom of Varying Cross-section.*—The complete stress distribution in the sheet is determinable if the strain in the boom is known, and it has been shown¹¹ that unless the boom strain is zero at the root the shear stress there will be theoretically infinite. This means that for all booms of finite cross-section the shears become theoretically infinite at the root. However, the effect of rivet flexibility is to make the actual peak shear stress finite and such that it is reduced as the magnitude of the theoretical shear is reduced; a reduction in theoretical shear stress occurs if the boom area is increased, and so an actual reduction will occur also.

It has been considered worthwhile to investigate more fully the effect of varying the boom cross-sectional area in order to get some quantitative values for the stresses with various degrees of allowable rivet slip, and to suggest what increases, if any, should be made to the boom area when other stiffening is present.

It is shown in Part I (section 3.2) that an integral equation exists giving a relation between the boom cross-sectional area and the shear stress adjacent to the boom. This equation may be written in the form

$$2F = \frac{\pi t_s \int_x^\infty q(X) dX}{kx \int_0^\infty \frac{q(X) dX}{x^2 - X^2}} \quad \dots \quad \dots \quad \dots \quad \dots \quad \dots \quad \dots \quad \dots \quad \dots \quad \dots \quad (52)$$

where $q(X)$ is the shear stress at the point $x = X$.

If we prescribe a given form for $q(X)$ the necessary boom area is given immediately by equation (52).

The direct stress along the line of action of the applied load, obtained by putting y zero is

$$f_x = \frac{\delta P}{\pi \lambda t_s} J_b(x_2, X_2)$$

where

$$x_2 = x/k\lambda, \quad X_2 = X/k\lambda$$

and

$$\lambda = (kI/t_s)^{1/3}$$

(68)

$$J_b(x_2, X_2) = \frac{X_2}{x_2^2 - X_2^2} + \int_0^\infty \frac{e^{-(X_2+x_2)\theta}}{1+\theta^3} d\theta$$

from which it follows that the boom area required to give a prescribed shear stress distribution $q(x)$ is

$$2F(x_2) = \frac{\pi \lambda t_s \int_{x_2}^\infty q(X_2) dX_2}{\int_0^\infty q(X_2) J_b(x_2, X_2) dX_2}$$

(69)

This equation is of a more complex character than the corresponding equation (62) for the shear-stiffener case because the function J_b cannot be expressed in terms of known functions. Accordingly we shall confine our attention to the special case of constant boom area.

10.1. *Particular Case: Boom of Constant Cross-section.*—The complete stress distribution for this case is given in Appendix VI. The results are given in the form of definite integrals which are not expressible in simple form. The shear stress distribution adjacent to the boom is of practical importance and these distributions are plotted in Fig. 21 for various values of the non-dimensional parameter η , which is equal to $(kIt_s^2)^{1/3}/F$. It will be noticed that the shear stress is zero at the root and rises to a maximum value and then dies away slowly. From strength considerations the peak values of this shear stress are important and these may be obtained from Fig. 22.

10.1.1. *Example.*—Suppose that this form of stiffening is to be employed and the peak shear stress adjacent to the boom is to be limited to $0.6f_0$. How stiff must the bending-stiffener be?

Suppose the rest of the structure is specified by

$$2F = 8 \text{ in.}^2$$

$$t = 0.05 \text{ in.}$$

$$t_s = 0.08 \text{ in.}$$

$$G/E = 0.4.$$

This means that $\bar{k} = \sqrt{(Gt_s/Et)} = 0.8$.

Therefore, we require an I for the bending-stiffener to give an η corresponding to $q_{\max}/\bar{k}f_0 = 0.6/0.8 = 0.75$; and from Fig. 22 we accordingly take

$$\eta = 0.075$$

$$= (kIt_s^2)^{1/3}/F.$$

This is an equation for I , which may be solved to give

$$I = (0.075F)^3/kt_s^2$$

$$= 2.2 \text{ in.}^4$$

10.1.2. *Loads in the stiffener.*—The greatest bending moment in the stiffener occurs at the root and is given by

$$M_0 = \frac{PF}{t_s} \left[\frac{(2\pi/3\sqrt{3})\eta^2(1+\eta^2) - \frac{1}{2}\pi\eta^3 - \log \eta}{(4\pi/3\sqrt{3})(1-\eta^4)/\eta^2 + \pi\eta^3 + 2\log \eta} \right] \quad \dots \quad (70)$$

which has been plotted in Fig. 23.

In the numerical example considered above, in which the moment of inertia of the bending-stiffener was taken to be 2.2 in.⁴ and $\eta = 0.075$, the maximum bending moment will be $0.012 f_0 F^2/t_s$ from Fig. 23. If we limit the maximum stress in the stiffener to f_0 we can determine the depth of the bending-stiffener from the simple engineering formula. This gives the total depth of stiffening beam

$$\begin{aligned} &= \frac{2It_s}{0.012F^2} \\ &= 1.84 \text{ in.} \end{aligned}$$

The proportion of direct load transferred immediately by the bending-stiffener is a function of η alone,

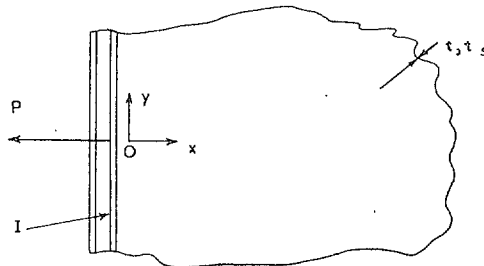
$$\Delta = \frac{\frac{\pi}{2}\eta^3 + \frac{8\pi}{27\eta}(1+\eta^2) - \frac{4\pi}{3\sqrt{3}}\eta^2 + \log \eta - \frac{4(1-\eta^2)}{3\eta\sqrt{3}}\log \eta}{\frac{\pi}{2}\eta^3 + \frac{2\pi(1-\eta^4)}{3\eta^2\sqrt{3}} + \log \eta} \quad \dots \quad (71)$$

which has been plotted in Fig. 24.

In the example considered earlier, in which $\eta = 0.075$, the proportion of load transferred is 0.17 and this means that the direct stress in the boom at the root, but on the sheet side of the stiffener, will be $(1 - 0.17)f_0 = 0.83f_0$.

We have previously implied that the boom cross-sectional area was the same on either side of the bending-stiffener, but, without changing the analysis given here, we can increase the efficiency of this form of load-diffusion by altering the boom areas on either side of the bending-stiffener in the ratio $1:(1 - \Delta)$. This would make the direct stresses on each side of the stiffener the same. A similar scheme could have been employed for the shear stiffener.

10.2. *Particular Case: No Boom.*—



DIAG. 17. Diagram showing notation.

This case may be regarded as a limiting case of that discussed in section 10, as X tends to zero, or as that discussed in section 10.1 as F tends to zero. The structure is of interest in that it can be compared with one discussed by Cox¹² in which it was stipulated that the sheet should be unstressed in shear, a somewhat drastic requirement which led that author to the conclusion that a bending-stiffener was not an efficient form of load distributor.

The stress distribution is readily found from Appendix IV by putting X zero. The stresses are obtained in the form of definite integrals which are not expressible in terms of known functions.

The direct stress along the line of action of the applied load is shown in Fig. 27, and the shear stress adjacent to the bending stiffener is shown in Fig. 28.

The maximum shear stress, occurring adjacent to the stiffener, is

$$q_{\max} = \frac{0.21\bar{k}P}{(\bar{k}It_s^2)^{1/3}} \dots \dots \dots (72)$$

and the maximum direct stress in the sheet, which occurs at the root, is

$$f_{\max} = \frac{0.385P}{(\bar{k}It_s^2)^{1/3}} \dots \dots \dots (73)$$

As \bar{k} is usually less than unity the sheet would, therefore, be expected to fail first in tension at the root.

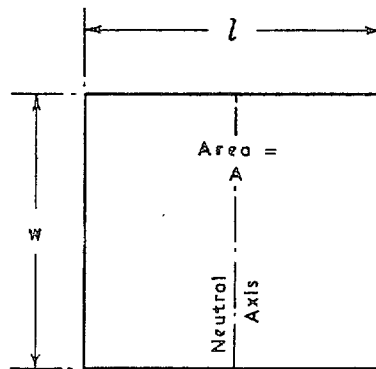
The greatest bending moment in the stiffener occurs at the root and is given by

$$M_0 = \left(\frac{2}{3\sqrt{3}}\right) P \left(\frac{kI}{t_s}\right)^{1/3} \dots \dots \dots (74)$$

If we assume that the bending-stiffener is symmetrical about its own bending axis we can calculate the overall depth of the stiffener to ensure that the maximum stress in the stiffener will not exceed a prescribed amount. A reasonable value for this maximum stress will be that given by equation (73), since this makes sheet and stiffener equally strong. Such a scheme gives a total depth of bending-stiffener of

$$2 \left(\frac{I}{\bar{k}t_s}\right)^{1/3} \dots \dots \dots (75)$$

If we limit our choice of stiffener to one of rectangular section such as shown in Diag. 18, we can obtain a relation



DIAG. 18.—Section of bending-stiffener.

between l and w (or between l and A , etc.), which is equivalent to equation (75). With the notation of Diag. 18 we have

$$l = \frac{2A}{3\bar{k}t_s} \dots \dots \dots (76)$$

and equation (73) now becomes:

$$f_{\max} = 1.16\bar{k}P/A \dots \dots \dots (77)$$

We shall defer this question of design of stiffeners until the next section where both bending and shear stiffnesses of the stiffeners are taken into account.

11. *Shear and Bending Stiffener: Boom on Constant Cross-section.*—The treatment given in sections 9.1 and 10.1 has been necessarily only approximate, because in considering the shear-stiffener we ignored its bending flexibility and in considering the bending-stiffener we ignored its

shear flexibility. These two cases may be regarded as upper and lower limits of the type of structure likely to occur in practice. To fix ideas let us consider a stiffener of rectangular cross-section, like that in Diag. 18. The shear stiffness of this section is proportional to the area (*i.e.*, to wl) and the bending stiffness is proportional to wl^3 . If, therefore, we let l become large, keeping wl unchanged, we have a shear-stiffener, since the stiffener has finite shear stiffness and infinite bending stiffness; and if we let l become very small, keeping wl^3 unchanged, we have a bending-stiffener, since the stiffener has finite bending stiffness and infinite shear stiffness (as the shear stiffness is now inversely proportional to l^2).

In considering the detailed design of such a stiffener it is clearly necessary to take account of both the bending and the shear stiffnesses of the stiffener, and this has been done here. From the analysis given in Appendix VI it appears that the complete stress distribution depends primarily on the two non-dimensional parameters η and ζ .

The shear stress in the stiffener at the root, which is also the shear stress in the sheet at the root, has been plotted in Fig. 29. The practical ranges of η and ζ have been covered.

The proportion of load transferred to the sheet by the stiffener is shown in Fig. 30.

The bending moment in the stiffener at the root is also a function of η and ζ alone and has been plotted in Fig. 31. The lines $\zeta = \infty$ shown in Figs. 30 and 31 correspond to the bending-stiffener case considered in section 10.1.

11.1. *Shear Stresses Adjacent to the Boom.*—The strength of a load diffusion structure, such as that considered here, depends usually on the shearing strength of the sheet and rivets adjacent to the boom. The maximum value of this shear stress is therefore of practical importance. Moreover, as we are interested in the design of a stiffener of least weight, it is reasonable to consider a series of stiffeners of equal weight (*i.e.*, equal cross-sectional area) but with differing shear and bending properties. If we now find that the peak shear stress in the sheet has a minimum value for a particular set of stiffnesses, then we can conclude that the stiffener material has then been used to the best advantage*.

The simplest shape of stiffener to consider is that of rectangular cross-section, and the weight of such a stiffener varies as the cross-sectional area—as does the shear stiffness. This means that ‘equal weight’ is the same as ‘equal shear stiffness’, and this in turn means that we can consider a series of stiffeners with varying η but constant ζ .

There is, of course, an infinite number of possible shapes from which to choose, but for purposes of analysis it is convenient to regard all those in which the sectional area is in a fixed proportion to the shear stiffness as belonging to one group in which ζ will be constant. This means, for example, that all I-beams for which the ratio of flange area to web area is constant belong to one particular group.

The shear stress adjacent to the boom has been plotted in Fig. 32 for a number of values of η keeping ζ constant. The value of ζ , 0.3, is typical of current practice.

Over the upper range of η , that is to say $\eta > 0.247$, the stiffener may be said to behave like a shear-stiffener in that the shear stress in the sheet adjacent to the boom has a peak value at the root and decreases steadily along the boom. This peak value is also the shear stress in the stiffener and, as ζ is constant, this will be proportional to the direct load transferred by the stiffener, which clearly becomes less if η becomes less. This accounts for the drop in the peak shear stress as η drops to 0.247. It will be further noticed that the two curves for values of $\eta = 0.247$ and $\eta = \infty$, cross each other some distance along the boom, since the higher the root shear stress the lower is the proportion of load to be transferred by the shear stress along the boom.

* Subject, of course, to the assumptions made which may restrict our scope of design somewhat: the most serious of these restrictions is probably that of constant stiffener properties along its length.

- The range from $\eta = 0.247$ to $\eta \approx 0.1$ must be regarded as a transition from a predominantly shear- to a predominantly bending-stiffener. For all values of η less than 0.247 the shear stress increases in magnitude along the boom to a maximum value and then decreases steadily. As η decreases from 0.247 to about 0.15 these maximum values decrease steadily to a minimum. From $\eta = 0.15$ to $\eta = 0$ these maximum values increase steadily in magnitude.

It is possible to plot the peak (or maximum) values of the shear stress as η varies. This has been done in Fig. 33 for these values of ζ : 0.2, 0.3 and 0.5. An efficiently designed structure would have values of η and ζ lying close to the broken line of Fig. 33 which is drawn through the minimum values of peak shear stress.

These curves of peak shear stress plotted against η are of considerable interest and one such curve ($\zeta = 0.3$) has been re-plotted in Fig. 34 to show how the curve is composed of two distinct analytic parts, and to show the asymptotes.

11.2. *Effect of Variation of Shear Stress across Width of Stiffener.*—We have hitherto assumed that the shear stress was constant across the width of the stiffener. This is approximately true for the bending-stiffener as the width will usually be comparatively small, but for the predominantly shear type of stiffener there will be an appreciable variation in shear stress across the stiffener. And in the limiting case in which the shear-stiffener has become very wide, and can be regarded as merely a slight thickening of the sheet, the structure degenerates into the no-stiffener class.

Any attempt to estimate accurately the increase in the peak shear stress due to the variation in shear across the stiffener width demands a knowledge of the dimensions of the stiffener flanges (from the point of view of local bending) and the method of attachment of the stiffener and sheet to the boom.

In Figs. 35, 36 and 37 the broken curves of constant ζ show the theoretical variation of the peak shear stress as the width of stiffener varies. Each figure applies to one particular value of n ($n = \text{total flange area of stiffener}/\text{total web area of stiffener}$), and these figures are accordingly on a strictly equal weight basis. The full lines are attempts to include the effect of shear variation across the stiffener width, which makes the minima of these curves more pronounced.

The connection between these curves of constant n , in which the variable is the width of the stiffener (l), and the fundamental curves of Fig. 33 in which the variable was η may be expressed as follows:

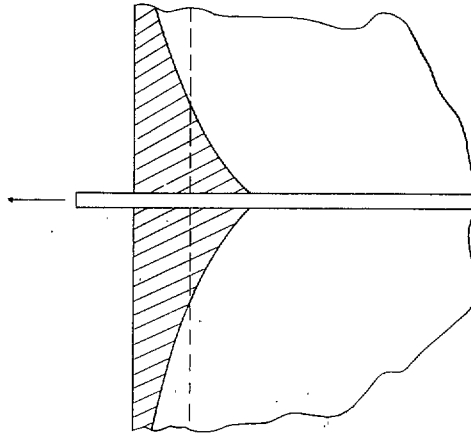
$$l \div \left(\frac{F}{t_s} \sqrt{\frac{G}{E}} \right) = \left(\frac{12\eta^3}{(3n+1)\zeta} \right)^{1/2} \cdot \dots \dots \dots \dots \dots \dots (78)$$

In Fig. 38, a curve of peak shear stress plotted against n is drawn where the stiffener weight is kept constant and the stiffener width is at its optimum. It will be seen that the peak shear stress is lowest when n is zero, though in practice the peak shear stress does not increase greatly with n if n is small.

The optimum width of stiffener has been plotted in Fig. 39 with n as the variable. The curve is practically independent of the stiffener section area.

11.3. *Final Remarks.*—In the discussion of section 11 it was shown that if we limit our choice of stiffener to one with constant lengthwise properties we find that there is an optimum shape for this stiffener. It is not intended that a designer should handicap himself by such a restriction but rather that the theoretical results presented here should provide a sound basis for design.

In the accompanying diagram the shaded area represents an intelligently designed stiffener based on the theoretical results shown by the broken line.



DIAG. 19.

12. *Conclusions.*—A theoretical investigation has been made of ways in which a sheet can be relieved of the high stresses which occur near the free edge of the sheet and adjacent to a direct load carrying boom attached to the sheet.

The following conclusions of practical importance are drawn.

If no stiffening of the sheet is present :

- (i) The shear stresses may be reduced by reducing the boom strain in the neighbourhood of the root : for booms of equal weight/strength properties the most efficient is one whose Young's-modulus/weight ratio is the highest.
- (ii) A boom designed to give a flat shear stress distribution is lighter than one designed to give an exponential shear-stress distribution.
- (iii) A line of rivets attaching sheet to boom will not appreciably relieve the shear stresses in the sheet if the rivet slip factor is constant along the line : the shear stresses at the root will be reduced if the rivets are very flexible at the root and have graded flexibilities down to zero a short distance from the root ; rivet flexibility some distance from the root will increase the shear stress at the root.

If there is a stiffener attached to the free edge of the sheet and the boom area is constant :

- (iv) For a given weight of stiffener material there exists a particular shape of stiffener which gives the lowest peak stresses in the sheet.
- (v) This optimum shape of stiffener is such that the stiffener acts as a bending-stiffener rather than a shear-stiffener ; the section area of this stiffener (assumed to be unaltered along its length) is about 20 per cent of the total boom area, and is in the form of a deep beam with small flanges, if any.

Acknowledgement.—The author is indebted to Miss G. M. Chitty for her help with the computation.

LIST OF SYMBOLS

Structure Properties:

$2F$	Main boom area
t	Thickness of sheet
t_s	Stringer-sheet thickness (total equivalent thickness capable of taking direct load)
R	Section area of stiffener resisting shear
I	Moment of inertia of stiffener
l	Width of stiffener in direction of main boom
w	Thickness of stiffener of rectangular cross-section
$A = wl$	
E, G	Elastic moduli
ε	Maximum allowable rivet slip

Parameters:

$\lambda = (kI/t_s)^{1/3}$	
n	Ratio of total flange area of stiffener/total web area of stiffener
$k = (Et_s/Gt)^{1/2}$	} non-dimensional parameters
$\bar{k} = (Gt_s/Et)^{1/2}$	
$\zeta = \bar{k}R/F$	
$\eta = (kIt_s^2)^{1/3}/F$	

Scales:

Ox, Oy	Co-ordinate axes such that Ox lies along main boom
X	Distance of concentrated applied load from free edge ; a 'travelling' value of x
$x_1, X_1 = xt/R, Xt/R$	
$y_1 = ykt/R$	
$x_2, X_2 = x/k\lambda, X/k\lambda$	
$y_2 = y/\lambda$	
$x' = xt_s/kF$	
$y' = yt_s/F$	

Stresses and Loads:

P	Applied load
f_{xx}	General expression for direct stress in sheet
q_{xy}	General expression for shear stress in sheet
f_{\max}, q_{\max}	Maximum values of these stresses
q, q'	Shear stress adjacent to boom
q_{m-a}	Maximum allowable value of q

LIST OF SYMBOLS—*continued*

f	Direct stress in boom
f_0	Root boom stress= $P/2F$
f_0^+	Direct stress in main boom at root on sheet side of stiffener
Δ	Proportion of direct load transferred immediately by stiffener
M_0	Bending moment in stiffener at root
α, α'	Arbitrary constants

Functions:

J_s	Defined in equation (61)
J_b	Defined in equation (68)
Ei x , si x , Ci x	Exponentials, sine and cosine integrals and are defined as follows ¹⁸ :

$$\text{Ei } x = \int_{\infty}^{-x} \frac{e^{-\theta}}{\theta} d\theta$$

$$\text{si } x = \int_{\infty}^x \frac{\sin \theta}{\theta} d\theta$$

$$\text{Ci } x = \int_{\infty}^x \frac{\cos \theta}{\theta} d\theta$$

Additional Symbols used only in the Appendices:

u	Displacement in the x -direction		
$\bar{u}, \bar{f}_{xx}, \bar{q}_{xy}$	Values of these functions when no stiffener is present		
		<i>First introduced in:</i>	
$u_r, u_s, u_b,$ equation (131)	
r	} Independent variables	} equations (83), (94)	
ϱ			equation (91)
ϕ			equation (101)
θ			equations (106), (130)
$R(r)$ equation (83)	
$R'(r)$ equation (94)	
$\phi_1(\theta)$ equation (106)	
$\phi_2(\theta)$ equation (106)	
$\phi(\theta)$ equations (114), (130)	
Z equations (119), (139)	
C	} Constants of integration	} equations (120), (140)	
C_n			equation (143)
C_{-1}			equation (146)
C_0			equation (146) } <i>et supra</i>
T, U, V, W equation (147)	
N equation (148)	

REFERENCES

<i>No.</i>	<i>Author</i>	<i>Title, etc.</i>
11	E. H. Mansfield	The Diffusion of Load into a Semi-infinite Sheet. Part I. November 1947. A.R.C. Report 11,268, Part I of this report.
12	H. L. Cox, H. E. Smith and C. G. Conway.	Diffusion of Concentrated Loads into Monocoque Structures. R. & M. 1780. April, 1937.
13	W. J. Duncan	Diffusion of Load in Certain Sheet-stringer Combinations. R. & M. 1825. January, 1938.
14	D. Williams, R. D. Starkey and R. H. R. H. Taylor.	Distribution of Stress between Spar Flanges and Stringers for a Wing under Distributed Loading. R. & M. 2098. January, 1939.
15	E. H. Mansfield	The Effect of Spanwise Rib-Boom Stiffness on the Stress Distribution near a Wing Cut-out. R. & M. No. 2663. December, 1947.
16	M. Fine and H. G. Hopkins	Stress Diffusion Adjacent to Gaps in the Interspar Skin of a Stressed Skin Wing. R. & M. 2618. May, 1942.
17	J. Hadji-Argyris	Diffusion of Symmetrical Loads into Stiffened Parallel Panels with Constant Area Edge Members. R. & M. 2038. 1944.
18	Jahnke and Emde	<i>Table of Functions</i>

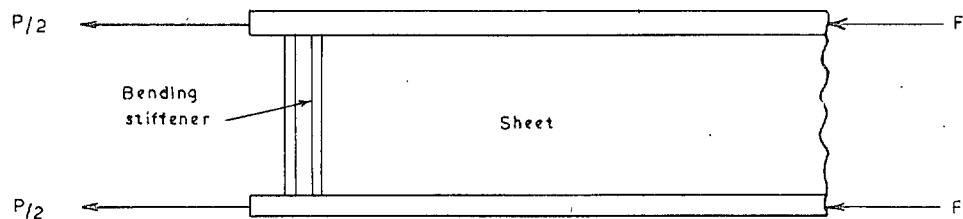
and see page at end of Part I.

APPENDIX II

Justification for assuming that the Stress System has a localised character

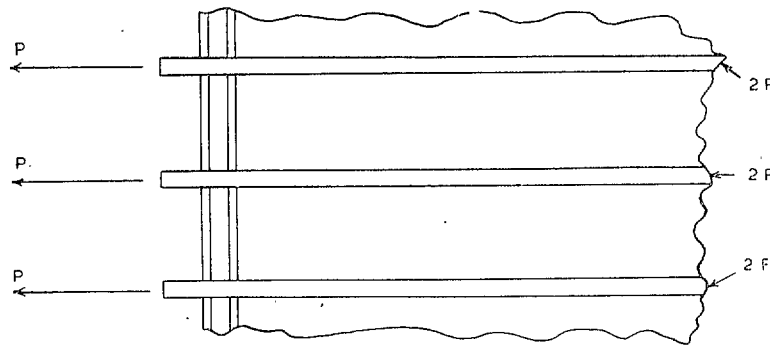
Comparison with Panels of Finite Width.—The high stresses which occur in the unstiffened sheet near the boom-sheet junction are localised and are not appreciably affected either by the presence of further booms attached to the sheet or by changes in the width of the sheet. The presence of stiffening elements lowers these high stresses but also lowers their rates of die-away, though neither change is so great that the stresses are seriously affected by the presence of nearby booms, etc. This means that for the purpose of calculation a sheet of finite width and length can be regarded as semi-infinite.

Justification of a quantitative kind is given here for this assumption. We shall compare the bending moment in the bending-stiffener and the proportion of direct load transferred by the bending-stiffener for the infinitely wide sheet and for panels of finite width. These latter values are taken from R. & M. 2665¹⁵, where the general arrangement was as in Diag. 20.



DIAG. 20.

The stress distribution in such a system is identical with that of Diag. 21, where the sheet is infinitely wide and there are infinitely many booms attached to it.



DIAG. 21. Multi-boom structure.

The discrepancies which exist in the values of maximum bending moment and proportion of load transferred by bending-stiffener in the two cases of 'single-boom' structure (as represented by the simplified structure considered in this report) and the 'multi-boom' structure (as represented by Diag. 21) may be regarded as due to the relieving effects of the loads in all the booms on either side of the one under consideration. The greatest relief is, of course, afforded by the two booms immediately adjacent to the one under consideration.

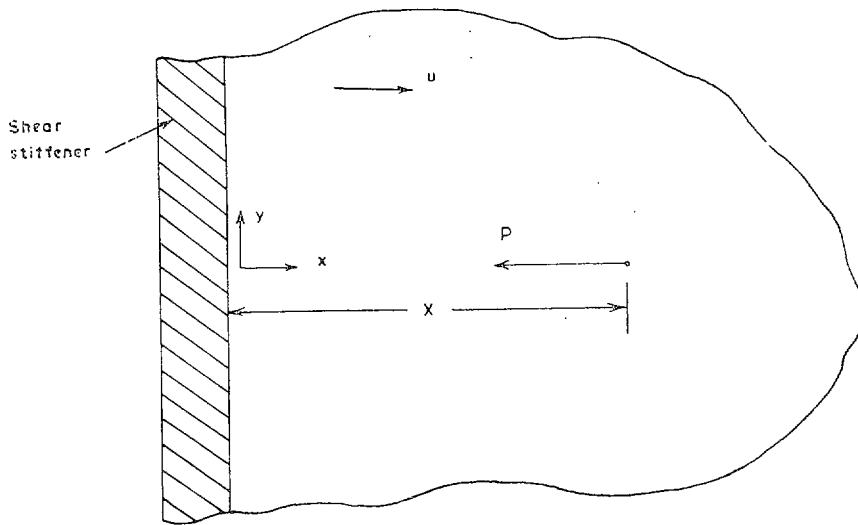
The results of this comparison are shown graphically in Figs. 25 and 26, where a panel width parameter has been introduced. The discrepancy in both cases is of the order of 5 to 10 per cent for most practical cases, and it is unlikely to exceed 20 per cent. These facts are regarded as sufficient justification for assuming that the stress system has a localised character.

A further comparison can be made by comparing the maximum shear stress adjacent to the boom. We should expect these to be more widely differing because the peaks occur some way from the root section where the presence of adjacent booms would naturally have a greater effect on the 'local' stress pattern.

For the numerical example considered in section 10.1.1 the peak shear stress was $0.6f_0$ whereas for a panel of width 100 in. the peak is $0.51f_0$.

APPENDIX III

Point load in semi-infinite sheet with shear-stiffener



DIAG. 22. Diagram showing notation.

When there is no stiffener the displacement u in the x -direction is given by¹¹

$$u = \frac{P}{4\pi \sqrt{(EGtt_s)}} \log \{(x - X)^2 + k^2y^2\} \{(x + X)^2 + k^2y^2\} \quad \dots \quad (79)$$

$\equiv \bar{u}$, say,

and the corresponding direct and shear stresses in the sheet are

$$\bar{f}_{xx} = \frac{kP}{\pi t_s} \cdot \frac{x(x^2 + k^2y^2 - X^2)}{\{(x + X)^2 + k^2y^2\} \{(x - X)^2 + k^2y^2\}} \quad \dots \quad (81)$$

and

$$\bar{q}_{xy} = \frac{kP}{\pi t} \cdot \frac{y(x^2 + k^2y^2 + X^2)}{\{(x + X)^2 + k^2y^2\} \{(x - X)^2 + k^2y^2\}} \quad \dots \quad (82)$$

In considering the problem when the stiffener is present it is convenient to search for a solution in the form

$$u = \bar{u} + \int_0^\infty R(r) e^{-rx/k} \cos ry \cdot dr, \quad \dots \quad (83)$$

which can be differentiated once with respect to x and once with respect to y .

Equation (83) satisfies the stringer-sheet equation

$$\frac{\partial^2 u}{\partial x^2} + \frac{1}{k^2} \frac{\partial^2 u}{\partial y^2} = 0, \quad \dots \quad (84)$$

the equilibrium condition obtained by integrating along any closed contour round the applied load P (since the \bar{u} term accounts for this and the other term contributes nothing) and the condition that $u(y) = u(-y)$; and the equilibrium of the shear stiffener will now be considered.

Differentiating equation (83) with respect to x and multiplying by E gives the stress in the x -direction:

$$f_{xx} = \bar{f}_{xx} - \frac{E}{\bar{k}} \int_0^\infty rR(r) e^{-rx/\bar{k}} \cos ry \cdot dr \quad \dots \quad \dots \quad \dots \quad \dots \quad (85)$$

$$= -\frac{E}{\bar{k}} \int_0^\infty rR(r) \cos ry \cdot dr \text{ along } x = 0 \quad \dots \quad \dots \quad \dots \quad \dots \quad (86)$$

But the direct load per unit length, $t_s f_{xx}$ is also given by

$$- GR \left(\frac{\partial^2 u}{\partial y^2} \right)_{x=0} \quad \dots \quad \dots \quad \dots \quad \dots \quad \dots \quad \dots \quad (87)$$

from considerations of equilibrium of the shear stiffener.

Multiplying equation (86) by t_s and equating to (87) gives, on integrating with respect to y :

$$\begin{aligned} -RG \left(\frac{\partial u}{\partial y} \right)_{x=0} &= -\frac{Et_s}{\bar{k}} \int_0^\infty R(r) \sin ry \cdot dr \\ &= \frac{-PR}{\pi kt} \left(\frac{y}{(X/\bar{k})^2 + y^2} \right) + GR \int_0^\infty rR(r) \sin ry \cdot dr \quad \dots \quad \dots \quad \dots \quad (88) \end{aligned}$$

Equation (88) is true for all values of y and $R(r)$ is therefore determinable. We observe that*

$$\frac{y}{(X/\bar{k})^2 + y^2} = \int_0^\infty e^{-rx/\bar{k}} \sin ry \cdot dr \quad \dots \quad \dots \quad \dots \quad \dots \quad \dots \quad \dots \quad (89)$$

and $R(r)$ is accordingly given by

$$R(r) = \frac{PR}{\pi Et_s} \left\{ \frac{e^{-rX/\bar{k}}}{1 + \left(\frac{\bar{k}R}{t_s} \right) r} \right\} \quad \dots \quad \dots \quad \dots \quad \dots \quad \dots \quad (90)$$

If we write

$$\left. \begin{aligned} \varrho &= r\bar{k}R/t_s \\ X_1 &= Xt/R \\ x_1 &= xt/R \\ y_1 &= ykt/R \end{aligned} \right\} \text{(non-dimensional)} \quad \dots \quad \dots \quad \dots \quad \dots \quad \dots \quad (91)$$

the expressions for the stresses become,

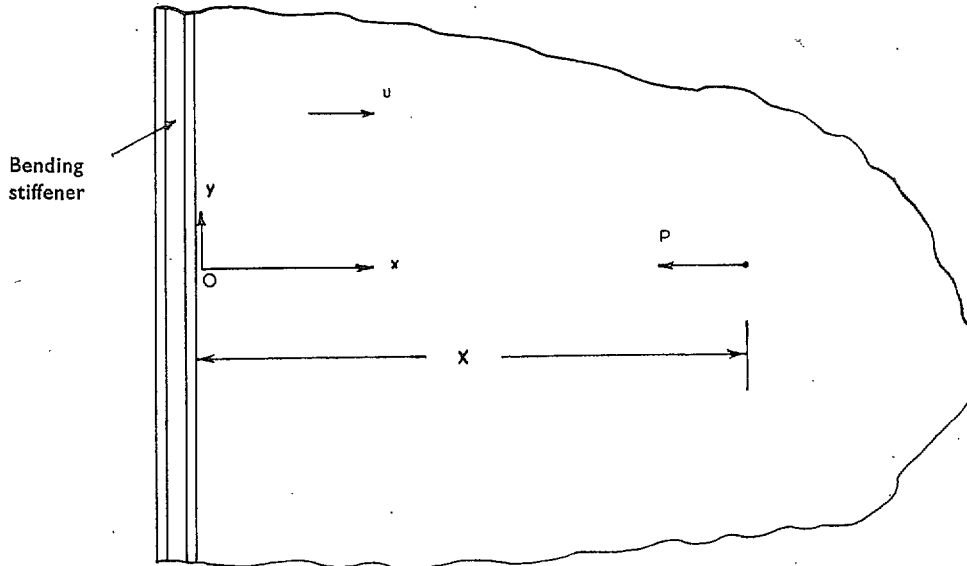
$$f_{xx} = \bar{f}_{xx} - \frac{P}{\pi \bar{k}R} \int_0^\infty \frac{\varrho e^{-\varrho(x_1+X_1)} \cos \varrho y_1}{1 + \varrho} d\varrho \quad \dots \quad \dots \quad \dots \quad \dots \quad \dots \quad (92)$$

$$q_{xy} = \bar{q}_{xy} - \frac{P}{\pi R} \int_0^\infty \frac{\varrho e^{-\varrho(x_1+X_1)} \sin \varrho y_1}{1 + \varrho} d\varrho \quad \dots \quad \dots \quad \dots \quad \dots \quad \dots \quad (93)$$

* See, for example, Copson's *Functions of a Complex Variable*. Page 130. 1944.

APPENDIX IV

Point load in semi-infinite sheet with bending-stiffener



DIAG. 23. Diagram showing notation.

Once again we search for a solution in the form

$$u = \bar{u} + \int_0^\infty R'(r) e^{-rx/k} \cos ry \cdot dr, \quad \dots \dots \dots (94)$$

where the barred term represents the displacement when there is no stiffener.

Along $x = 0$ the direct and shear stresses are given by

$$E \left(\frac{\partial u}{\partial x} \right)_{x=0} = - \frac{E}{k} \int_0^\infty r R'(r) \cos ry \cdot dr \quad \dots \dots \dots (95)$$

$$G \left(\frac{\partial u}{\partial y} \right)_{x=0} = \frac{P}{\pi k t} \left(\frac{y}{(X/k)^2 + y^2} \right) - G \int_0^\infty r R'(r) \sin ry \cdot dr. \quad \dots \dots \dots (96)$$

Considering the equilibrium of the bending-stiffener we therefore have

$$\begin{aligned} \left(\frac{\partial^4 u}{\partial y^4} \right)_{x=0} &= \frac{t_s}{I} \left(\frac{\partial u}{\partial x} \right)_{x=0} \\ &= \frac{-t_s}{kI} \int_0^\infty r R'(r) \cos ry \cdot dr. \quad \dots \dots \dots (97) \end{aligned}$$

Integrating equation (97) three times with respect to y gives

$$\left(\frac{\partial u}{\partial y} \right)_{x=0} = \frac{t_s}{kI} \int_0^\infty \frac{R'(r)}{r^2} \sin ry \cdot dr + \text{terms which are zero by virtue of the fact that } \frac{\partial u}{\partial y}$$

is zero for large values of y . \dots \dots \dots (98)

This expression for the slope of the bending-stiffener may be compared with that given by equation (96), i.e.,

$$\frac{P}{\pi k t G} \left(\frac{y}{(X/k)^2 + y^2} \right) = \int_0^\infty r R'(r) \left(1 + \frac{t_s}{kI r^3} \right) \sin ry \cdot dr. \quad \dots \dots \dots (99)$$

The function of y in the brackets in equation (99) may be expressed in the form of a Fourier sine integral and we have:

$$\frac{y}{(X/k)^2 + y^2} = \int_0^\infty e^{-rX/k} \sin ry \cdot dr \quad \dots \quad (89 \text{ bis})$$

Equations (99) and (89 bis) determine $R'(r)$:

$$R'(r) = \frac{PI}{\pi G t_s} \left(\frac{r^2 e^{-rX/k}}{1 + (kI/t_s)r^3} \right) \quad \dots \quad (100)$$

If we write

$$\lambda = \left(\frac{kI}{t_s} \right)^{1/3} \quad \dots \quad (101)$$

and

$$\phi = r\lambda \quad (\text{non-dimensional}) \quad \dots$$

and

$$\left. \begin{aligned} X_2 &= X/k\lambda \quad (\text{non-dimensional}) \quad \dots \\ x_2 &= x/k\lambda \quad (\text{non-dimensional}) \quad \dots \\ y_2 &= y/\lambda \quad (\text{non-dimensional}) \quad \dots \end{aligned} \right\} (102)$$

we can now write

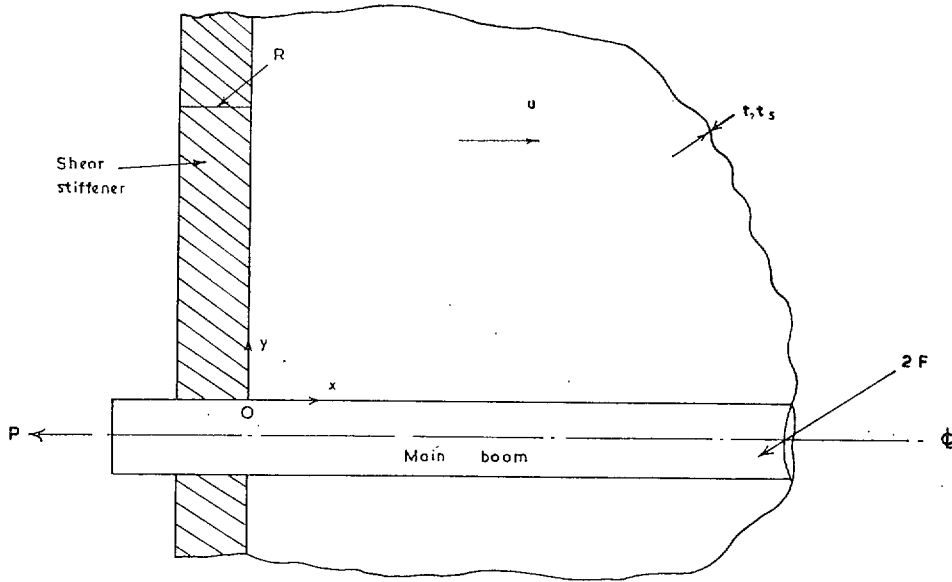
$$u = \bar{u} + \frac{P}{\pi k t G} \int_0^\infty \left(\frac{\phi^2}{1 + \phi^3} \right) e^{-(X_2+x_2)\phi} \cos y_2\phi \cdot d\phi \quad \dots \quad (103)$$

$$f_{xx} = \bar{f}_{xx} - \frac{P}{\pi} (kI t_s^2)^{-1/3} \int_0^\infty \left(\frac{\phi^3}{1 + \phi^3} \right) e^{-(X_2+x_2)\phi} \cos y_2\phi \cdot d\phi \quad \dots \quad (104)$$

$$q_{xy} = \bar{q}_{xy} - \frac{P}{\pi k t \lambda} \int_0^\infty \left(\frac{\phi^3}{1 + \phi^3} \right) e^{-(X_2+x_2)\phi} \sin y_2\phi \cdot d\phi \quad \dots \quad (105)$$

APPENDIX V

Constant area boom and shear-stiffener



DIAG. 24. Diagram showing notation.

We consider that part of the structure for which y is positive and search for a solution in the form

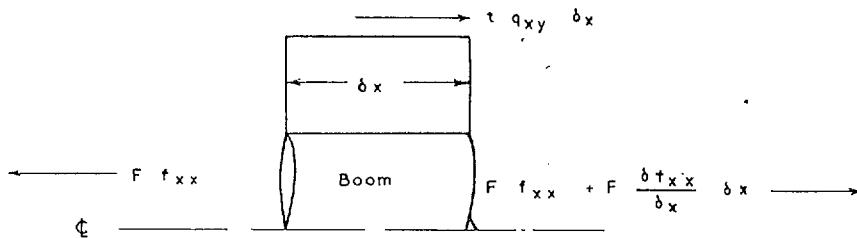
$$u = \int_0^{\infty} [\phi_1(\theta) \cos \theta y + \phi_2(\theta) \sin \theta y] e^{-\theta x/k} d\theta \quad \dots \quad (106)$$

which satisfies the stringer-sheet equation

$$\frac{\partial^2 u}{\partial x^2} + \frac{1}{k^2} \frac{\partial^2 u}{\partial y^2} = 0, \quad \dots \quad (107)$$

and which diminishes steadily as x and y increase. A relationship between ϕ_1 and ϕ_2 will now be obtained which satisfies the conditions along the boom-to-sheet connection ($y = 0$).

Consider the equilibrium of an element of skin adjacent to the boom, as in the diagram below.



DIAG. 25.

We see that for equilibrium

$$t q_{xy} + F \frac{\partial f_{xx}}{\partial x} = 0 \quad \dots \quad (108)$$

i.e.,

$$Gt \frac{\partial u}{\partial y} + EF \frac{\partial^2 u}{\partial x^2} = 0 \quad \dots \quad (109)$$

Substituting from equation (106) and observing that expressions for all the derivatives of u exist provided $x > 0$, we find that

$$Gt \int_0^{\infty} \theta \phi_2(\theta) e^{-\theta x/k} d\theta + \frac{EF}{k^2} \int_0^{\infty} \theta^2 \phi_1(\theta) e^{-\theta x/k} d\theta = 0 \quad \dots \dots \dots (110)$$

for all values of x .

Dropping the integration signs, and using the fact that $k^2 = Et_s/Gt$, gives a relation between $\phi_2(\theta)$ and $\phi_1(\theta)$:

$$\phi_2(\theta) = -\frac{\theta F}{t_s} \phi_1(\theta) \quad \dots \dots \dots (111)$$

Equation (106) can now be written in the form

$$u = \int_0^{\infty} \left(\cos \theta y - \frac{\theta F}{t_s} \sin \theta y \right) e^{-\theta x/k} \phi_1(\theta) d\theta, \quad \dots \dots \dots (112)$$

which may be further simplified by putting

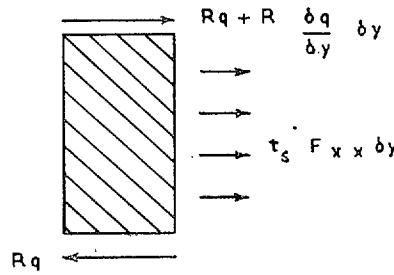
$$\left. \begin{aligned} \theta F/t_s &= \theta \\ y' &= y t_s/F \\ x' &= x t_s/kF \end{aligned} \right\} \text{(non-dimensional)} \quad \dots \dots \dots (113)$$

which gives

$$u = \int_0^{\infty} \phi(\theta) e^{-\theta x'} (-\cos \theta y' + \theta \sin \theta y') d\theta \quad \dots \dots \dots (114)$$

$\phi(\theta)$ will now be determined by the conditions of equilibrium of the shear-stiffener ($x = 0$).

Consider an elemental part of the shear-stiffener as represented in the accompanying diagram.



DIAG. 26.

Equilibrium of the element gives

$$R \frac{\partial q}{\partial y} + t_s f_{xx} = 0, \quad \dots \dots \dots (115)$$

where q is the shear stress in the shear-stiffener, which is also the shear stress, from compatibility of displacements, in the adjacent sheet.

In terms of the displacement u equation (115) may be written

$$\left(RG \frac{\partial^2 u}{\partial y^2} + Et_s \frac{\partial u}{\partial x} \right)_{x=0} = 0 \quad \dots \dots \dots (116)$$

This gives on simplifying and rearranging

$$\int_0^{\infty} \phi(\theta) (1 + \zeta \theta) \theta \cos \theta y' d\theta - \int_0^{\infty} \phi(\theta) (1 + \zeta \theta) \theta^2 \sin \theta y' d\theta = 0 \quad \dots \dots \dots (117)$$

where

$$\zeta = \bar{k}R/F \quad \dots \dots \dots (118)$$

and is, therefore, a non-dimensional measure of the stiffness of the shear-stiffener.

The above equation for $\phi(\theta)$, which is true for all values of y' , may be solved as follows:

Denoting the first integral by Z the equation can be put in the form

$$Z + \frac{\partial Z}{\partial y'} = 0 \quad \dots \dots \dots (119)$$

the solution of which is

$$Z = C e^{-y'} \quad \dots \dots \dots (120)$$

where C is some constant.

Now $C e^{-y'}$ can be expressed as a Fourier integral,

$$\left. \begin{aligned} C e^{-y'} &= \frac{2C}{\pi} \int_0^{\infty} \frac{\cos \theta y'}{1 + \theta^2} d\theta \\ &= -\frac{2C}{\pi} \int_0^{\infty} \frac{\theta \sin \theta y'}{1 + \theta^2} d\theta \end{aligned} \right\} \dots \dots \dots (121)$$

Equating the first of these to Z , or the second to $\partial Z/\partial y'$, and dropping the $\int_0^{\infty} \cos \theta y' d\theta$ and $\int_0^{\infty} \theta \sin \theta y' d\theta$ operators gives the following equation for $\phi(\theta)$,

$$\phi(\theta) = \frac{2C}{\pi \theta (1 + \zeta \theta) (1 + \theta^2)} \quad \dots \dots \dots (122)$$

where C is yet to be determined.

This form for $\phi(\theta)$ gives the stresses in the following form:

$$\begin{aligned} f_{xx} &= E \frac{\partial u}{\partial x} \\ &= \frac{2CEt_s}{\pi kF} \int_0^{\infty} \frac{(\cos \theta y' - \theta \sin \theta y') e^{-\theta x}}{(1 + \zeta \theta) (1 + \theta^2)} d\theta \quad \dots \dots \dots (123) \end{aligned}$$

and

$$\begin{aligned} q_{xy} &= G \frac{\partial u}{\partial y} \\ &= \frac{2CGt_s}{\pi F} \int_0^{\infty} \frac{(\sin \theta y' + \theta \cos \theta y') e^{-\theta x}}{(1 + \zeta \theta) (1 + \theta^2)} d\theta \quad \dots \dots \dots (124) \end{aligned}$$

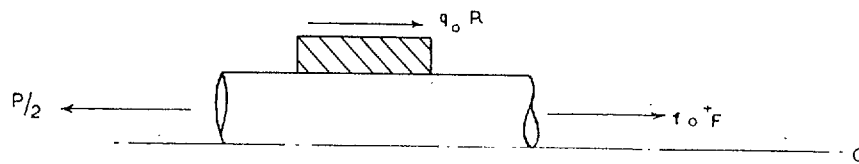
At the origin these become

$$f_0^+ = \frac{2CEt_s}{\pi kF} \int_0^{\infty} \frac{d\theta}{(1 + \zeta \theta) (1 + \theta^2)} \quad \dots \dots \dots (125)$$

and

$$q_0 = \frac{2CGt_s}{\pi F} \int_0^{\infty} \frac{\theta d\theta}{(1 + \zeta \theta) (1 + \theta^2)} \quad \dots \dots \dots (126)$$

If now we make a small rectangular cut through the boom and shear-stiffener, as in the diagram below,



DIAG. 27.

we have for equilibrium of the element of boom cut out at the origin,

$$P/2 = f_0 + F + q_0 R \quad \dots \dots \dots (127)$$

$$= \frac{2C}{\pi} \sqrt{(EGt_s)} \int_0^\infty \frac{d\theta}{(1 + \zeta\theta)(1 + \theta^2)} + \frac{2C}{\pi} \sqrt{(EGt_s)} \left(\frac{kR}{F} \right) \int_0^\infty \frac{\theta d\theta}{(1 + \zeta\theta)(1 + \theta^2)}$$

$$= \frac{2C}{\pi} \sqrt{(EGt_s)} \int_0^\infty \frac{(1 + \zeta\theta) d\theta}{(1 + \zeta\theta)(1 + \theta^2)}$$

$$= C\sqrt{(EGt_s)} \quad \dots \dots \dots (128)$$

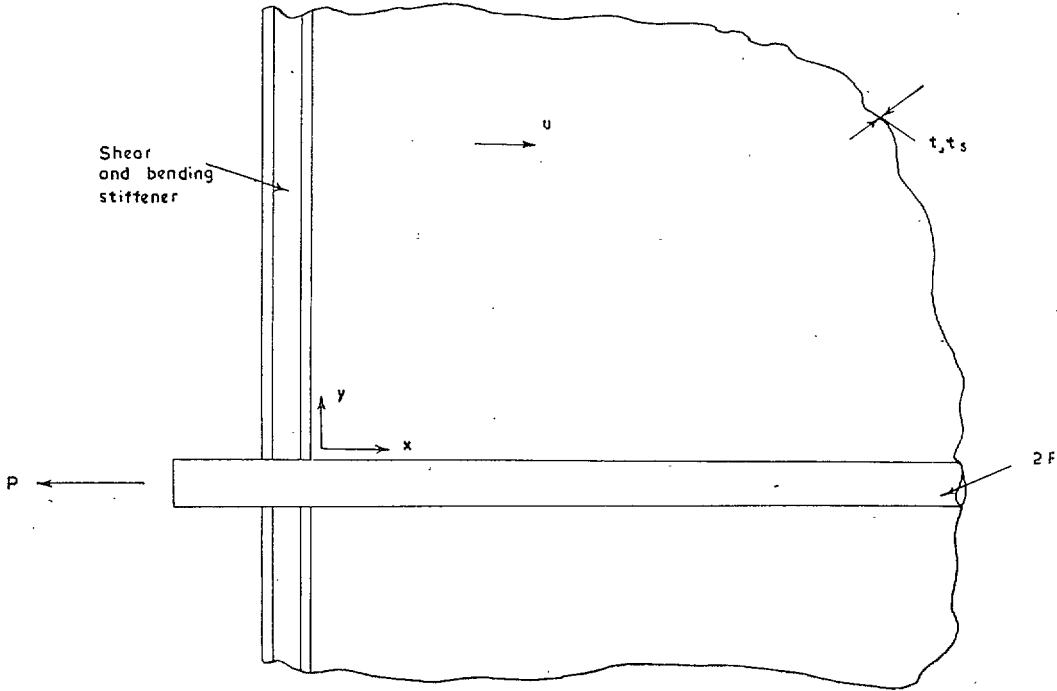
i.e.,

$$C = P/2 \sqrt{(EGt_s)} \quad \dots \dots \dots (129)$$

This value of C substituted in equations (123) and (124) determines the complete stress distribution throughout the structure.

APPENDIX VI

Constant area boom and shear + bending stiffener



DIAG. 28. Diagram showing notation.

As in Appendix V we search for a solution in the form

$$u = \int_0^{\infty} \phi(\theta) e^{-\theta x'} \{-\cos \theta y' + \theta \sin \theta y'\} d\theta \quad \dots \quad (130)$$

which satisfies the conditions of equilibrium adjacent to the main boom ($y = 0$). x' and y' are defined by equation (113), and equation (130) is again assumed valid for positive y' .

$\phi(\theta)$ will now be found to satisfy conditions adjacent to the stiffener.

It is convenient here to regard the deflection u_r of the stiffener as made up of two parts, u_s due to shear deflection and u_b due to bending, *i.e.*,

$$\begin{aligned} u_r &= (u)_{x=0} \text{ because of compatibility of displacement,} \\ &= u_s + u_b \quad \dots \quad (131) \end{aligned}$$

and hence

$$\frac{\partial^2 u_r}{\partial y^2} = \frac{t_s^2}{F^2} \int_0^{\infty} \theta^2 \phi(\theta) (\cos \theta y' - \theta \sin \theta y') d\theta \quad \dots \quad (132)$$

$$= \frac{\partial^2 u_s}{\partial y^2} + \frac{\partial^2 u_b}{\partial y^2} \quad \dots \quad (133)$$

Considering now the deflection due to shear alone

$$\frac{\partial^2 u_s}{\partial y^2} = -\frac{Et_s}{RG} \left(\frac{\partial u}{\partial x} \right)_{x=0} \quad \dots \quad (134)$$

as in equation (116),

$$= \frac{-Et_s^2}{kRGF} \int_0^{\infty} \theta \phi(\theta) (\cos \theta y' - \theta \sin \theta y') d\theta \quad \dots \quad (135)$$

from equation (130).

Considering the deflection due only to bending gives

$$\begin{aligned} \frac{\partial^4 u_b}{\partial y^4} &= \frac{t_s}{I} \left(\frac{\partial u}{\partial x} \right)_{x=0} \text{ as in Appendix IV} \\ &= \frac{t_s^2}{kFI} \int_0^\infty \theta \phi(\theta) (\cos \theta y' - \theta \sin \theta y') d\theta \end{aligned} \quad \dots \quad \dots \quad \dots \quad \dots \quad (136)$$

Integrating this equation twice with respect to y gives

$$\frac{\partial^2 u_b}{\partial y^2} = \frac{-F}{kI} \int_0^\infty \frac{\phi(\theta)}{\theta} (\cos \theta y' - \theta \sin \theta y') d\theta$$

+ terms which are zero because $\partial^2 u_b / \partial y^2$ is zero for large values of y (137)

Equations (135) and (137) in (133) give an equation for determining $\phi(\theta)$; on simplifying and rearranging we have

$$\int_0^\infty \frac{\phi(\theta)}{\theta} \left\{ 1 + \eta^3 \theta^2 \left(\theta + \frac{1}{\xi} \right) \right\} \cos \theta y' d\theta - \int_0^\infty \phi(\theta) \left\{ 1 + \eta^3 \theta^2 \left(\theta + \frac{1}{\xi} \right) \right\} \sin \theta y' d\theta = 0 \quad \dots \quad (138)$$

which is true for all values of y' .

This equation may be solved by a method similar to that used in Appendix IV. Denoting the first integral by Z the equation can be written in the form

$$Z + \frac{\partial Z}{\partial y'} = 0, \quad \dots \quad \dots \quad \dots \quad \dots \quad (139)$$

the solution of which is

$$Z = C e^{-y'} \quad \dots \quad \dots \quad \dots \quad \dots \quad (140)$$

where C is an arbitrary constant.

$C e^{-y'}$ can be expressed as a Fourier integral,

$$\left. \begin{aligned} C e^{-y'} &= \frac{2C}{\pi} \int_0^\infty \frac{\cos \theta y'}{1 + \theta^2} d\theta \\ &= \frac{-2C}{\pi} \int_0^\infty \frac{\theta \sin \theta y'}{1 + \theta^2} d\theta \end{aligned} \right\} \quad \dots \quad \dots \quad \dots \quad \dots \quad (141)$$

Now we also have the relation that

$$e^{-y'} \equiv \frac{\partial^{2n} e^{-y'}}{\partial (y')^{2n}} \quad \dots \quad \dots \quad \dots \quad \dots \quad (142)$$

and we accordingly take the most general form for equation (141) and write

$$\left. \begin{aligned} C e^{-y'} &= \frac{2}{\pi} \int_0^\infty \frac{\Sigma C_n \theta^{2n} \cos \theta y'}{1 + \theta^2} d\theta \\ &= \frac{2}{\pi} \int_0^\infty - \frac{\Sigma C_n \theta^{2n+1} \sin \theta y'}{1 + \theta^2} d\theta \end{aligned} \right\} \quad \dots \quad \dots \quad \dots \quad \dots \quad (143)$$

where the C_n are arbitrary constants which will be determined partly by the overall equilibrium of the system, partly by the fact that there is no change of slope due to bending at the root, and

partly by the fact that expressions for the stresses are necessarily everywhere convergent. (We could have used these more general expressions in Appendix V, though we should merely have found that the other C 's were all zero.)

Equating the first of equation (141) to Z , or the second to $-\partial Z/\partial y'$, and dropping the $\int_0^\infty \dots \cos \theta y' d\theta$ and $\int_0^\infty \dots \theta \sin \theta y' d\theta$ operators gives the following equation for $\phi(\theta)$,

$$\phi(\theta) = \frac{2 \sum C_n \theta^{2n+1}}{\pi(1 + \theta^2) \left\{ 1 + \eta^3 \theta^2 \left(\theta + \frac{1}{\zeta} \right) \right\}} \dots \dots \dots (144)$$

and the stresses, obtained by differentiating u , will be integrals containing the functions

$$\theta \phi(\theta) \{-\cos \theta y' + \theta \sin \theta y'\} \quad \text{or} \quad \theta \phi(\theta) \{\sin \theta y' + \theta \cos \theta y'\}$$

which are only convergent if all the C_n except C_{-1} and C_0 are zero. (This is best seen by considering the behaviour of $\partial u/\partial y$ along the line $x = 0$.)

C_{-1} and C_0 will now be determined from the fact that the stiffener is built-in at the root (since it is continuous there), and from overall conditions of equilibrium. This first condition may be written as

$$\begin{aligned} \frac{\partial u}{\partial y} \text{ at root} &= \text{slope due entirely to shear in stiffener} \\ &= \text{slope due to } t_s \int_0^\infty (f_{xx})_{x=0} dy. \end{aligned}$$

i.e.,

$$\frac{\partial u}{\partial y} = \frac{t_s E}{RG} \int_0^\infty \left(\frac{\partial u}{\partial x} \right)_{x=0} dy. \dots \dots \dots (145)$$

Substituting from equations (130) and (144) and rearranging gives

$$\zeta \int_0^\infty \frac{(\theta C_{-1} + \theta^3 C_0) d\theta}{(1 + \theta^2)(1 + \eta^3 \theta^2 (\theta + 1/\zeta))} = \int_0^\infty \int_0^\infty \frac{(C_{-1} + \theta^2 C_0) (\cos \theta y' - \theta \sin \theta y') d\theta dy'}{(1 + \theta^2) \{1 + \eta^3 \theta^2 (\theta + 1/\zeta)\}} \dots (146)$$

This relation between C_{-1} and C_0 can be simplified by employing the notation:

$$\left. \begin{aligned} T &= \int_0^\infty \frac{\theta^3 d\theta}{(1 + \theta^2) \{1 + \eta^3 \theta^2 (\theta + 1/\zeta)\}} \\ U &= \int_0^\infty \frac{\theta^2 d\theta}{(1 + \theta^2) \{1 + \eta^3 \theta^2 (\theta + 1/\zeta)\}} \\ V &= \int_0^\infty \frac{\theta d\theta}{(1 + \theta^2) \{1 + \eta^3 \theta^2 (\theta + 1/\zeta)\}} \\ W &= \int_0^\infty \frac{d\theta}{(1 + \theta^2) \{1 + \eta^3 \theta^2 (\theta + 1/\zeta)\}} \\ &\equiv \frac{\pi}{2} - \eta^3 T - \frac{\eta^3 U}{\zeta}. \end{aligned} \right\} \dots \dots \dots (147)$$

This gives

$$\frac{C_0}{C_{-1}} = \frac{\eta^3}{\xi} - \frac{\xi V}{U + \xi T} = N, \text{ say.} \quad \dots \dots \dots (148)$$

The condition of overall equilibrium is the same as equation (127) of Appendix V, *i.e.*,

$$P/2 = f_0^+ F + q_0 R \quad \dots \dots \dots (149)$$

$$= \frac{2Et_s}{\pi k} (WC_{-1} + UC_0) + \frac{2RGt_s}{\pi F} (VC_{-1} + TC_0)$$

$$= \frac{2}{\pi} \sqrt{(EGtt_s)} \{ (W + \xi V)C_{-1} + (U + \xi T)C_0 \}$$

$$= \sqrt{(EGtt_s)} C_{-1}, \text{ using equations (147) and (148)}$$

i.e.,

$$C_{-1} = P/2 \sqrt{(EGtt_s)}. \quad \dots \dots \dots (150)$$

The values of C_{-1} and C_0 given by equations (150) and (148) give the following expressions for the stresses in the sheet,

$$f_{xx} = \frac{2}{\pi} f_0 \int_0^\infty \frac{(1 + N\theta^2) e^{-\theta x'} (\cos \theta y' - \theta \sin \theta y') d\theta}{(1 + \theta^2) \{1 + \eta^3 \theta^2 (\theta + 1/\xi)\}}, \quad \dots \dots \dots (151)$$

$$q_{xy} = \frac{2}{\pi} k f_0 \int_0^\infty \frac{(1 + N\theta^2) e^{-\theta x'} (\sin \theta y' + \theta \cos \theta y') d\theta}{(1 + \theta^2) \{1 + \eta^3 \theta^2 (\theta + 1/\xi)\}}. \quad \dots \dots \dots (152)$$

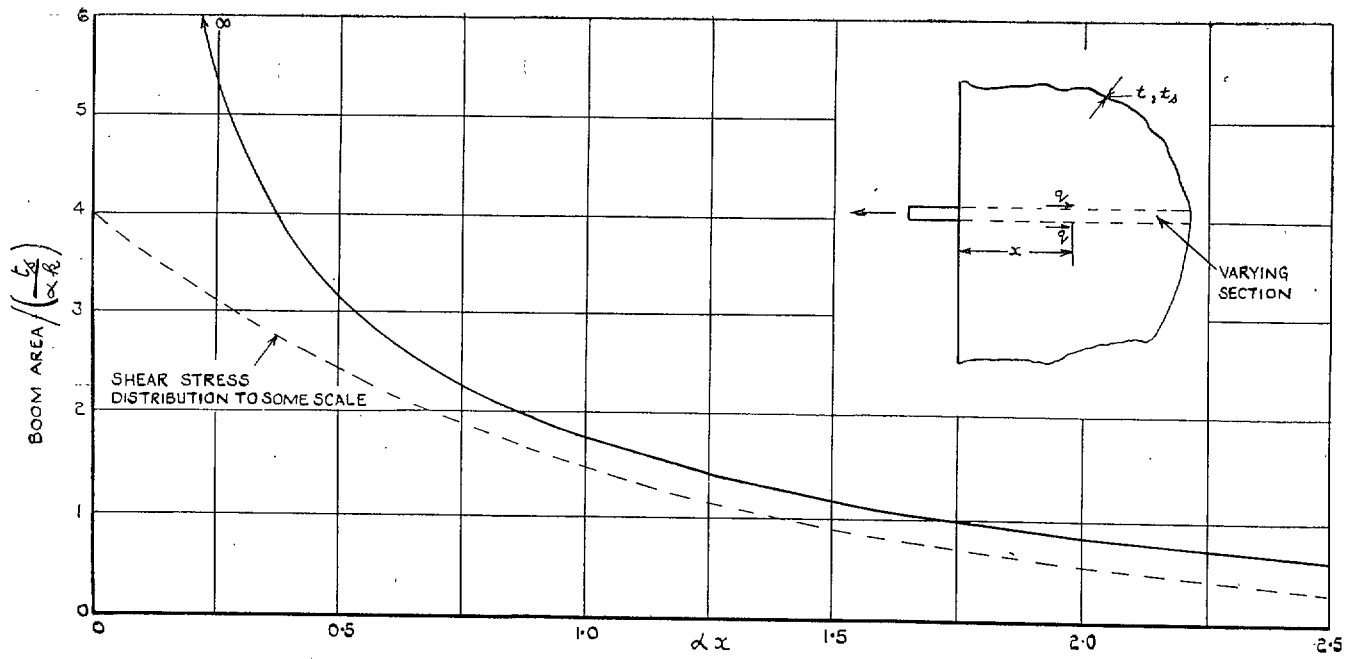


FIG. 8. Required boom sectional area to produce exponential shear stress adjacent to the boom.

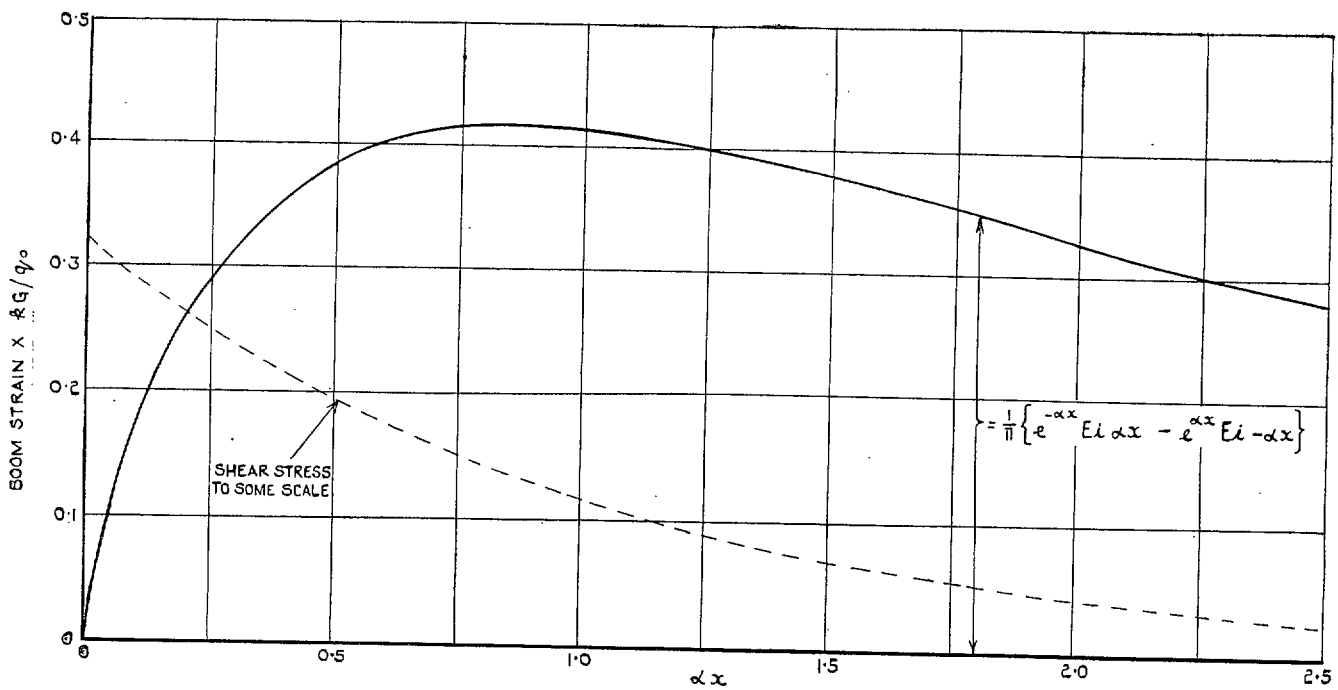


FIG. 9. Required boom strain to produce exponential shear stress adjacent to the boom.

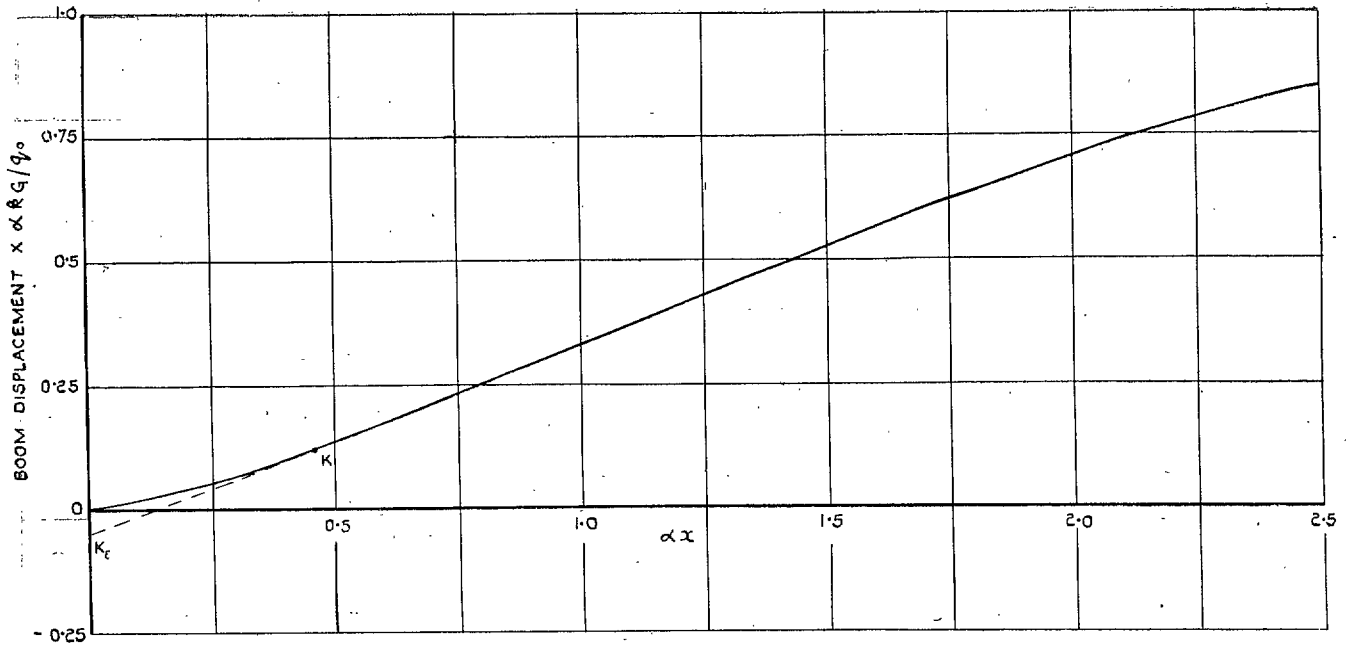


FIG. 10. Boom displacement consistent with exponential shear-stress distribution.

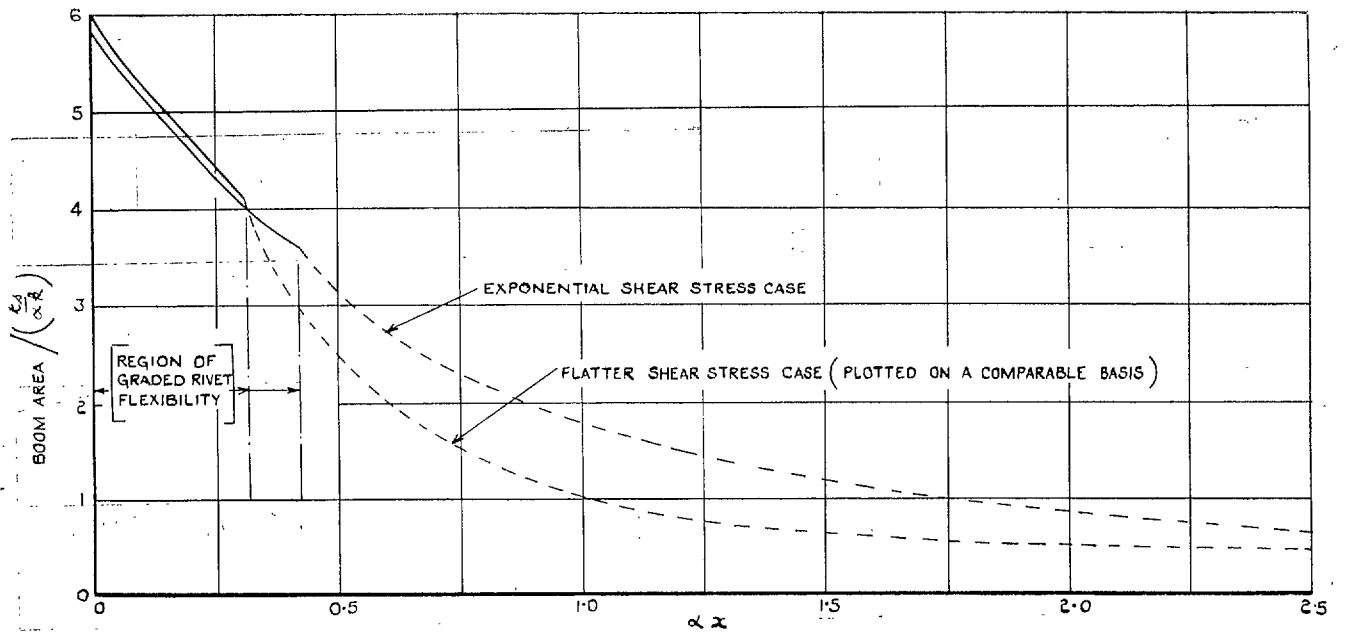


FIG. 11. Boom areas with appropriate rivet slip in neighbourhood of root.

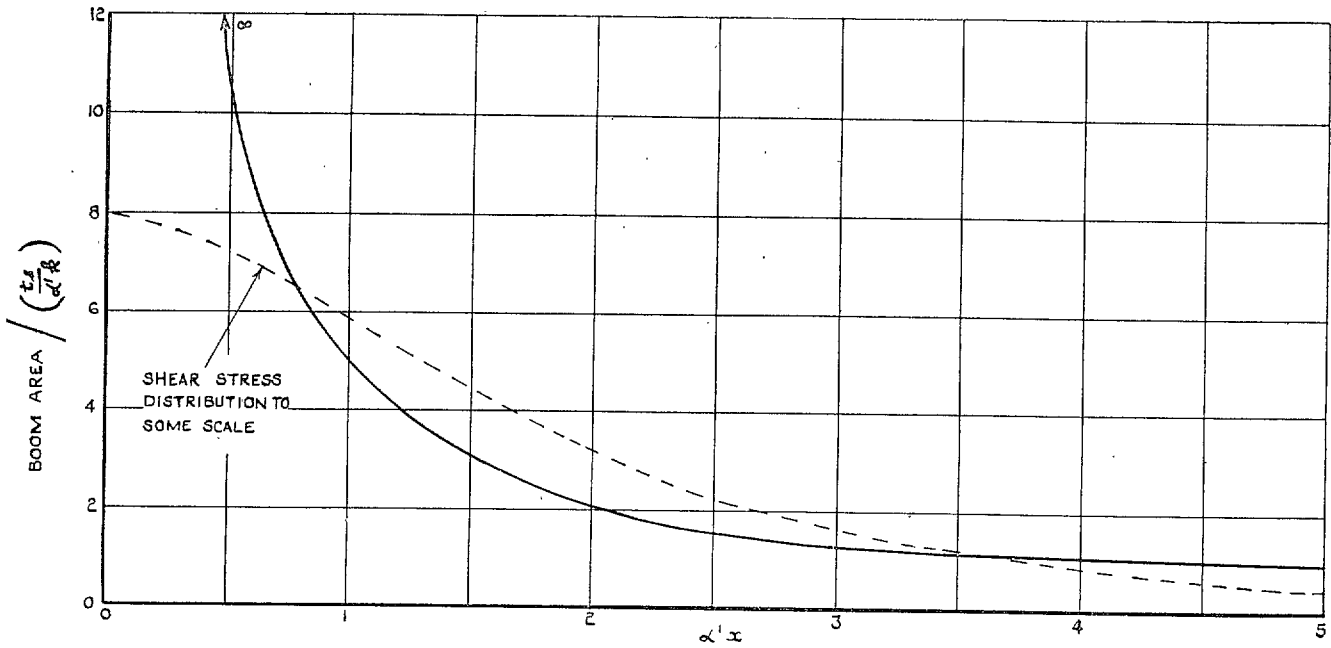


FIG. 12. Required boom sectional area to produce flutter shear stress adjacent to the boom.

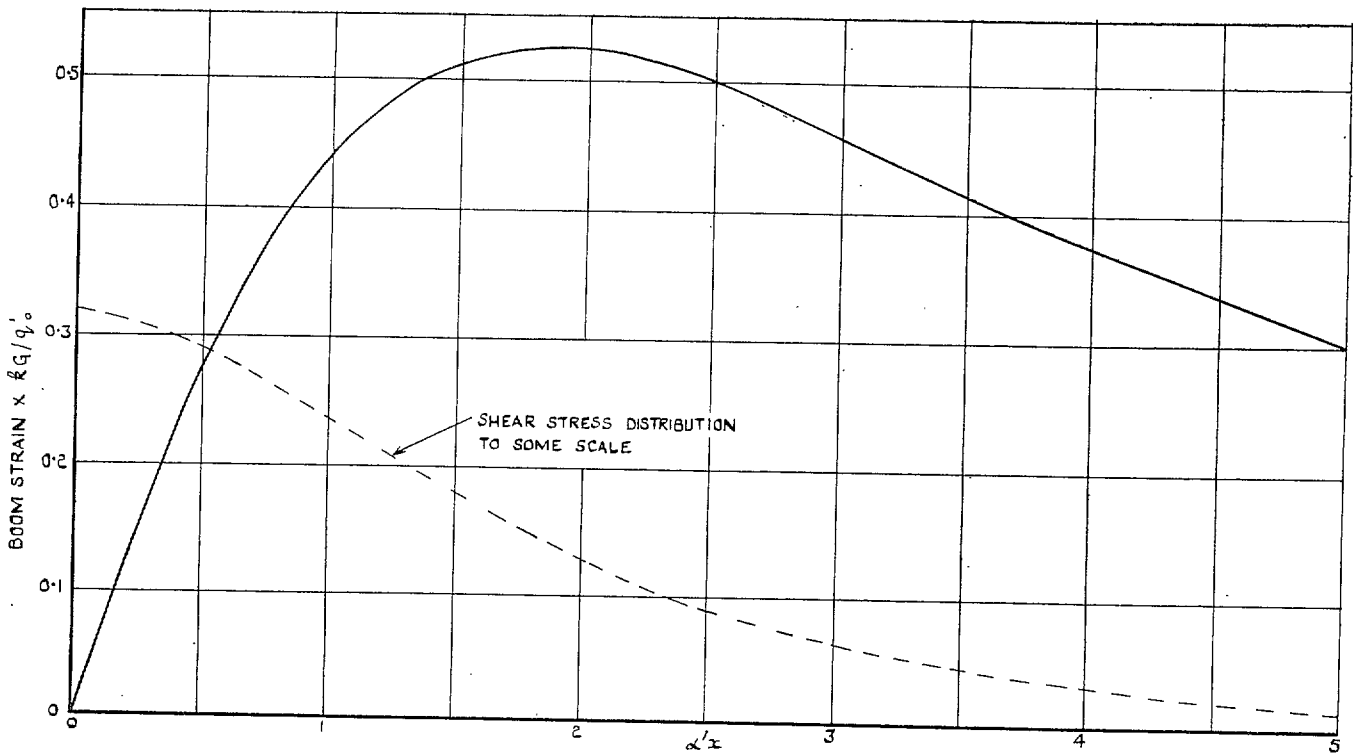


FIG. 13. Required boom strain to produce flutter shear-stress distribution adjacent to the boom.

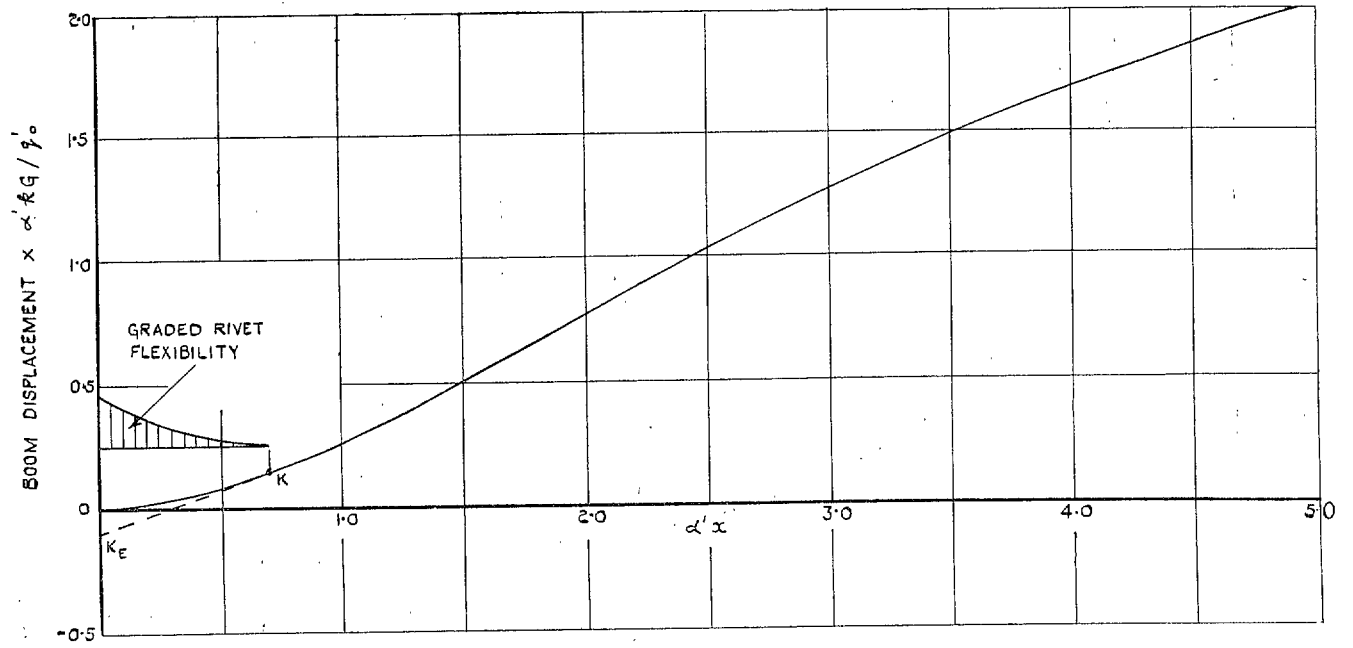


FIG. 14. Boom displacement consistent with flatter shear-stress distribution.

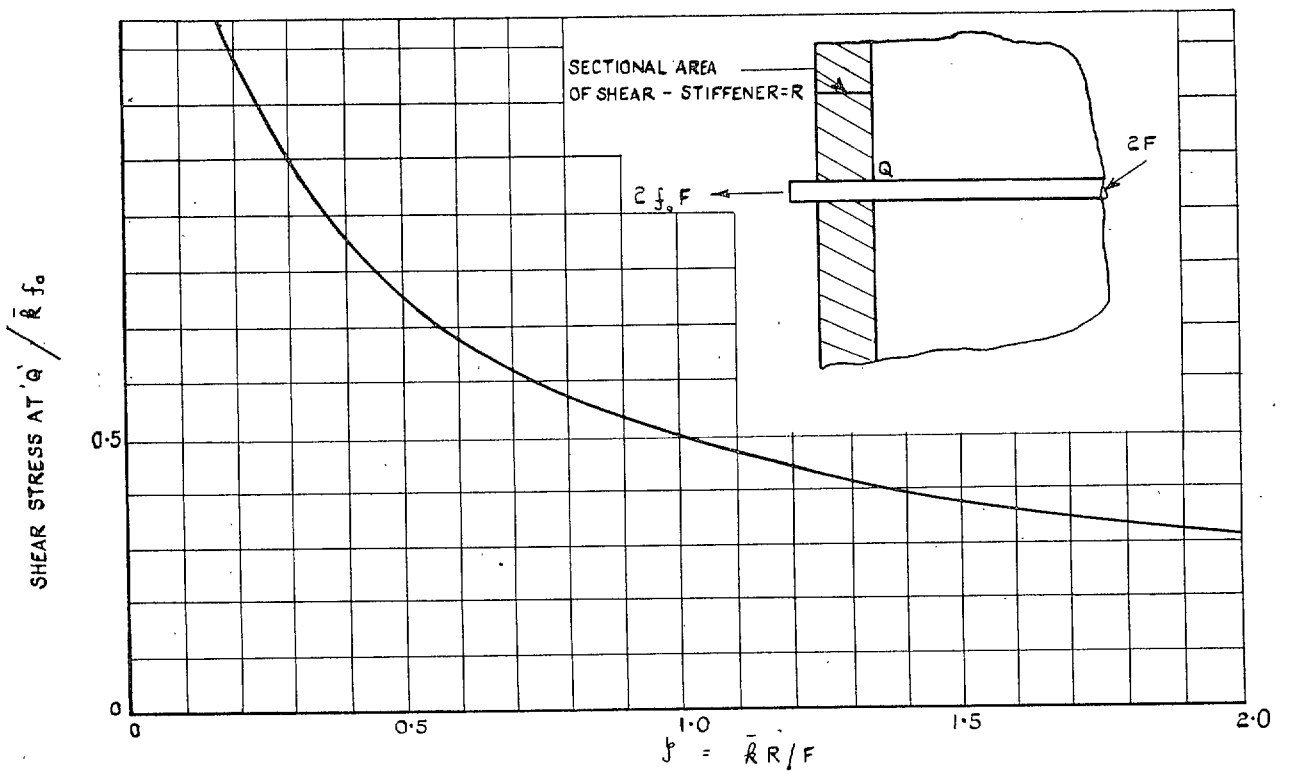


FIG. 15. Peak shear stress in sheet (boom plus shear-stiffener).

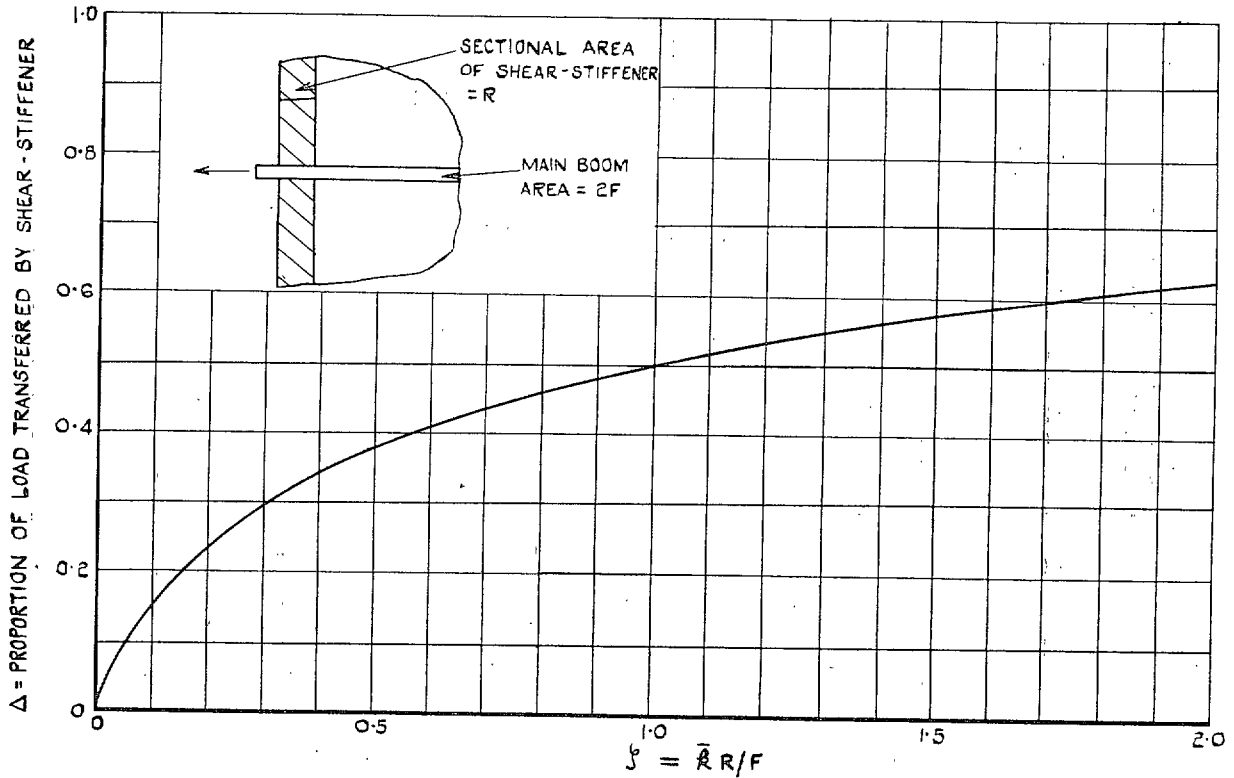


FIG. 16. Proportion of load transferred to sheet by shear-stiffener.

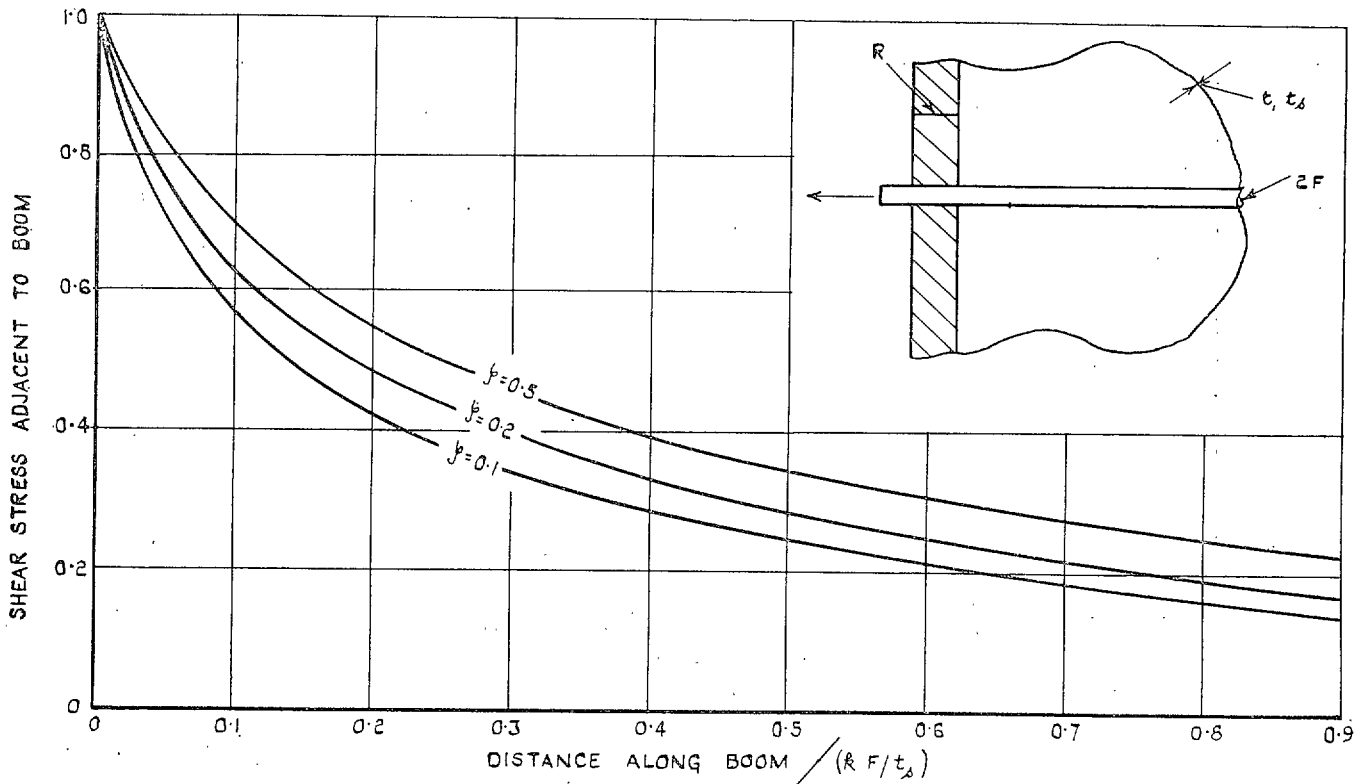


FIG. 17. Variation of shear die-away forms with different shear-stiffeners.

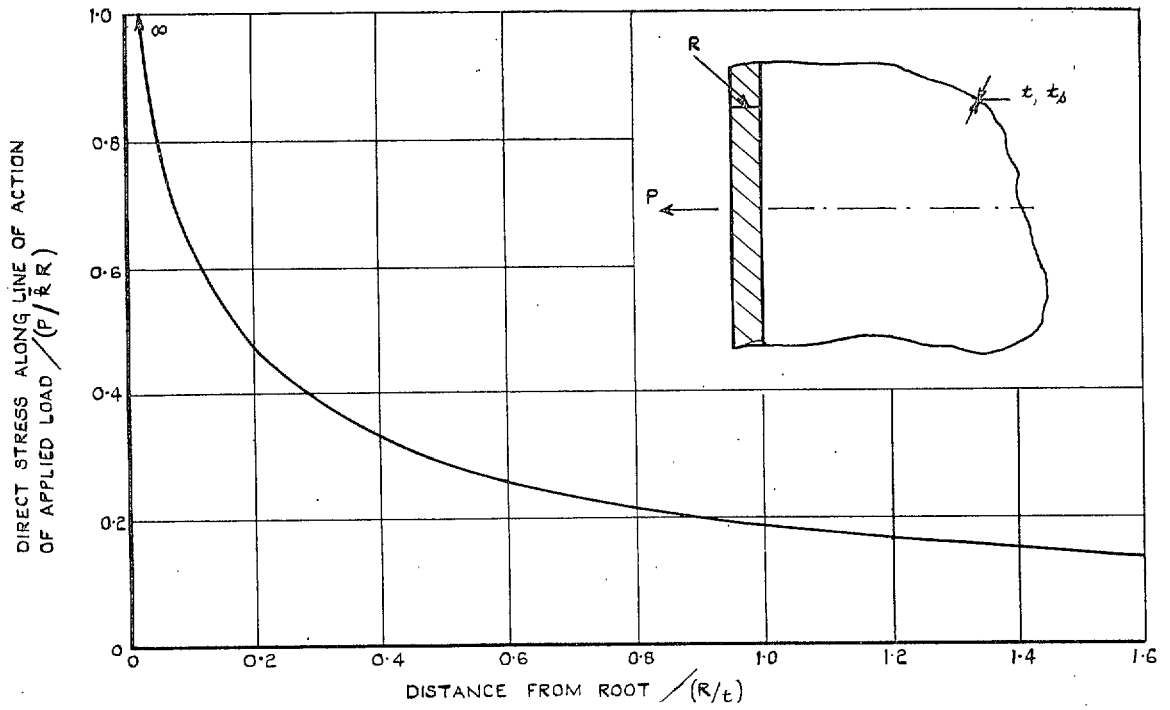


FIG. 18. Direct stress distribution with shear-stiffener and no main boom.

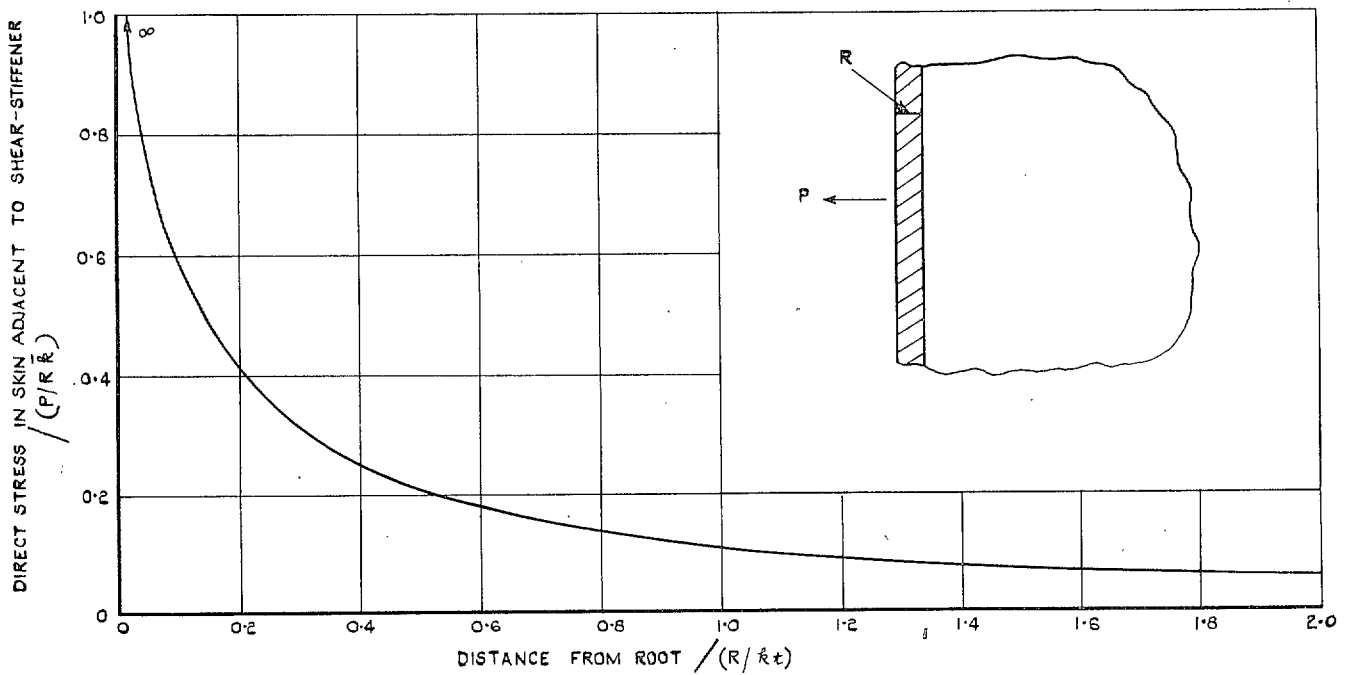


FIG. 19. Direct stress in skin adjacent to shear-stiffener (no main boom).

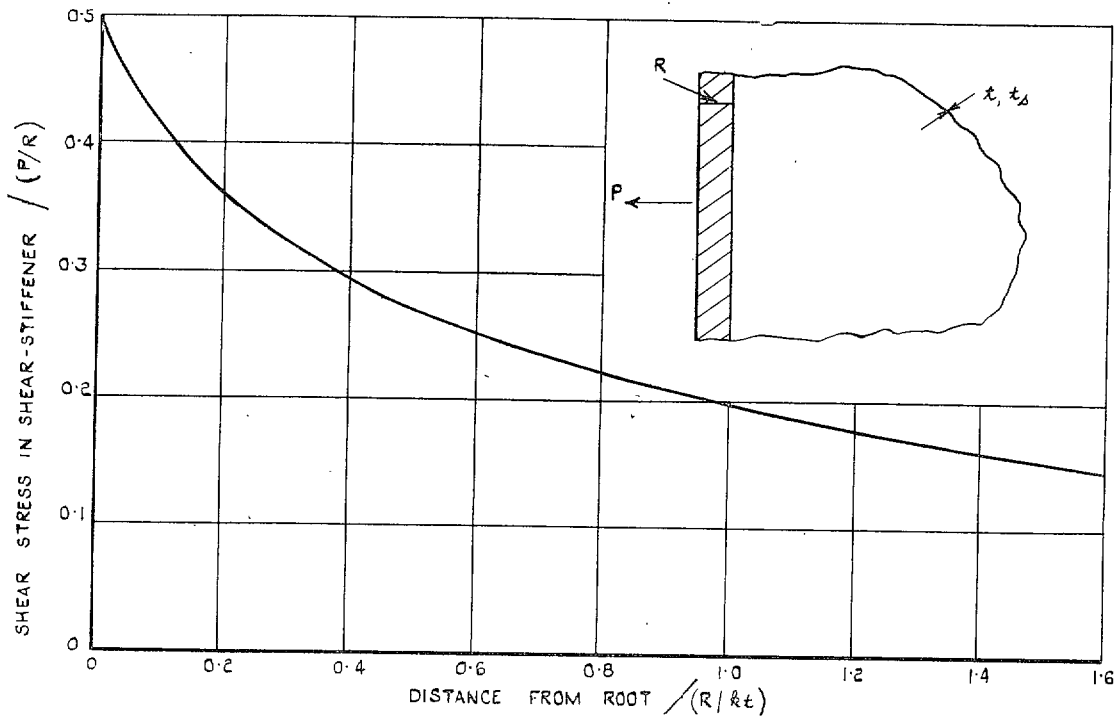


FIG. 20. Shear stress in shear-stiffener (no main boom).

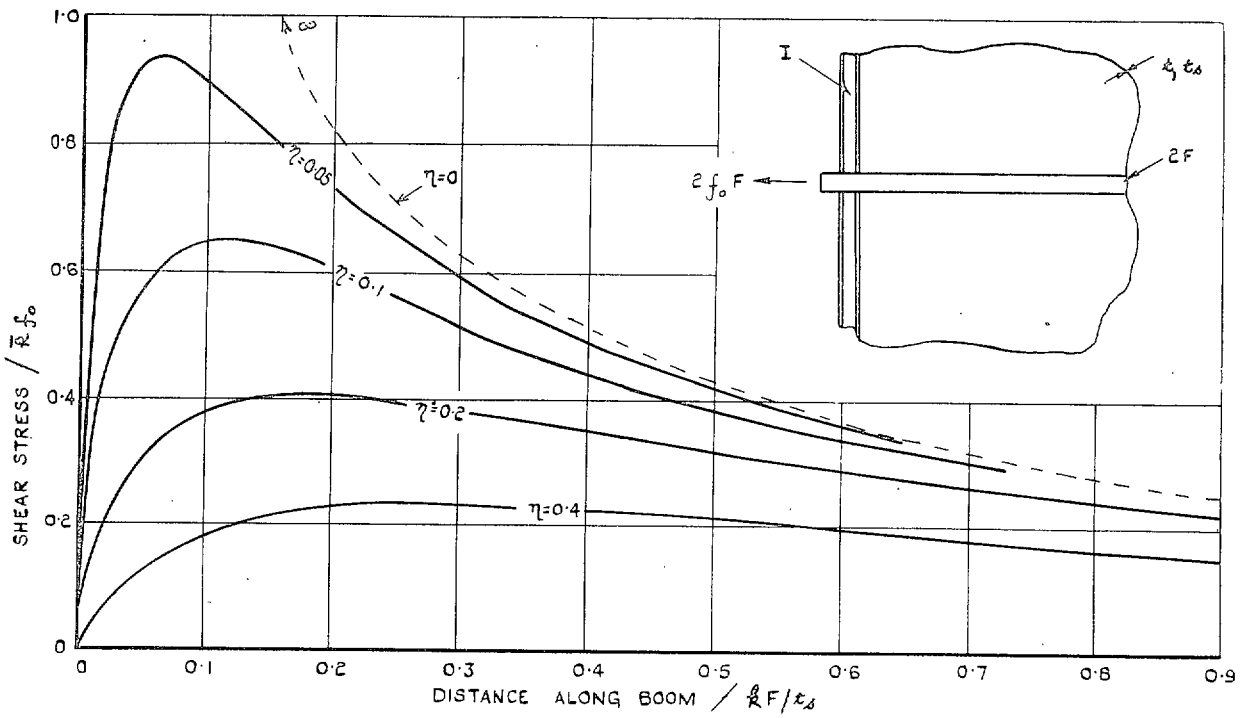


FIG. 21. Shear stress adjacent to boom (boom plus bending-stiffener).

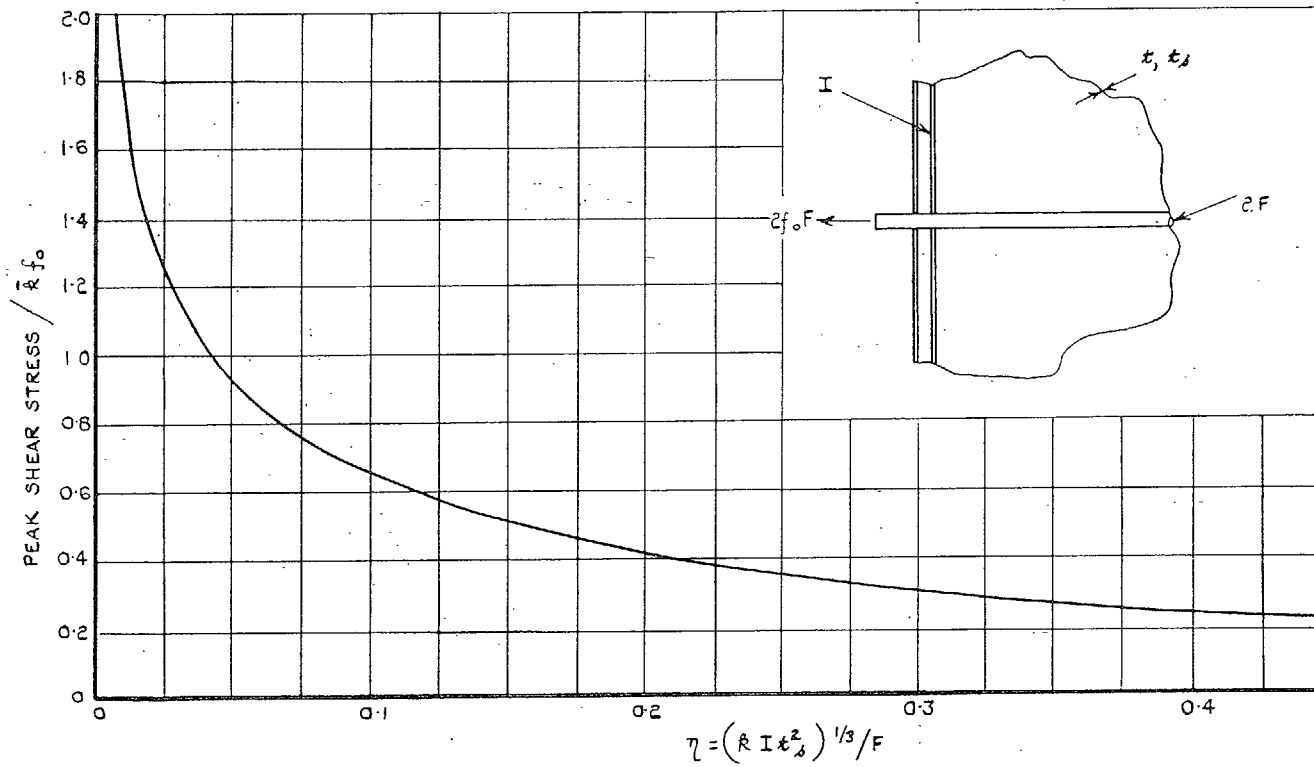


FIG. 22. Peak shear stress in sheet adjacent to boom (boom plus bending-stiffener).

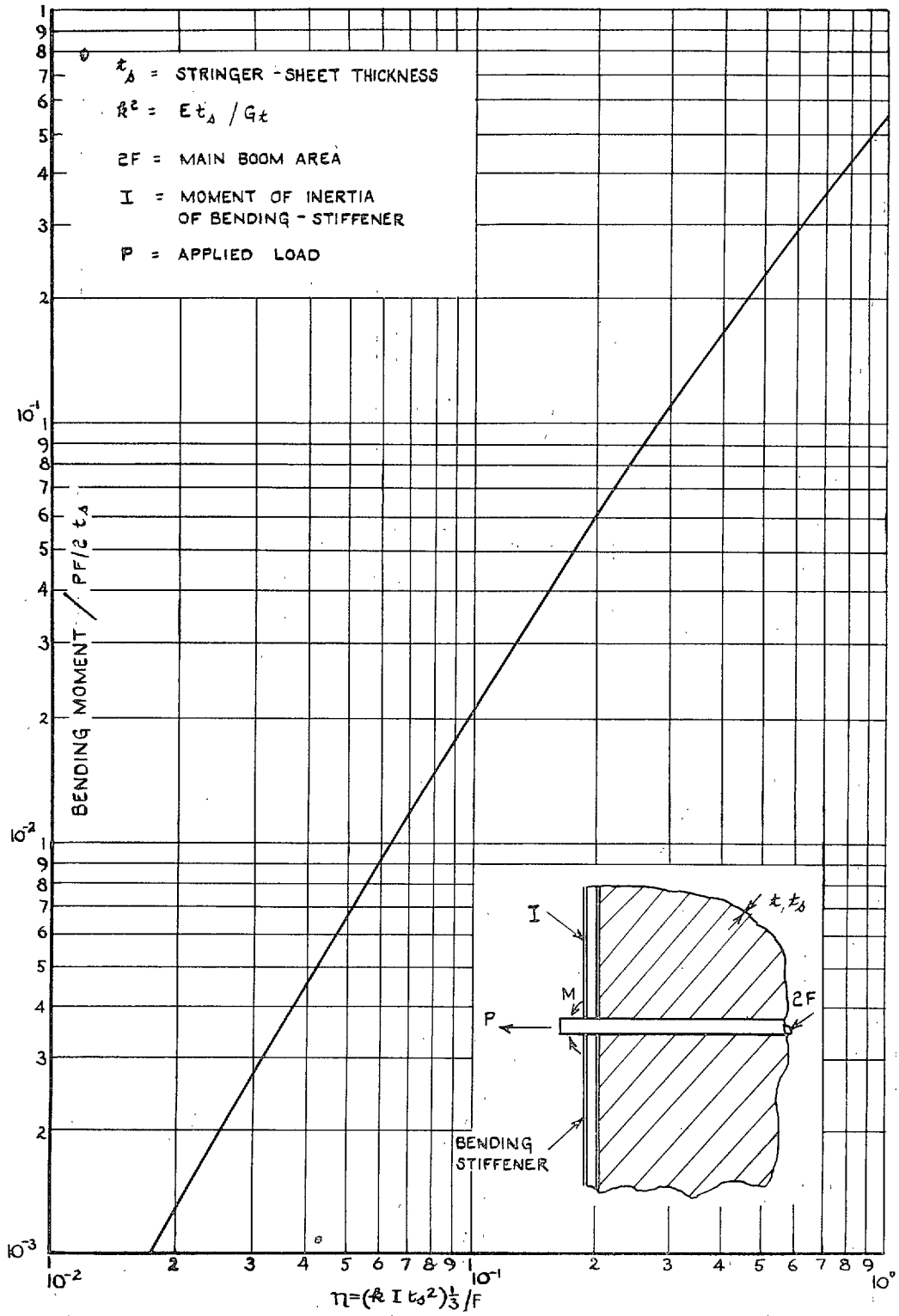


FIG. 23. Bending moment in bending-stiffener.

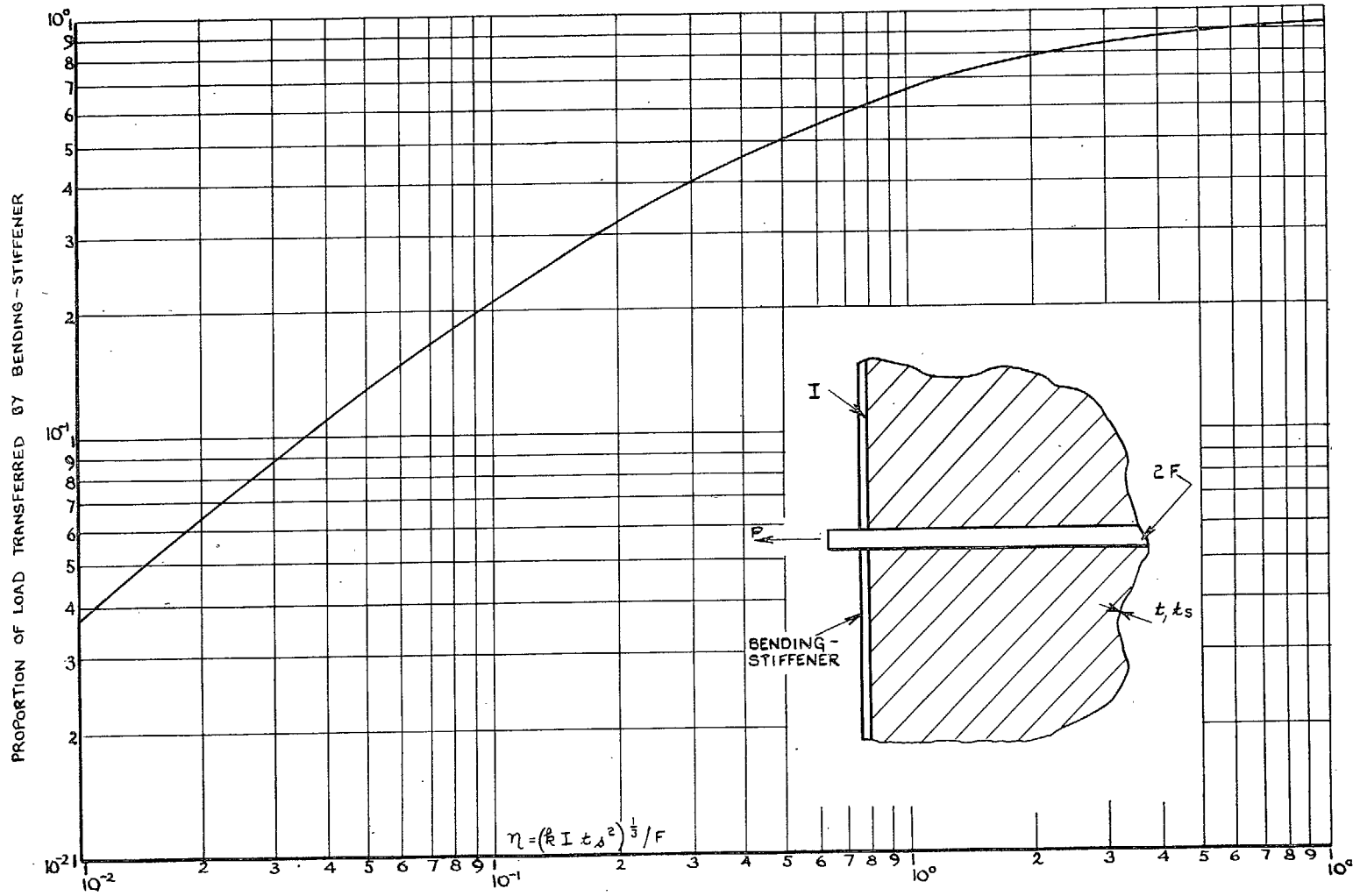


FIG. 24. Proportion of load transferred to sheet by bending-stiffener.

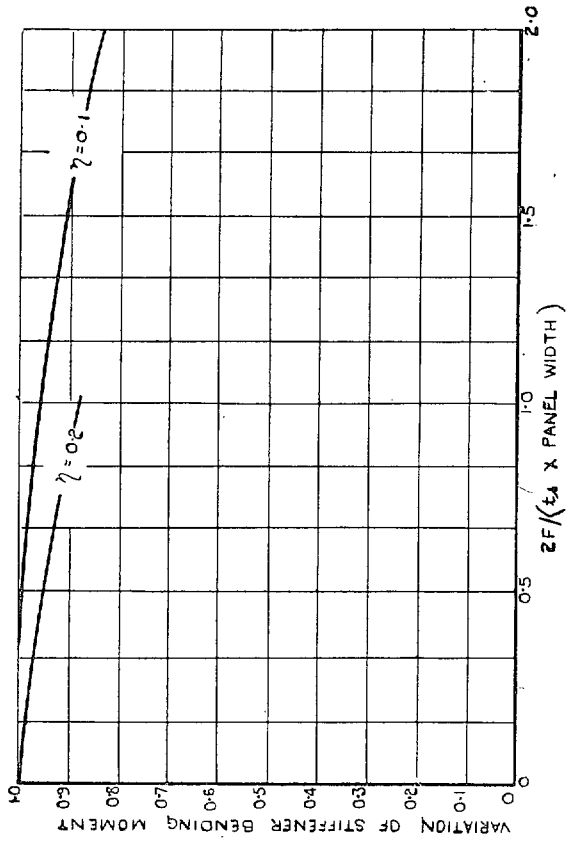


FIG. 25

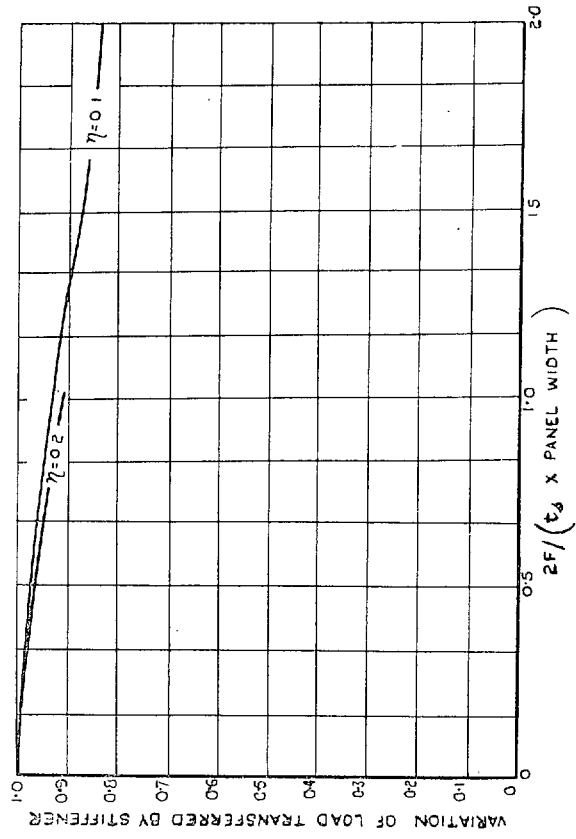


FIG. 26

Comparison with panels of finite width.

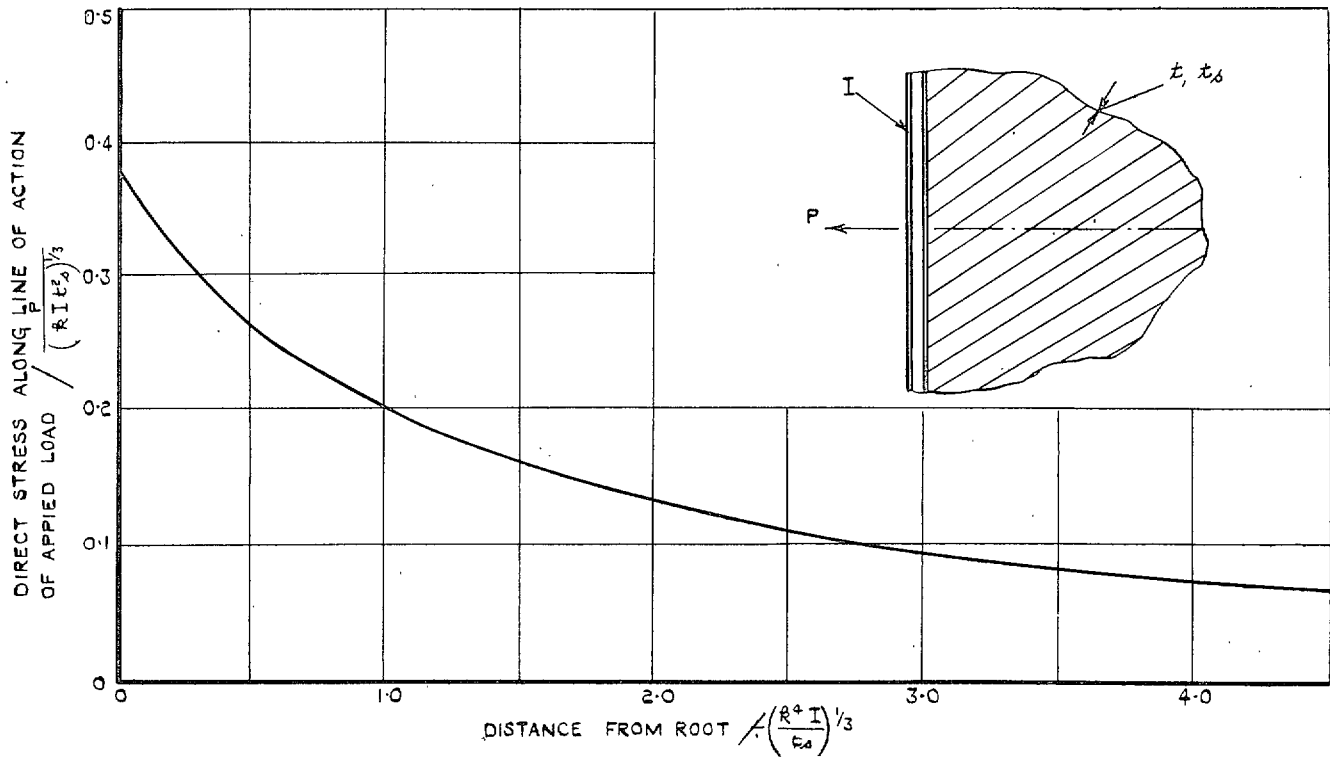


FIG. 27. Direct stress distribution with bending-stiffener and no main boom.

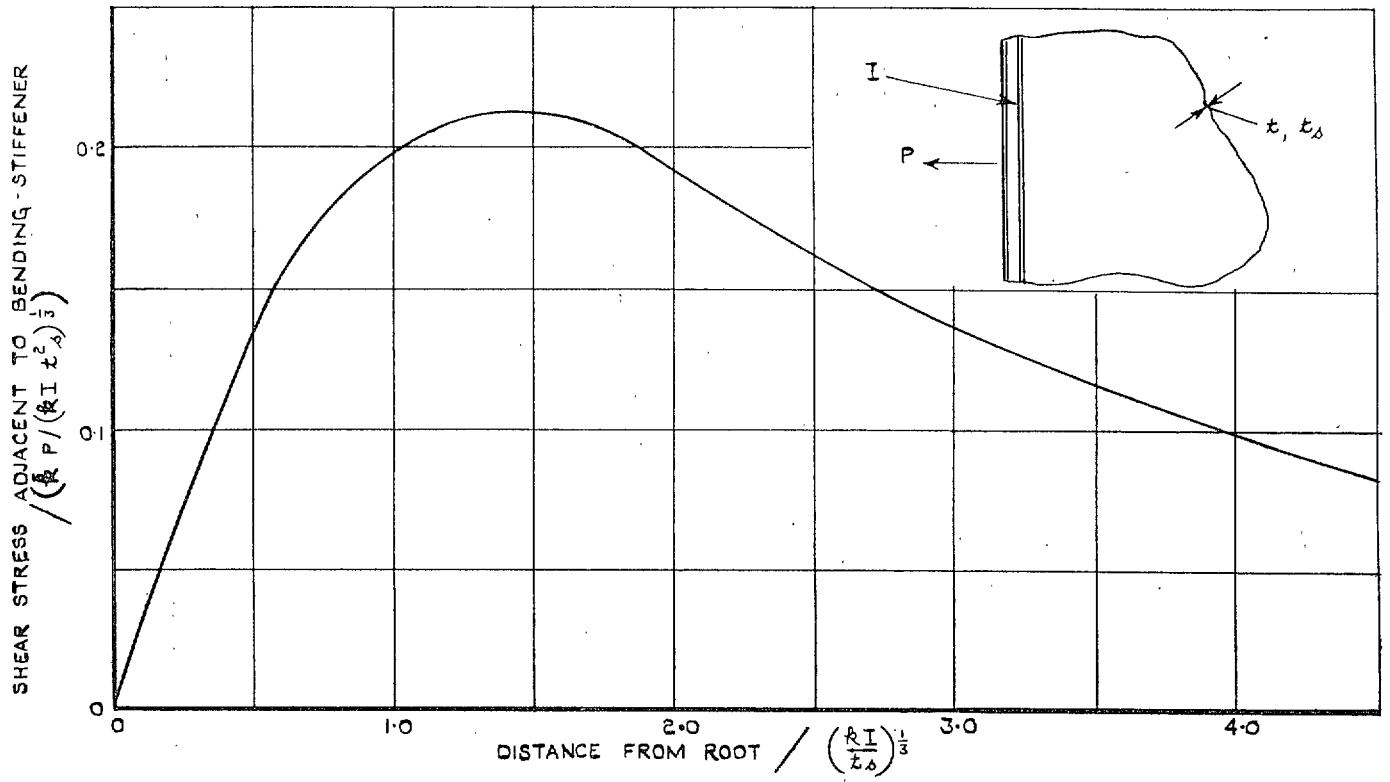


FIG. 28. Shear stress in sheet adjacent to bending-stiffener (no main boom).

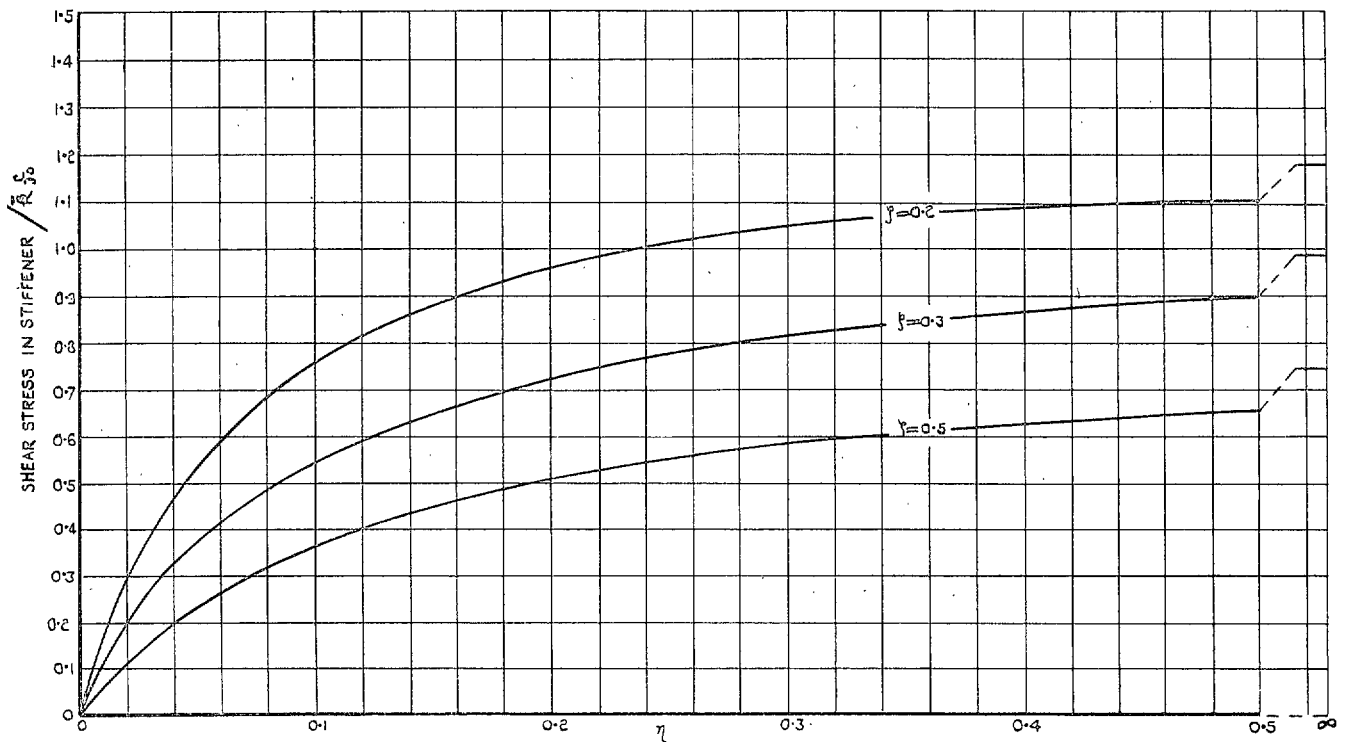


FIG. 29. Shear stress in stiffener.

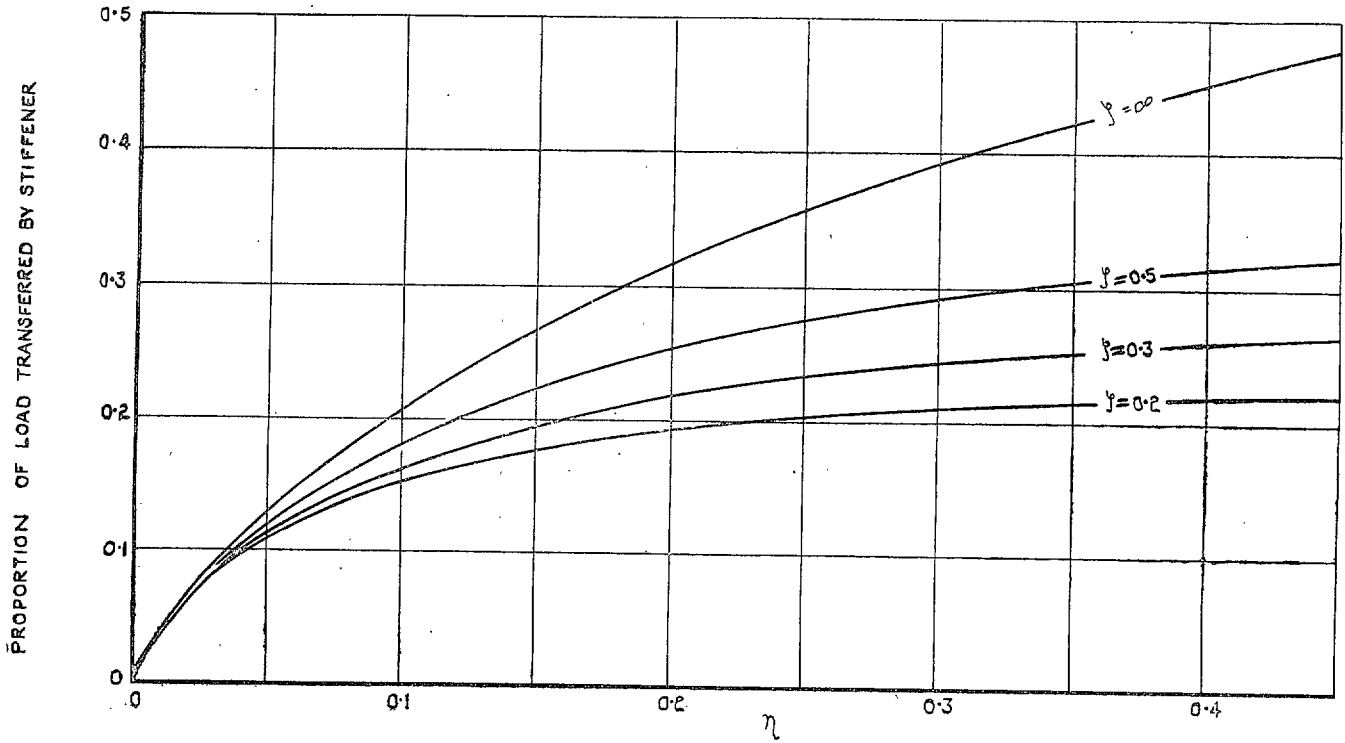


FIG. 30. Proportion of load transferred to sheet by stiffener.

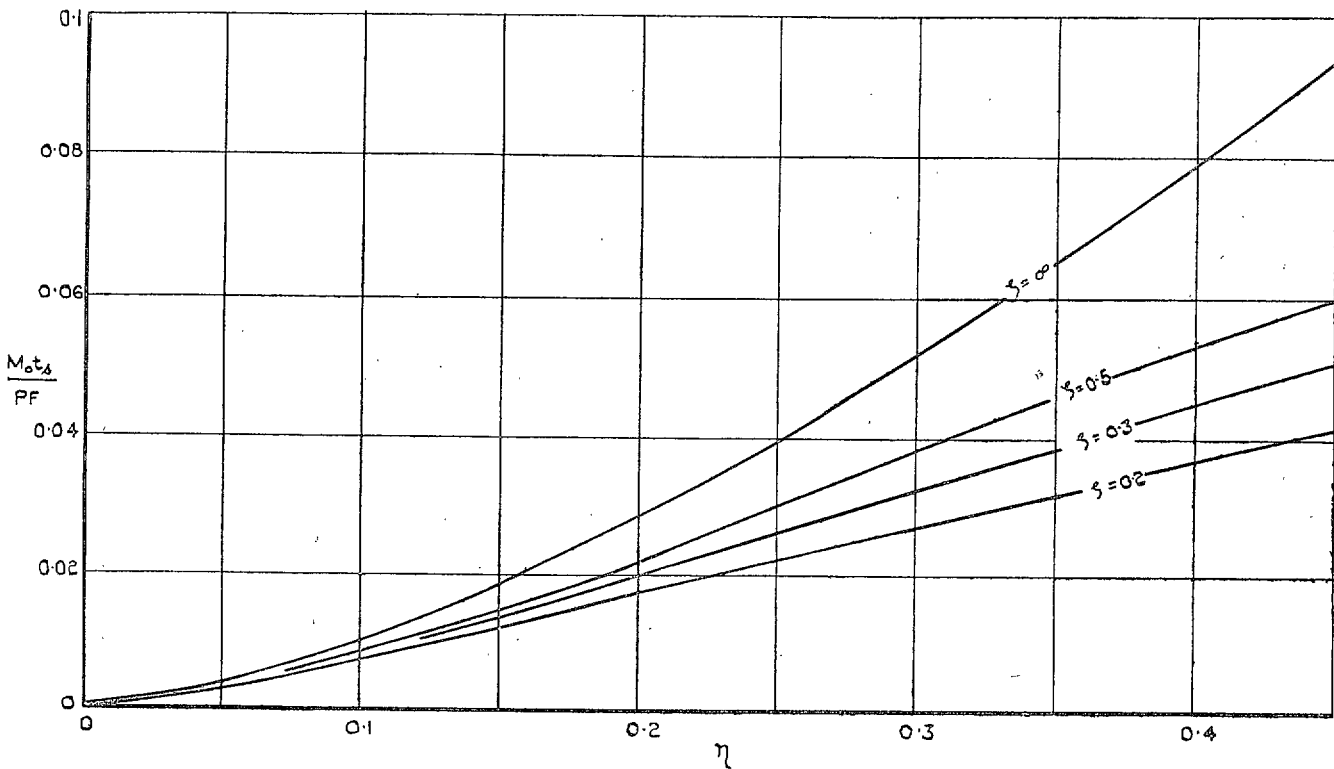


FIG. 31. Bending moment in stiffener.

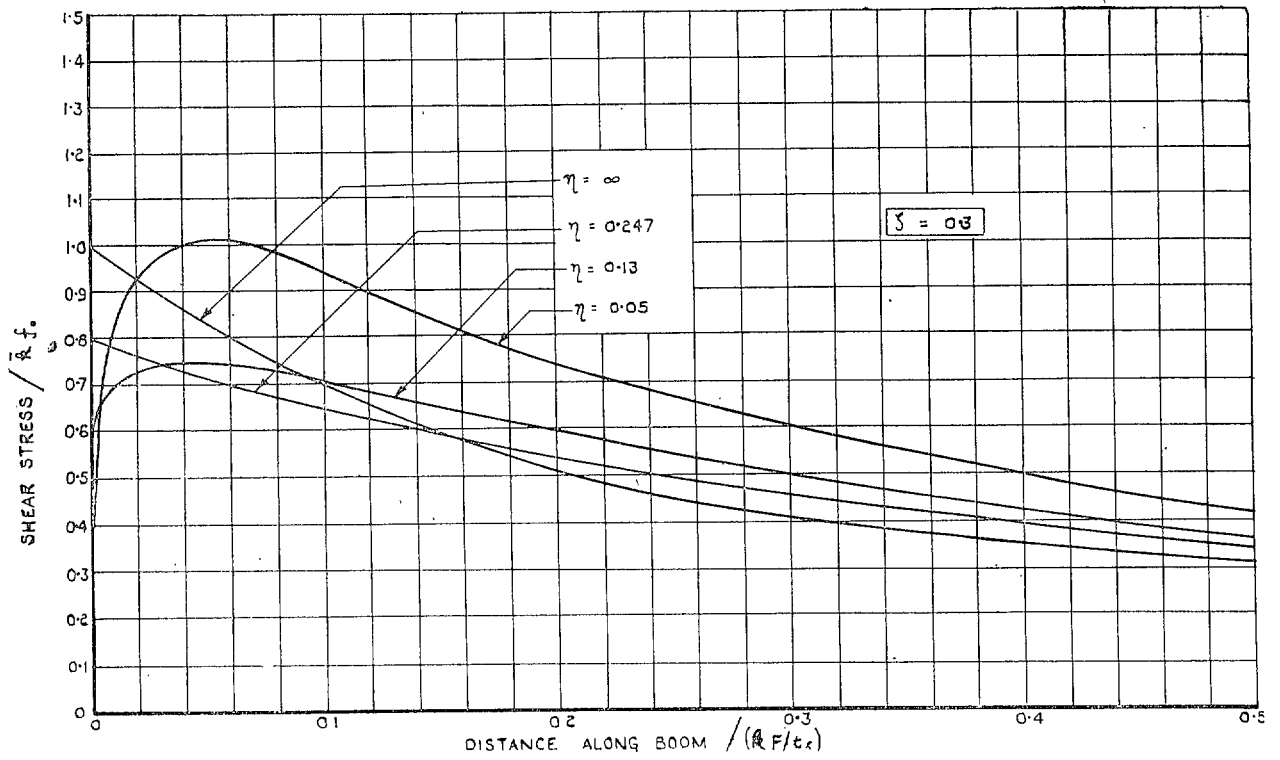


FIG. 32. Variation of shear-stress distribution with η .

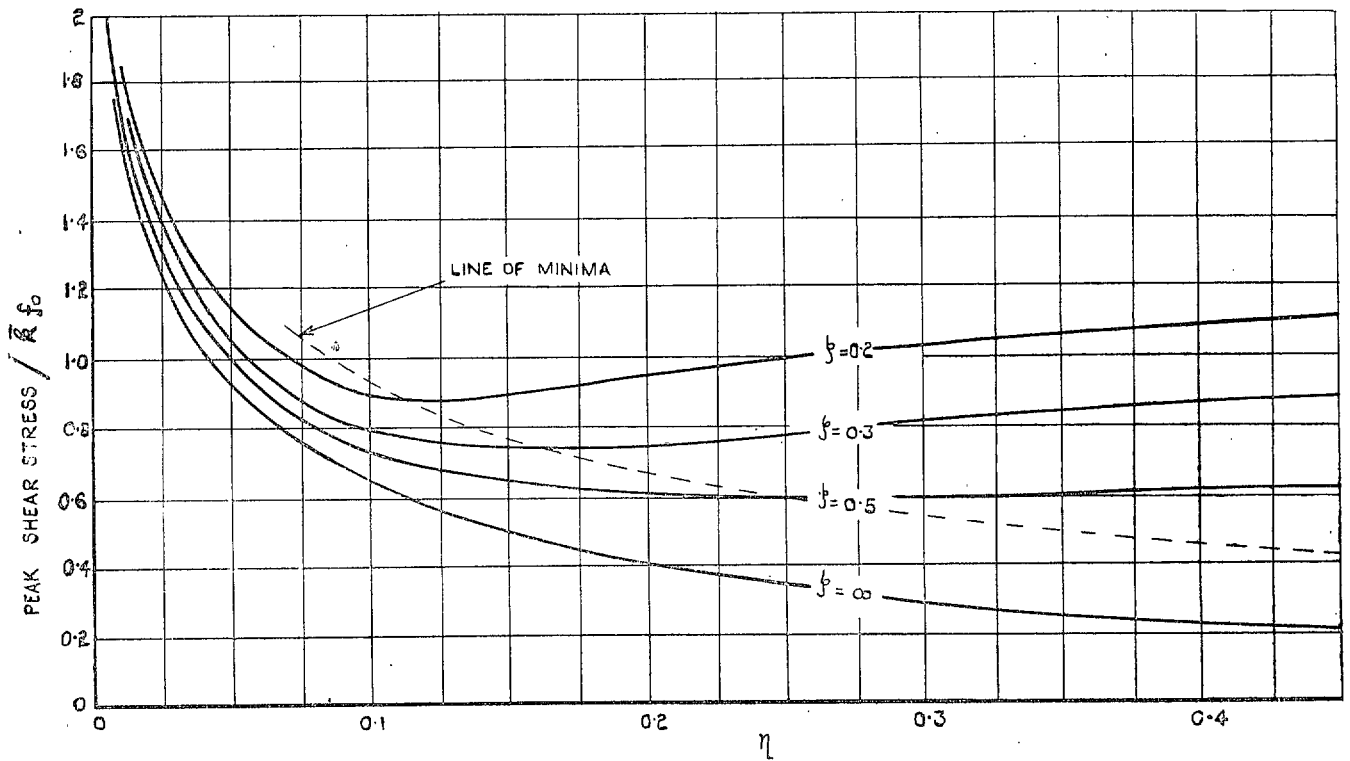


FIG. 33. Peak values of shear adjacent to the boom (variation with η).

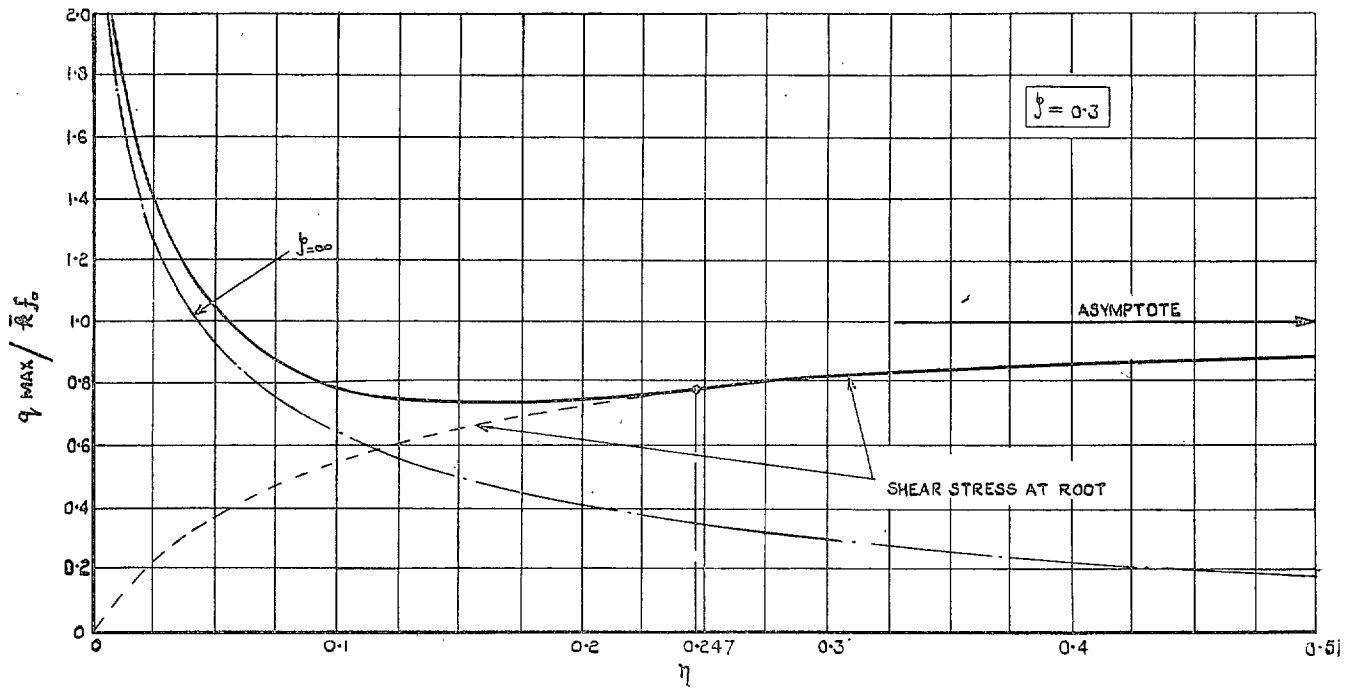


FIG. 34. Analysis of typical peak shear-stress curve.

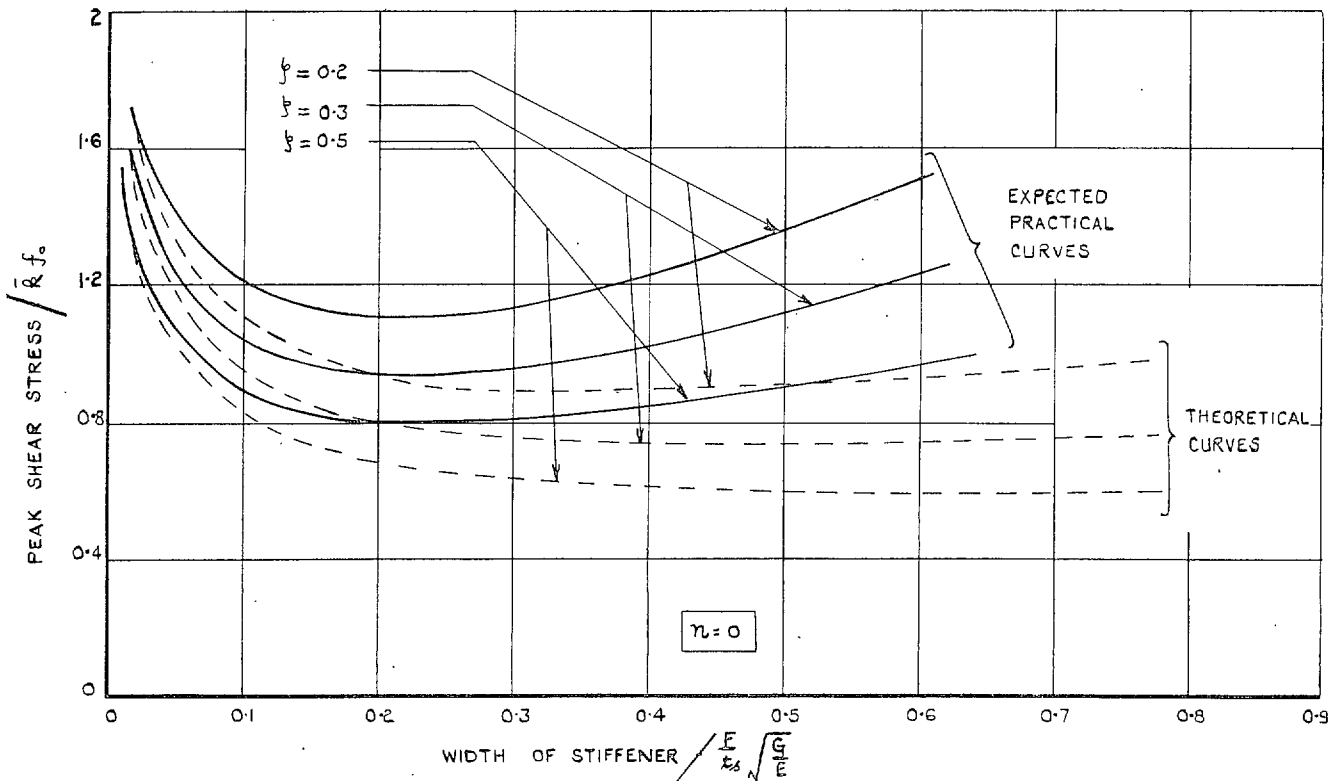


FIG. 35. Peak shear stress as influenced by stiffener width ($n = 0$).

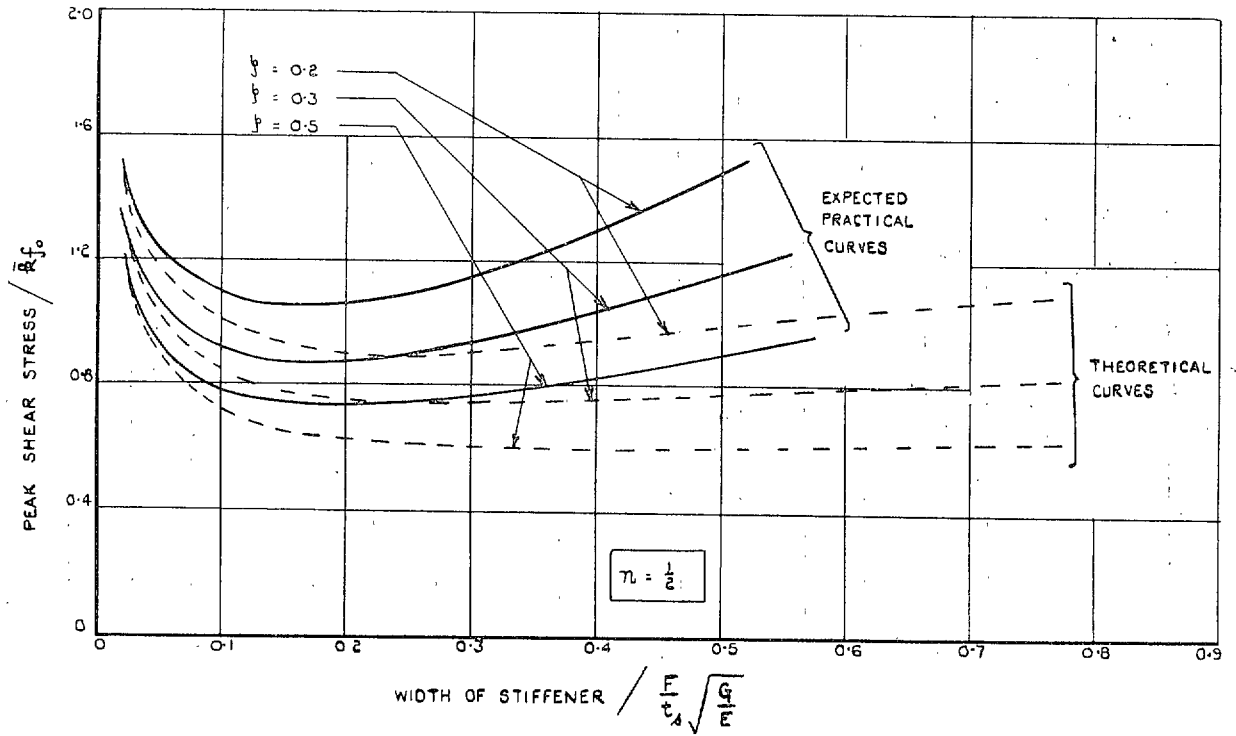


FIG. 36. Peak shear stress as influenced by stiffener width ($n = \frac{1}{2}$).

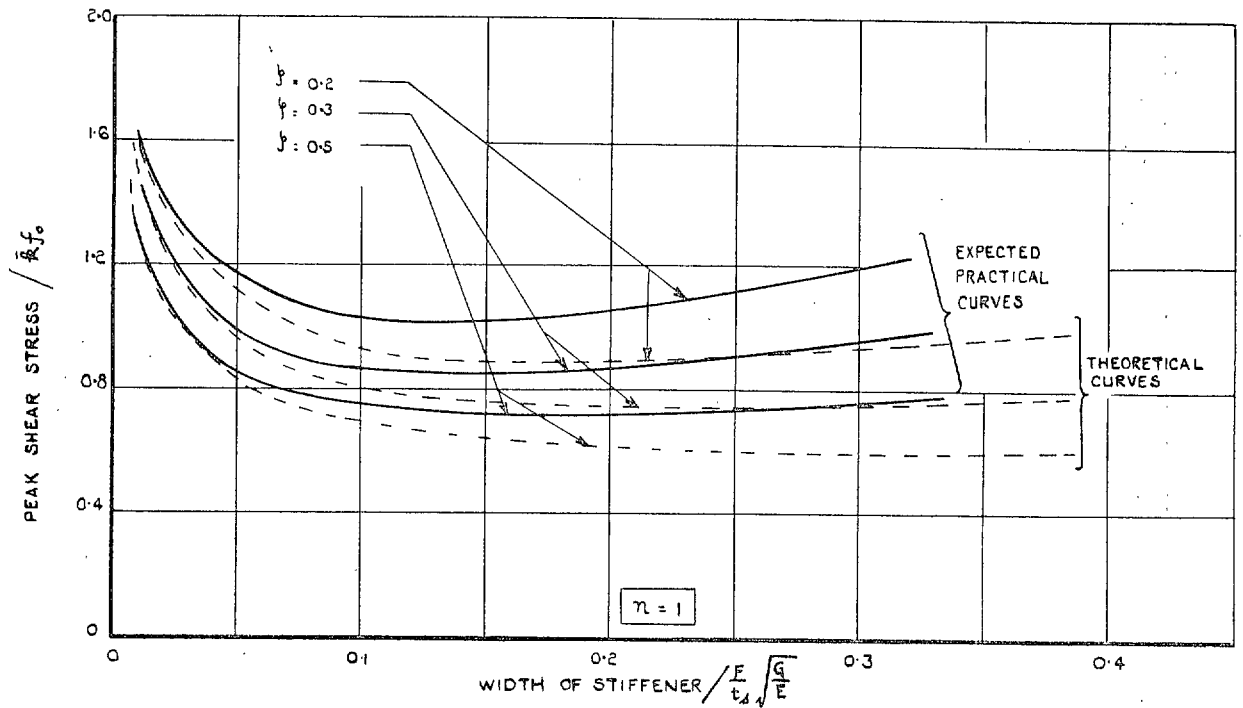


FIG. 37. Peak shear stress as influenced by stiffener width ($n = 1$).

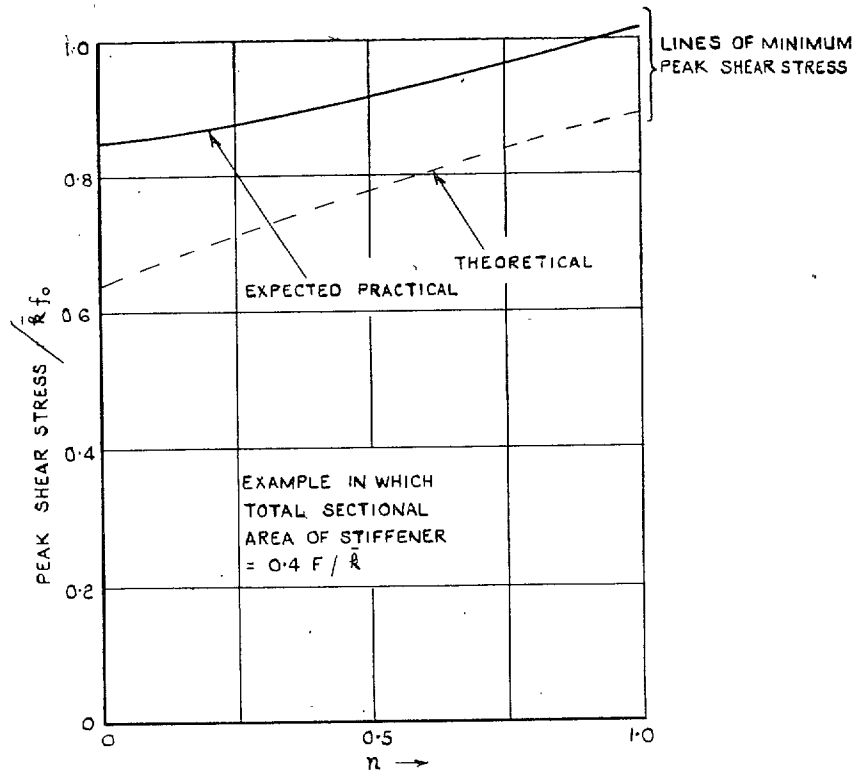


FIG. 38. Typical curve showing variation of peak shear stress with n .

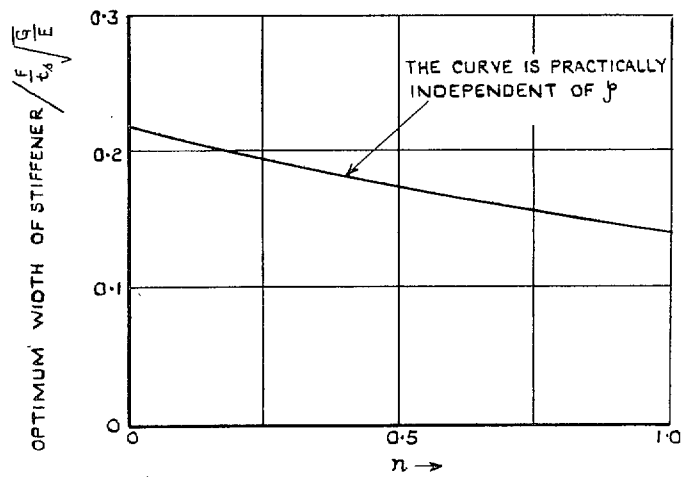


FIG. 39. Optimum width of stiffener consistent with a given n .

Publications of the Aeronautical Research Council

ANNUAL TECHNICAL REPORTS OF THE AERONAUTICAL RESEARCH COUNCIL (BOUND VOLUMES)

- 1936 Vol. I. Aerodynamics General, Performance, Airscrews, Flutter and Spinning. 40s. (40s. 9d.)
 Vol. II. Stability and Control, Structures, Seaplanes, Engines, etc. 50s. (50s. 10d.)
- 1937 Vol. I. Aerodynamics General, Performance, Airscrews, Flutter and Spinning. 40s. (40s. 10d.)
 Vol. II. Stability and Control, Structures, Seaplanes, Engines, etc. 60s. (61s.)
- 1938 Vol. I. Aerodynamics General, Performance, Airscrews. 50s. (51s.)
 Vol. II. Stability and Control, Flutter, Structures, Seaplanes, Wind Tunnels, Materials. 30s.
 (30s. 9d.)
- 1939 Vol. I. Aerodynamics General, Performance, Airscrews, Engines. 50s. (50s. 11d.)
 Vol. II. Stability and Control, Flutter and Vibration, Instruments, Structures, Seaplanes, etc.
 63s. (64s. 2d.)
- 1940 Aero and Hydrodynamics, Aerofoils, Airscrews, Engines, Flutter, Icing, Stability and Control,
 Structures, and a miscellaneous section. 50s. (51s.)
- 1941 Aero and Hydrodynamics, Aerofoils, Airscrews, Engines, Flutter, Stability and Control,
 Structures. 63s. (64s. 2d.)
- 1942 Vol. I. Aero and Hydrodynamics, Aerofoils, Airscrews, Engines. 75s. (76s. 3d.)
 Vol. II. Noise, Parachutes, Stability and Control, Structures, Vibration, Wind Tunnels
 47s. 6d. (48s. 5d.)
- 1943 Vol. I. (*In the press.*)
 Vol. II. (*In the press.*)

ANNUAL REPORTS OF THE AERONAUTICAL RESEARCH COUNCIL—

1933-34	1s. 6d. (1s. 8d.)	1937	2s. (2s. 2d.)
1934-35	1s. 6d. (1s. 8d.)	1938	1s. 6d. (1s. 8d.)
April 1, 1935 to Dec. 31, 1936.	4s. (4s. 4d.)	1939-48	3s. (3s. 2d.)

INDEX TO ALL REPORTS AND MEMORANDA PUBLISHED IN THE ANNUAL TECHNICAL REPORTS, AND SEPARATELY—

April, 1950 - - - - R. & M. No. 2600. 2s. 6d. (2s. 7½d.)

AUTHOR INDEX TO ALL REPORTS AND MEMORANDA OF THE AERONAUTICAL RESEARCH COUNCIL—

1909-1949. R. & M. No. 2570. 15s. (15s. 3d.)

INDEXES TO THE TECHNICAL REPORTS OF THE AERONAUTICAL RESEARCH COUNCIL—

December 1, 1936 — June 30, 1939.	R. & M. No. 1850.	1s. 3d. (1s. 4½d.)
July 1, 1939 — June 30, 1945.	R. & M. No. 1950.	1s. (1s. 1½d.)
July 1, 1945 — June 30, 1946.	R. & M. No. 2050.	1s. (1s. 1½d.)
July 1, 1946 — December 31, 1946.	R. & M. No. 2150.	1s. 3d. (1s. 4½d.)
January 1, 1947 — June 30, 1947.	R. & M. No. 2250.	1s. 3d. (1s. 4½d.)
July, 1951.	R. & M. No. 2350.	1s. 9d. (1s. 10½d.)

Prices in brackets include postage.

Obtainable from

HER MAJESTY'S STATIONERY OFFICE

York House, Kingsway, London, W.C.2; 423 Oxford Street, London, W.1 (Post Orders:
 P.O. Box 569, London, S.E.1); 13a Castle Street, Edinburgh 2; 39, King Street, Manchester, 2;
 2 Edmund Street, Birmingham 3; 1 St. Andrew's Crescent, Cardiff; Tower Lane, Bristol 1;
 80 Chichester Street, Belfast, or through any bookseller